DISSERTATION

PARSIMONY AND COMPLEXITY IN EPIDEMIOLOGICAL MODELS FOR DECISION SUPPORT IN ANIMAL HEALTH

Submitted by

Francisco J. Zagmutt

Department of Clinical Sciences

In partial fulfillment of the requirements

For the Degree of Doctor of Philosophy

Colorado State University

Fort Collins, Colorado

Fall 2012

Doctoral Committee:

Advisor: Steven W. Dow
Co-Advisor: Ashley Hill

Colleen T. Webb
Bruce A. Wagner

ABSTRACT

PARSIMONY AND COMPLEXITY IN EPIDEMIOLOGICAL MODELS FOR DECISION SUPPORT IN ANIMAL HEALTH

This thesis is concerned with epidemiological models used as decision-support tools in animal health. By definition, models are representations of reality, and the epidemiological models I examine here are a simplification of complex ecological systems involving the interactions of host, agent, and environment. The development of new analytical methods and tools, and faster computing capabilities has motivated the creation of increasingly realistic epidemiological models. The development and parameterization of such sophisticated models can take considerable time and effort, and can potentially reduce the model's transparency when communicating the modeling results to decision makers. Hence, it is relevant to evaluate whether extra model complexity provides more accurate or useful information for health policy than more parsimonious modeling approaches.

The overall objective of this thesis was to evaluate the role that parsimony and complexity has in epidemiological models used to inform animal health policy. For this, I developed and used several models to explore different aspects of model parsimony and complexity in the context of animal health policy.

Chapter 1 provides an introduction to the subject of epidemiological models, parsimony and complexity in modeling, and a review of the different models used in animal health policy, focusing on the levels of complexity and parsimony approaches used in the published literature. For this, I make a distinction between complexity in the model structure (structural complexity) and in the corresponding parameters used in the epidemiological models (parameter complexity), and I use examples such as the 2001 Foot-and-mouth disease (FMD) outbreak in the UK to depict how complexity and parsimony can directly affect health policy. In general, consensus on the level of complexity necessary to provide useful information for animal health policy doesn't seem to exist, as some researchers advocate very realistic (and thus, complex) models, whereas others use simplistic (parsimonious) models to inform policy.

In Chapter 2, I explore the effect that structural complexity and parsimony in the model (specifically, population, contact, and spatial heterogeneity) can have in the results commonly used for policy. For this, I developed a flexible herd-level model that simulates the spatial and temporal spread of infectious diseases between animal populations, and used it to evaluate sixteen scenarios , involving combinations of multiple production-types (PT) with heterogeneous contact structure versus single PT with homogeneous contact structure; random versus actual spatial distribution of population units (based on an existing dataset from the state of Minnesota); high versus low disease infectivity; and no vaccination versus preemptive ring vaccination. The results from the scenarios revealed that for fast spreading epidemics, the actual locations of population units (e.g. herds) may not be as relevant to predict outbreak size and duration as information on population and contact heterogeneity.

Nonetheless, both population and spatial heterogeneity might be important to model slower spreading epidemic diseases. This information is relevant to inform data collection and model building efforts for epidemiological models used to inform health policy.

In chapter 3, I used an epidemiological modeling framework to estimate the potential losses from a new emerging disease (ED) in channel catfish ponds in Mississippi, with the purpose of estimating animal inventory losses for agricultural insurance purposes. Given the uncertain epidemiology of a new ED, the predictions naturally have a high level of uncertainty, which motivated the design of a structurally complex model to try to evaluate the potential spread of the disease from the "bottom-up". For this, I used two coupled stochastic models that simulate the spread of an ED between and within ponds under high, medium, and low disease impact scenarios, which were parameterized based on a meeting with fish disease experts. The mean (95% prediction interval (PI)) proportion of ponds infected within disease-impacted farms was 7.6% (3.8%, 22.8%), 24.5% (3.8%, 72.0%), and 45.6% (4.0%, 92.3%), and the mean (95%PI) proportion of fish mortalities in ponds affected by the disease was 9.8% (1.4%, 26.7%), 49.2% (4.7%, 60.7%), and 88.3% (85.9%, 90.5%) for the low, medium and high impact scenarios respectively. The farm-level mortality losses from an ED were up to 40.3% of the total farm inventory. The models provided a systematic method to organize the current knowledge on the emerging disease perils and, ultimately, use this information to help develop actuarially sound agricultural insurance policies and premiums. The conclusions from this chapter was that a structurally complex model was necessary to make inferences about a hypothetical ED for which no empirical data is available, but the estimates obtained included a large amount of

uncertainty driven by the stochastic nature of disease outbreaks, by the uncertainty in the frequency of future ED occurrences, and by the often sparse data available from past outbreaks.

After reviewing the impact of structural complexity and parsimony in chapter 2, and the application of a structurally complex model in chapter 3, chapter 4 evaluates the impact that parsimony and complexity in model parameters can have in model predictions. For this, I developed a Bayesian model that estimates the confidence on individual infection progression using longitudinal screening test results, and use the results to estimate infectious disease model parameters using a Monte Carlo simulation model. Test results from a *Mycobacterium avium* subsp. *paratuberculosis* (MAP) control program from three Wisconsin dairy herds were used to build a stochastic Markov Chain model for the within-herd spread of MAP and estimate its parameters. The infection/disease states were Susceptible, Non-shedder adult, Latent, Low Shedder, Heavy Shedder, Clinical, and Culled. Test parameters estimated with a latent-class Bayesian model were used to simulate a longitudinal disease trajectory for each tested animal and for the herd. The disease trajectories were used to estimate the joint uncertainty distributions of the transition probabilities of the stochastic Markov Chain model, and were then used to project the yearly progression of disease in 20 years. The joint uncertainties in both, the test characteristics and the disease parameters exhibited a significant level of correlation, and sensitivity analysis showed that ignoring parameter correlation considerably underestimated the variance of the model predictions. The main conclusion from this chapter is that the correlation between disease parameters can have an important impact in the variance

of relevant disease model outputs and therefore, this correlation should be taken into account when parameterizing stochastic epidemic models. In other words, assuming a more parsimonious structure in the correlation parameters underestimated the variance of the results, justifying the model complex methodology used to derive the correlated parameters.

This thesis explored different aspects of parsimony and complexity in the structure and parameters of epidemiological models used for decision support in animal health. From the studies, I conclude that complexity in both, the model structure and its parameters can be needed depending on the disease modeled and types of results required from the model. However, in other instances a more parsimonious model structure could have yielded equivalent results and thus, should be favored. Although aspects of this work agree with the literature, the results from this thesis are novel, as all models used were created in response to a specific animal health application and thus, have direct application to animal health policy.

ACKNOWLEDGEMENTS

I would like to express my deepest gratitude to Dr. Dow and Dr. Hill for their guidance and encouragement during the completion of my thesis. I could not have done this without you!
I am also indebted to Dr. Wagner and Dr. Webb for going above and beyond their committee responsibilities to make me a better scientist and for their significant scientific input during the development of my PhD program.

Much of this research was partially supported by different institutions, including USDA-VS-APHIS-CEAH and CSU-APHI (chapter 2), USDA-RMA-Federal Crop Insurance Corporation (chapter 3), and USDA-NIFA (chapter 4).

Many people provided essential discussion, advice, and guidance during my PhD program, so I apologize in advance if your name is not listed here. Dr. Mark Schoenbaum patiently taught me how to program in Delphi, and was a key collaborator for chapter 2 in this thesis, whereas Dr. Barbara Corso provided valuable discussion and expert opinion to parameterize the model in chapter 2. I am also grateful to Dr. Paul Anderson for allowing me to use the herd location dataset used in chapter 2, and to Mr. Ryan Miller and Dr. Anne Seitzinger for their assistance in the addition of beef herds to the dataset.
Dr. Terry Hanson and Mr. Steve Sempier's expert knowledge of the catfish and aquaculture industry were instrumental in the development and submission of chapter 3, and the fish

disease experts that participated in the expert consultation meeting were essential to develop the parameters and models used.

My thanks also go to my external collaborators for chapter 4; Drs. Luis A. Espejo, Joao R. Lima, Elizabeth Patton, and Scott Wells for the great team work to develop the paratuberculosis modeling framework. I very much enjoyed and learned from our meetings and discussions about this rather puzzling disease.

I would also like to thank Dr. Mowafak (Mo) Salman from the Animal Population Health Institute (APHI) for his input during the earlier stages of my PhD program.

I am much obliged to my friend and business partner, Dr. Huybert Groenendaal, not only for his input on chapter 4, but also for his encouragement to “get it done” and for shouldering a sizable part of my work responsibilities while I was working long hours to finish this thesis. Dank je wel, mijn vriend!

And last but not least, I am eternally indebted to my parents, who taught me to embrace all forms of knowledge, and to keep an open mind even under the direst circumstances.

DEDICATION

To Solenne; your unconditional love and constant support were vital to complete this work.

TABLE OF CONTENTS

CHAPTER 1: PARSIMONY AND COMPLEXITY IN EPIDEMIOLOGICAL MODELS USED TO SUPPORT ANIMAL HEALTH DECISION-MAKING

"With four parameters I can fit an elephant, and with five I can make him wiggle his trunk."

- John Von Neumann

1 Introduction

Livestock production is continuously faced with significant disease challenges, from Transboundary Animal Diseases (highly contagious infectious diseases that spread rapidly regardless of country borders) with significant impact on trade [(1)], to endemic diseases that affect production, and zoonotic diseases that can also affect humans [(2)]. In response to the challenge imposed by animal diseases, a wide range of quantitative models have been developed to support animal health decisions, ranging from simple empirical statistical models, to sophisticated mechanistic models that simulate the dynamics of disease transmission in populations [(3)].

This work is concerned with epidemiological models used as decision-support tool for animal health management. Such models are described in the literature with a variety of names, such as *disease spread models, epidemic models, mathematical models, disease models, and infectious disease models*. Here I use the term "epidemiological models" exclusively to describe mechanistic models that simulate disease spread in animal populations.

At this point it is important to make a distinction between empirical and mechanistic models: empirical models attempt to best match the observed pattern in the data using mathematical

functions and/or probability theory [4]. In contrast, mechanistic models specify the underlying processes that are hypothesized to have generated the observed data [4]. For example, when fitting a time series model to disease incidence data we find the set of parameters that best match the data, but the parameters may not directly explain what caused the incidence pattern. In contrast, if an epidemiological model was used on the same dataset, the model parameters and relationships could implicitly incorporate the underlying disease mechanisms such as transmission rates and population dynamics.

Although the basis of the epidemiological models used today dates back to a landmark article published over 80 years ago [5], the first formal treatment on the subject was provided relatively recently by Anderson and May [6]. Nowadays, epidemiological models are described extensively in the literature. For instance, Vynnycky and White [7] provide an excellent introductory reference book to epidemiological modeling, whereas Keeling and Rohani [8] present a more detailed treatment of infectious diseases models used in both humans and animals. Hollingsworth [9] offers a brief review of selected epidemiological models for controlling infectious disease outbreaks in humans, and Eisenberg et al. [10] discuss the application of epidemiological modeling to support decision making in public health, highlighting that models can be used both to identify data gaps, and to aid in decision making, and therefore models create a link between science and policy. Garner and Hamilton [11] recently discussed the principles and applications of epidemiological models in animal health, while others have reviewed the applications of models to animals diseases such as foot-and-mouth disease (FMD) [12] and avian influenza [13]. Woolhouse [14] connects both worlds by examining models used to

predict diseases in humans and animals, and calls for more complex models that incorporate exogenous factors such as human behavior and climate change.

By definition, epidemiological models are a simplification of complex ecological systems involving the interactions of host, agent, and environment [7]. Nonetheless, the advance of new analytical methods and tools, and faster computing capabilities has motivated the creation and adoption of increasingly realistic epidemiological models [11]. The development and parameterization of such sophisticated models can take considerable time and efforts, and can potentially reduce the model's transparency when communicating the modeling results to decision makers or even between modeling practitioners. Hence, it is relevant to evaluate whether extra model complexity provides more accurate or useful information for health policy than more parsimonious modeling approaches.

The overall objective of this thesis was to evaluate the role that parsimony and complexity has in epidemiological models used to inform animal health policy.

2 Model parsimony and complexity

Parsimony can be loosely described as the general principle of favoring simplicity over complexity. In the scientific literature, this is often equaled to Occam's (Ockam's) razor principle, which (translated from Latin) states that "entities should not be multiplied unnecessarily" [15]. Although this quote is highly cited in a wide range of scientific work, the vague nature of the statement makes it widely open to interpretation, but in general, the

concept is commonly understood as “all other things being equal, scientists ought to prefer simpler theories” [16]. The direct implication of the principle of parsimony in modeling is that the simplest of competing models providing equally compelling explanation about a natural process should be preferred to the more complex model. Therefore, parsimony and complexity are opposite directions in any modeling effort.

Abundant literature exists arguing in favor [15-16], and against [17-18] parsimony in statistical modeling. For example, a prominent Bayesian statistician and his colleagues [18] discuss the practical limitations of traditional compartmental pharmacokinetics models in which model complexity is largely reduced to be able to estimate parameters, and presents an alternative complex hierarchical Bayesian model, arguing that the hierarchical structure of the model decreases the risk of overfitting, without losing predictive power. However, his criticism appears to be confined to parsimony in hierarchical Bayesian models, as overfitting remains a problem for statistical models that use optimization methods such as Maximum Likelihood Estimation (MLE) to fit model parameters. Indeed, Hitchcock and Sober [19] discuss the importance of differentiating prediction vs. accommodation (i.e. using observation(s) to formulate a theory) in scientific theory, and Forster [20] more specifically argues that tests for parsimony in MLE-based statistical models, such as Akaike’s Information Criterion (AIC) only account for parsimony to minimize the potential errors in parameter estimation, while failing to incorporate the potential for errors of extrapolation or generalization, which are relevant to models with the goal of making predictions.

Although the aforementioned principles may also apply to mechanistic models, less work directly address the role of parsimony and complexity in such models. In an opinion article discussing general rules to judge ecological theories, Ginzburg and Jensen [21] provide discussion and examples in favor of parsimony, and conclude that if a theory greatly exceeds the complexity of the problem it addresses, it should be rejected. Asgharbeygi et al. [22] present an innovative model selection algorithm where an initial model, a data set, and a set of allowed revisions are used to explore alternative parameterizations of the model that may explain the dataset. Cox et al. [23] applies a simplified version of the Asgharbeygi et al. [22] algorithm to compare thousands of reduced formulations of a published radiocaesium plant-uptake model, based on goodness-of-fit measures on existing data and also to predict an independent dataset, and conclude that the simplified models provide a better fit both for the existing and independent datasets.

Parsimony and complexity in epidemiological models has also been directly addressed by some authors. Bauch and Bhattacharyya [24] present a modified Susceptible-Infectious-Recovered (SIR) epidemiological model that incorporates social learning and game theory to model disease incidence and vaccine coverage during a vaccine scare, reporting that a structurally more complex model consistent with human behavior improved the model fit with little parsimony penalty. In another example, as the persistence of low pathogenic avian influenza in waterfowl in North America could not be explained with traditional SIR models, Breban et al. [25] incorporated environmental transmission in a simple SIR model, providing a parsimonious explanation of the observed incidence patterns. Wearing et al. [26] describe how the commonly

used assumption of exponentially distributed latent and infectious periods in models of diseases in humans can have a direct impact on public health policy, by overestimating the value of potential management options. In this case, the authors proposed replacing the Exponential with a Gamma distribution, which only results in one extra (shape) parameter. In all three examples, the authors favored slightly more complex models to be able to explain empirical observations not supported by their simpler models. However, their solutions can still be considered parsimonious, as the complexity added was small relative to the extra knowledge gained by the addition of the extra parameters.

In contrast, many authors advocate the use of much more realistic and thus, complex epidemiological models. For instance, Eubank et al.[27] used a sophisticated model that includes urban traffic simulations, land-use, and population-mobility data to evaluate strategies to contain smallpox spread, and concluded that targeted vaccination and early detection could be used in favor of mass vaccination. Similarly complex models are also described in the veterinary literature [28-31], and will be discussed in the next section.

3 Parsimony and complexity in models used for supporting animal health decision making

A wide range of quantitative models are used to support animal health decisions. Singer et al [3] found that thirteen out of the 35 animal health-related scientific opinions adopted by the Animal Health and Animal Welfare panel of the European Food Safety Authority relied on at least one quantitative model, resulting in a total of 23 models used. Three of those models were epidemiological SIR-type of models, with two of them being based on systems of

differential equations, and one of them being a spatially explicit, individual-based model. Although this number might seem small relative to the total models used, the other models were used to answer non-transmission questions such as diagnostic test evaluation, and introduction and exposure risk assessments. In an article advocating the use of quantitative modeling for the evaluation of strategies for animal disease control, Saegerman et al. [32] categorizes models as descriptive, predictive, and explicative, including epidemiological models in the explicative category. The authors argue that modeling is one of the "key investments in Veterinary services for the future" and modeling efforts should make the "fewest assumptions possible". Although the recommendations do not seem to be derived directly from their findings, the authors seem to advocate for more realistic (and thus, more complex) models.

Epidemiological models are indeed increasingly being used for animal health policy. Garner et al [33] review the role of epidemiological models to support policy, and advocate the use of models for informing disease control policy before an outbreak, particularly in the areas of retrospective outbreak analysis, contingency planning, resource planning, risk assessments, and training, while cautioning on the use of models during an outbreak, a point also made by Keeling [34] when describing the models used to inform policy during the 2001 FMD outbreak in the UK. In contrast, other authors seem to advocate the use of models to inform policy during animal disease outbreaks [35]. The use of models to support policy during an outbreak remain controversial, and their usage during the 2001 FMD outbreak in the UK has been particularly criticized [36-37]. For instance, in a critical review of the modeling efforts during the 2001 FMD outbreak in the UK, Taylor [38] highlighted that some complex features in the models used to

inform a controversial “contiguous culling” policy may not have been well understood by the non-modeling experts in the FMD Science Group appointed by the UK veterinary authority to advise policy during the outbreak. Although 3 of the 4 models used to inform policy were fairly simple extensions to the SIR model [34], the confusion and criticism created by the use of these models during an outbreak highlights the difficulties in communicating the results of epidemiological models to decision makers, and thus why this should be taken into account when deciding in the level of complexity of a model.

The types of epidemiological models used to inform policy varies considerably. For example, during the aforementioned FMD outbreak in the UK, the models used ranged from a simple deterministic SIR model [39], to a very detailed stochastic simulation model [40] that explicitly modeled multiple modes of direct and indirect spread. Although both approaches are applied to a variety of other applications, more detailed stochastic simulation models seem to be more commonly adopted by national veterinary authorities, especially for the purpose of emergency planning. Some of the most widely known models used for emergency planning and policy evaluation are the InterSpread Plus [30] from New Zealand, the InterFMD model from The Netherlands [41], the AusSpread from Australia [28], and the North American Animal Disease Simulation Model (NAADSM) [29]. Although the aforementioned models are unique, a common trait among them is that they tend to be more structurally complex than more traditional epidemiological models based on differential equations. For example, all four models allow for the inclusion of detailed population data and the explicit modeling of multiple modes of transmission. Some example applications of these models include:

- InterSpread/InterSpread Plus: Prediction of control strategies during the FMD epidemic in the US [40]; evaluation of different control strategies for an FMD outbreak in Korea [42]; evaluation of control strategies against Classical Swine Fever in Denmark [43]; assessment of the use of antiviral supplementation as an alternative to stamping using a modified version of the model [44].
- AusSpread: Garner and Becket [28] describe how the model is used by the Australian Government Department of Agriculture, Fisheries and Forestry for emergency preparedness purposes.
- InterFMD: Evaluation of movement restrictions to reduce FMD spread [41]
- NAADSM: this model is used by veterinary authorities in North and South America for the purpose of emergency preparedness for a variety of transboundary infectious diseases [45-46],and to quantify the value of animal traceability [47].

Dubé et al. [48] compared the predictions of an FMD outbreak from NAADSM, AusSpread, and InterSpread plus and found that although the model predictions were different, they would not have affected the management decisions adopted based on the models results.

Beyond the application to epidemics and emergency management, epidemiological models are also used to support decisions for a variety of endemic diseases. Examples include the development of a national control program for Johne's disease [49], economic evaluation of badger culling strategies to reduce tuberculosis in UK cattle [50], and the evaluation of surveillance protocols for a swine disease [51].

The common denominator in all applications of the epidemiological models described is that researchers must decide on the level of complexity in their models based on *a priori* understanding of the epidemiology and ecology of the disease being modeled, but the potential impact that such structural assumptions have in the outputs used for animal health policy is rarely tested explicitly. An example of such tests is provided by Tildesley et al.[35], who used a spatially explicit model to evaluate the level of spatial granularity required to determine optimal ring vaccination strategies against FMD, and concluded that using herds randomly generated (without spatial clustering) from aggregate US county-scale data was sufficient to closely determine an optimal ring culling strategy, and did not significantly modify the prediction of epidemic size when compared against a fully spatial model containing representative herd locations. Likewise, Danon [52] discusses the hypothetical effect that movement of humans have on the spread of FMD, concluding that more realistic routine movements (such as daily commuting) resulted in slower epidemic spread compared to the movements with random destinations which are typically assumed in epidemiological models. Such findings show that the structural complexity of a model can impact animal health policy, and thus deserve further exploration.

Just as the assumptions on the structure of a model may impact predictions, the correct selection and modeling of model parameters can also have a considerable impact in the model predictions. The most intuitive challenge when modeling disease spread is that of determining the correct parameter estimates (e.g. the proper distribution of contact distances or animal level latent duration), but a more insidious and less addressed problem is that of correctly

modeling the joint uncertainties (i.e. the correlations) in model parameters that are not perfectly known. For example, diagnostic tests such as serological or culture tests that are commonly used to infer disease status in populations can be correlated [53]. Incorrectly accounting for parameter correlations can alter the scale and shape of the model predictions, and thus, potentially bias the information provided to animal health decision makers. Traditionally, this problem has been avoided by using point estimates of epidemiological parameters [6], while still sometimes allowing for stochasticity in the disease spread dynamics [29, 42, 54]. As uncertainty analysis is now a fundamental part of decision support models, many of them now include parameters with uncertainty, but often correlations are ignored as their estimation from observational data is not straightforward, or in many instances such as Morris et al [40], parameter estimates rely on expert opinion. Capaldi et al.[55] recently provided a statistical assessment of estimation and correlation of the parameters of the simple SIR model, and reported that the transmission parameter and recovery rates are correlated. The fact that parameters are correlated even in the simplest of epidemiological models suggests that much more research should be focused on this neglected area.

4 Objectives of this thesis

The primary aim of this thesis was to compare parsimony and complexity approaches in the design and parameterization of epidemiological models used as decision aid tools in animal health. The following sub-objectives were established to achieve the primary objective:

1. To develop and use a generic model for an epidemic disease to evaluate the impact of different degrees of complexity in the structure of epidemiological models, and evaluate their impact in disease predictions used to establish animal health policy;
2. To develop and use a model that quantifies the potential impact of an emerging disease in an animal production system, to explore the level of complexity needed to provide predictions for a disease risk transfer strategy (insurance);
3. To develop and use a model for the spread of an endemic disease to evaluate the effect of different degrees of complexity in the modeling of parameter uncertainty.

5 Outline of this thesis

Chapter 2 describes a study designed to explore the effect of structural complexity and parsimony in epidemiological models, in the form of population, contact, and spatial heterogeneity, and how variations in this complexity can affect the results commonly used for policy. For this, I developed an epidemiological simulation model that simulates the spatial and temporal spread of infectious diseases in large scale populations, and used it to explore a range of combinations of alternative model structures and parameterizations.

Chapter 3 then describes the application of a structurally complex epidemiological modeling framework to predict the potential spread a new emerging disease in channel catfish ponds in Mississippi, with the goal of estimating animal inventory losses for agricultural insurance purposes. Given the uncertain epidemiology of a new emerging disease, the predictions have a high level of uncertainty, which motivated the design of a structurally complex model that

attempts to evaluate the potential spread of the disease more mechanistically than the more parsimonious models usually applied to model epidemics.

Chapter 4 then focuses on parameter complexity, with the goal of evaluating the impact that parsimony and complexity in the estimation and representation of model parameters can have in model predictions. This is approached with a Bayesian modeling framework that estimates the confidence on the infection progression of individual animals using longitudinal screening test results, and uses the results to estimate infectious disease model parameters using a Monte Carlo simulation model. The model is applied to results from a *Mycobacterium avium* subsp. *paratuberculosis* (MAP) control program, and highlights the impact that different parameter assumptions can have in the model predictions.

Finally, chapter 5 discusses the approaches and main findings of this thesis, and their practical implications to epidemiological models used to support animal health decisions.

CHAPTER 2: THE QUANTITATIVE IMPACT OF POPULATION, CONTACT, AND SPATIAL HETEROGENEITY TO MODEL INFECTIOUS ANIMAL DISEASES[1]

Summary

Epidemiological simulation models are increasingly used to support human and animal health policy. Models vary in complexity, ranging from simple differential equations, to complex mechanistic models considering the spatial and demographic components of the disease spread. The development and parameterization of such sophisticated models may take considerable time and effort and can reduce the model's transparency. Hence, it is relevant to evaluate whether the extra complexity provides more accurate or useful information for health policy.

The objective of this study was to evaluate the effect that complexity in the form of different levels of spatial, population, and contact heterogeneity have in the predictions of a mechanistic model for the spread of infectious animal diseases.

A flexible herd-level model that simulates the spatial and temporal spread of infectious diseases between animal populations was developed.

Sixteen scenarios were analyzed, involving combinations of the following factors: multiple production-types (PT) with heterogeneous contact structure versus single PT with homogeneous contact structure, random versus actual (clustered) spatial distribution of population units, high versus low infectivity, and no vaccination versus preemptive ring

[1] Simulation scenarios and model developed in collaboration with Dr. Mark A. Schoenbaum (USDA-APHIS-VS)

vaccination. The mean epidemic size (cumulative number of infected population units at the end of the outbreak) and duration was considerably larger for scenarios with multiple PT than for scenarios with a single PT. Ignoring the actual unit locations did not appreciably affect the epidemic size in scenarios with multiple PT and high infectivity, but resulted in smaller epidemic sizes in scenarios using multiple PT and low infectivity.

In conclusion, knowing the actual locations of population units may not be as relevant as collecting information on population and contact heterogeneity when modeling fast spreading epidemics. In contrast, both population and spatial heterogeneity might be important to model slower spreading epidemic diseases. Our findings can be used to inform data collection and model building efforts for mechanistic epidemic models used to inform health policy and planning.

1 Introduction

The emergence of economically important animal diseases such as H1N1 Avian Influenza has increased awareness of the importance of disease emergency planning [(56)]. One of the main tools used for emergency planning is simulation models that mimic the progress of the disease under different scenarios to evaluate disease control strategies, and that may be used to predict the potential impact of disease outbreaks [(31)].

Disease simulation models range from simple mass action models based on systems of ordinary differential equations [(57)], to complex models taking into account details such as the spatial and

demographic components of the disease spread [29, 58-60]. As modeling platforms and inexpensive computer capacity have become readily available, some researchers have naturally moved towards more complex simulation models that include further details on the dynamics of disease spread. However, complex models can have several caveats, including lack of data to support parameters [61], intractability of their calculations [62], difficulty to validate predictions [60], and more importantly, they may be less transparent and therefore harder to understand for non-modelers and decision makers. For example, a critical review of the modeling efforts during the 2001 FMD outbreak in the UK [38] highlighted that some complex features in the models used to inform a controversial "contiguous culling" outbreak control policy may not have been well understood by the non-modeling experts in the FMD Science Group appointed by the UK veterinary authority (formerly DEFRA) to advise policy during the outbreak. Thus, model complexity should only be justified when its components have a large enough impact on the final outcome such that decisions would change.

Several studies have explored the effect that model complexity has on model predictions, but they are largely focused on mathematical aspects [54], and/or on the impact of limited elements of the disease dynamic in human populations. For example, Hufnagel et al.[63] studied the effect of network heterogeneity in a severe acute respiratory syndrome (SARS) simulation model, but did not explicitly consider the effect of spatial heterogeneity and mixing. Similarly, Bombardt [64] compared predictions from a simple ordinary differential equations (ODE) model against a model based on contact networks of SARS, concluding that the simpler ODE model was adequate to assess the general impacts of disease progression control, whereas the network-

based model provided insights into disease transmission within and between connectivity classes. Diekmann et al.[65] and Kiss et al.[66] also explored the effect of contact heterogeneity and multiple transmission mechanisms in the reduction of infectious output, and final epidemic size respectively, but did not evaluate the effect of the spatial heterogeneity in the model predictions. Similarly, Dickey et al. [67] found that a mechanistic model with homogeneous contact parameters predicted fewer FMD infected premises than a model with heterogeneous operation-specific contact parameters. However, no comprehensive comparisons of the impact of different levels of population and spatial heterogeneity have been made for models of animal diseases used in practice to inform decision makers.

The objective of this study was to evaluate the effect that different levels of spatial, population, and contact heterogeneity have in the predictions of a mechanistic model for the spread of infectious animal diseases.

2 Materials and methods

A simulation model that takes into consideration spatial and demographic components relevant for the spread of infectious diseases was used to evaluate the impact of modeling multiple animal species and production systems versus modeling a single species and production system on the simulation output. The impact of the spatial distribution of the population units and of a ring vaccination strategy was also included.

2.1 Model description

A spatial stochastic model that simulates the spatial and temporal spread of infectious animal diseases was developed based on previous work by Schoenbaum and Disney [31]. As a description of a descendant version of the model for this study is published [29], only the model functions and features relevant to this study are described in the following sections.

2.2 Population units

The basic entity modeled is a collection of one or more animals called a unit (e.g. a herd or flock). Each unit has basic attributes including a point-based geographical location (latitude and longitude), the number of animals contained in the unit, and a user-defined production type (PT). A production type is typically an animal production system with distinct epidemiological features resulting in similar model parameters. For example, dairy and beef cattle can be of the same species, but usually have very different contact networks. Therefore, disease progression and spread parameters can be individually parameterized for each PTs to allow for scenarios with heterogeneous populations and contact structures.

2.3 Transition states

The disease progression is simulated and reported in daily time steps. A unit is Susceptible (Figure 2.1) when all the animals can contract the disease. If one or more animals in the unit are infected (effective exposure), the unit becomes Latent (infected but not infectious). A Latent unit naturally progresses to the Sub-Clinical state (infectious without clinical signs of disease), then to the Clinical state (infectious clinical animals) and if no interventions are implemented,

the unit progresses to the Natural Immune state. As natural immunity wanes, after a certain number of days a Natural Immune unit progresses to the Susceptible state. The progression between states and interventions occurs as following:

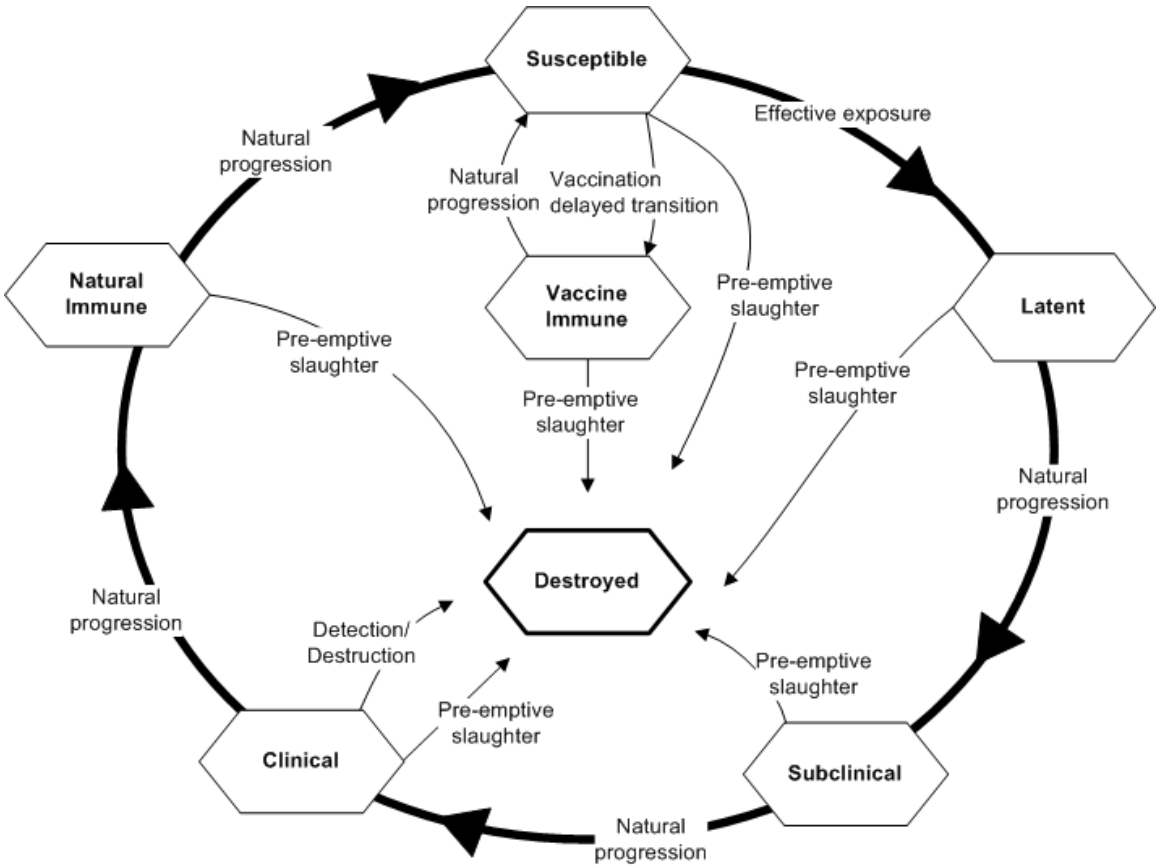

Figure 2.1. Transition states included in a simulation model for the spread of infectious animal diseases.

Natural progression: as time progresses in the simulation, a production unit transitions from one state to another (excluding susceptible and destroyed). When the unit originally enters a transition state the number of days for the unit to be in that state is randomly sampled from a user-defined probability distribution (PD). Each day of simulation decreases the days left for the unit in the state, and the unit transitions to the next state after the day drops to zero.

Vaccination: units can be vaccinated within a specified radius of detected, contagious units (ring vaccination). When units are vaccinated, they remain in their current state for a specified period of days before transitioning to the Vaccine Immune state. The time the unit will stay vaccine immune is randomly sampled from a user-defined PD. A unit is not revaccinated within a user-specified number of days. The maximum number of units to vaccinate per day and the prioritization order of vaccination can also be specified, to take into account resource constraints during an outbreak.

Exposure and infection: three possible modes of disease exposure are simulated: direct contact (animal movements), indirect contact (any other movements potentially resulting in disease transmission, e.g. feed trucks, veterinary visits, etc.), and airborne spread, taking into account the sizes and distances between the units. The infectivity (probability of infection given effective exposure to contagious unit) of direct and indirect contacts is a user defined parameter.

When two units are at the same distance from the infected unit, the probability of infection is weighted by the number of animals in the unit. The actual infection is modeled as *multinomial(n_i, pi)*, where n_i are the number of *i* units potentially receiving the infectious contact, and p_i are the probabilities of infection for each *i* unit, based on movement and airborne spread exposures and infectivity.

Movement exposures (direct and indirect contact) are based on the rate of daily movements (sampled from a Poisson distribution with a user-defined intensity rate) and random directional

movements within distances around contagious units. The distance of the movements from each unit is based on a user-defined PD.

Airborne spread is simulated with a user-specified infectivity parameter (probability of transfer from a contagious unit to a susceptible unit at a distance of 1 km). The probability of transfer decreases (with a user-defined function) as the distance from the contagious unit increases.

Detection/Destruction: Destruction or slaughter is based on the detection of contagious units via two user-defined time-series charts; daily probability of detection since the herd became clinically ill and daily probability of detection since first clinical detection of the outbreak. If detected units are chosen to be slaughtered during a simulation run, they are slaughtered at the end of the day that they are detected. The slaughter of the first confirmed case-unit can be delayed by a specified number of days. Capacity to slaughter can also be specified.

Pre-emptive slaughter: Units can be preemptively destroyed in three different ways: a) Within a specified radius of detected, contagious units (sometimes called ring slaughter), b) Units that had direct contact with the contagious unit during a specified time period, c) Units that had indirect contact with the contagious unit during a specified time period. Options b and c are determined from tracing activities, which are also user-defined.

The model is a standalone windows application developed with Delphi 7[2] and includes a user-friendly graphical user interface (GUI). All the simulation routines were tested using an automated suite that included comprehensive tests for each core function of the model (tests for transition between states, random number generators, generation of spatial movements, etc.). The model software and testing suite are available upon request from the authors.

2.4 Scenarios evaluated

A total of sixteen scenarios were used, involving all possible combinations of the following disease determinants: multiple production-types versus single production-type, random versus heterogeneous spatial distribution of population units, high versus low infectivity, and no vaccination versus 3km ring vaccination (Table 2.1). The scenario parameters are described below.

[2] Embarcadero Technologies, Inc., San Francisco, California, USA

Table 2.1. Summary of sixteen scenarios simulating a hypothetical outbreak of foot-and-mouth disease in a Midwestern US state.

Scenario ID	Spatial distribution	Population	Infectivity	Vaccination
1	Heterogeneous[†]	Single PT	High	No
2	Heterogeneous	Single PT	High	Yes
3	Heterogeneous	Single PT	Low	No
4	Heterogeneous	Single PT	Low	Yes
5	Heterogeneous	Multiple PTs	High	No
6	Heterogeneous	Multiple PTs	High	Yes
7	Heterogeneous	Multiple PTs	Low	No
8	Heterogeneous	Multiple PTs	Low	Yes
9	Homogeneous[‡]	Single PT	High	No
10	Homogeneous	Single PT	High	Yes
11	Homogeneous	Single PT	Low	No
12	Homogeneous	Single PT	Low	Yes
13	Homogeneous	Multiple PTs	High	No
14	Homogeneous	Multiple PTs	High	Yes
15	Homogeneous	Multiple PTs	Low	No
16	Homogeneous	Multiple PTs	Low	Yes

[†] Heterogeneous: actual unit locations based on data from a Midwestern US state. Beef herds randomly allocated based on survey data.
[‡]Homogeneous: unit locations created under Complete Spatial Randomness

2.4.1 Population location and demographics

Four population datasets with 4,048 animal population units were used to include the four combinations of spatial distribution (homogeneous and heterogeneous) and PTs (multiple and single). The latitude and longitude of the spatially heterogeneous population units were obtained from a randomly sampled subset of data from animal production units previously collected from a Midwestern US state[3]. A subset of the original population was used to have a reduced population dataset, increasing the simulation speed. Each unit included a PT identifier based on the main purpose of the production unit, and the number of animals in the unit

[3] Unpublished (2002). Courtesy of Dr. Paul Anderson, Minnesota State Board of Animal Health.

(Figure 2.2.a). Ripley's K-function [68] was calculated on the resulting dataset to evaluate spatial clustering.

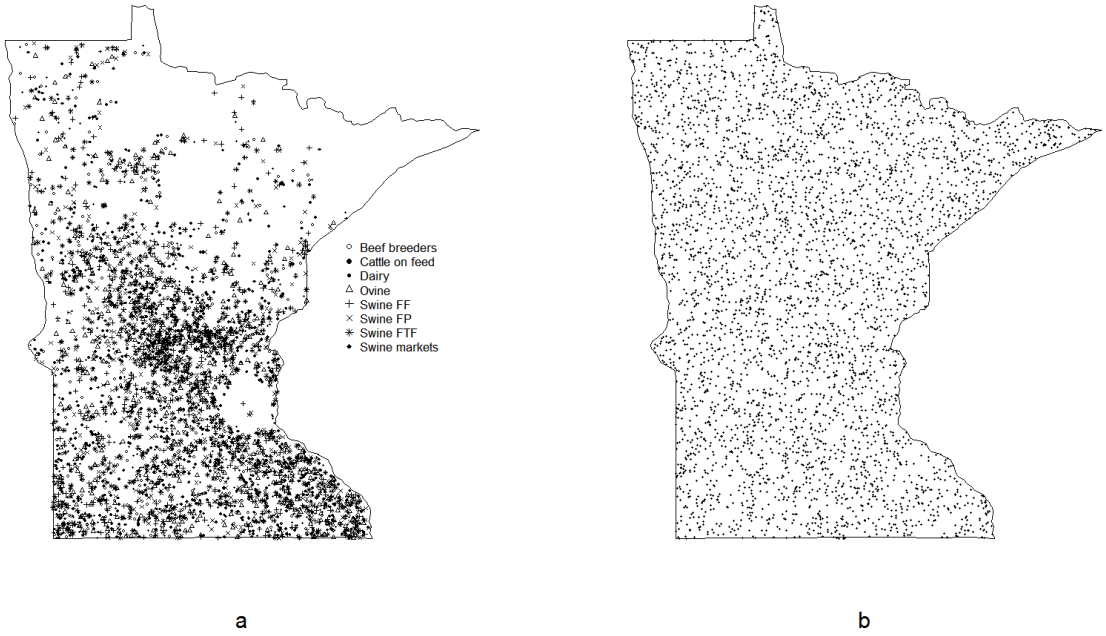

Figure 2.2. Spatial distribution for a sample of 4,048 actual animal population units from a Midwestern US state (a: heterogeneous locations), and for locations randomly generated under Complete Spatial Randomness (b: homogeneous locations).

The spatially homogeneous population dataset was constituted of geographic coordinates randomly generated under complete spatial randomness (CSR), using a spatial Poisson process. (Figure 2.2.b.).

Since the MN dataset did not contain beef herds or swine markets (Table 2.2), the production types *Beef breeders*, *Cattle on feed* and *Market* were added to provide a realistic population dataset. Herd locations were randomly generated, excluding geographical and natural boundaries such as cities, lakes, and rivers. The proportion of *beef breeders* and *cattle on feed*

herds, and the number of animals per unit were allocated to each unit randomly, based on Minnesota Beef cattle inventories for the 2002 US census of agriculture [69], resulting in 1556 beef breeders, 699 beef in feed, and 1 market. Therefore, the PTs included were b*eef breeders* (BEEFB), *cattle on feed* (BEEFF), dairy (BOV), sheep (OVI), farrow-to-finish pig (PORFTF), feeder pig (PORFP), finisher pig (PORFF), and pig market (MKT) (table 2.2)

Both the spatially heterogeneous and homogeneous datasets were populated with either the multiple PTs, or with a single PT for a total of 4 datasets

Table 2.2. Summary of population used in eight multiple production type scenarios simulating a hypothetical outbreak of foot-and-mouth disease in a Midwestern US state.

Production type (abbreviation	Number of units	Mean (SD) animals per unit
Dairy (BOV)	792	80.4 (99.59)
Beef breeder (BEEFB)	1556	28.1 (47.67)
Cattle on feed (BEEFF)	699	74.1 (147.35)
Pig - farrow-to-finish (PORKFTF)	437	934.2 (1698.93)
Pig - feeder (PORFP)	329	310.3 (955.14)
Pig - finishers (PORFF)	206	1143.7 (1725.06)
Ovine (OVI)	28	56.8 (66.99)
Pig Market (MKT)	1	2000.0 (-)

2.4.2 Contact rates, infectivity, and disease states duration

Direct and indirect contact rates and their infectivity for the multiple PT scenarios were derived from published survey data[70-72], an earlier version of this model [31] (Table 2.3), and expert opinion from the authors and an expert from the United States Department of Agriculture.

Table 2.3. Main baseline parameters used for in eight multiple production type scenarios simulating a hypothetical outbreak of foot-and-mouth disease in a Midwestern US state.

Parameter	All cattle	All swine	Ovine/goat	Generic	References[1]
Disease transitions					
Latent	*Pert(0,3.7,6.1)*	*Pert(0,6,8.7)*	*Pearson(15.3, 94.7)*	*Weighted*[2]	(71)
Subclinical-infection	*Pert(0,2.6,5.9)*	*Pert(0,4.3,10)*	*Pert(0,2.2,5.5)*	*Weighted*	(71)
Clinical infection	*Pert(7,18,60)*	*Pert(7,18,60)*	*Pert(7,18,60)*	*Weighted*	(72)
Distances					
Direct	*Weibull(.94,30.6)*	*Weibull(.94,30.6)*	*Weibull(.94,30.6)*	*Weighted*	(71)
Indirect- high	*Weibull(0.69, 13.7)*	*Weibull(0.69, 13.7)*	*Weibull(0.69, 13.7)*	*Weighted*	(71)
Indirect-low	*Weibull(.94,30.6)*	*Weibull(.94,30.6)*	*Weibull(.94,30.6)*	*Weighted*	(71)
Contacts[3]					
Direct	*Poisson(0.013)* *Poisson(0.157)*[4]	*Poisson(0.023)*	*Poisson(0.038)*	*Poisson(0.044)*	(70)
Indirect	*Poisson(1.135)* *Poisson(13.555)*[4]	*Poisson(15.087)*	*Poisson(1.352)*	*Poisson(6.924)*	(31, 70)

[1]Some published parameters were corrected to exclude unfeasible values (i.e. negative disease periods)

[2]Weighted: mixture distribution obtained by sampling disease duration from each individual PT, weighted by the number of units of each PT.

[3]Baseline contact rates only.

[4]Different parameter used for Dairy (BOV) herds.

The baseline contact rates for each production type were adjusted to account for heterogeneity in movements between PTs (Table 2.4). For most PTs, it was assumed that 90% of the movements occurred between the same PTs and the remaining 10% was evenly allocated to the other PTs. However, for the swine PTs the combination of contacts was weighted based on the knowledge of the US swine industry of one of the experts. For example, the movement of animals between Feeder-pig units was assumed to be smaller than to Feeder-finisher units (Table 2.4).

Table 2.4. Special cases of heterogeneous direct contact rates used to simulate a hypothetical outbreak of foot-and-mouth disease in a Midwestern US state. All other contact rates were assumed to be 90% movements between the same PT and 10% between all the others.

Source	Recipient	Percentage of baseline contact rate
PORFF	PORFF	5%
	PORMKT	90%
	Others	5%
PORFP	PORFP	5%
	PORFF	45%
	PORMKT	45%
	Others	5%
PORFTF	PORFTF	5%
	PORMKT	90%
	Others	5%
PORMKT	PORFP	32%
	PORFTF	32%
	PORFF	32%
	Others	4%

For the single PT scenarios, the mean of the production type specific direct and indirect contact rates were weighted by the number of units of each production type, to obtain a general direct

and indirect contact rate equivalent to the average rate for the multiple PT scenarios (Table 2.3).

The infectivity of direct contacts was set to 90% and 60% for the high and low infectivity scenarios respectively, and 1.5% and 1% for indirect contacts (modified from Schoenbaum and Disney [31], using expert opinion). The infectivity and maximum distance of airborne spread at 1km was 1% and .5% , and 4km and 2km for the high and low infectivity scenarios respectively. Airborne infectivity was intentionally high, to incorporate the effect of local disease spread beyond known movements described by Green et al [73].

2.4.3 Disease states periods

For the multiple PT scenarios, disease periods were parameterized using a PT-specific rate based on published data [70-72] and expert opinion (Table 2.3). In most instances, the same disease parameters were used for PTs of equal or similar species. Hence, parameters are presented for all cattle, all swine and Ovine/Goat.

Some of the previously reported distribution periods were modified to avoid unfeasible values. For example, Bates el al [71] reported a Subclinical period of Normal(2.6, 1.1) for cattle, which has a 2.2% chance of sample negative values, so this distribution was re-parameterized to Pert(0,2.6,5.9).

To make the disease states between multiple PT and single PT scenarios comparable, mixture distributions of disease periods for the single PT scenarios were approximated by sampling the distributions of disease periods for each production type, weighted by the number of units of each production type. The resulting distributions were normalized using a Gaussian kernel density estimator (Figure 2.3).

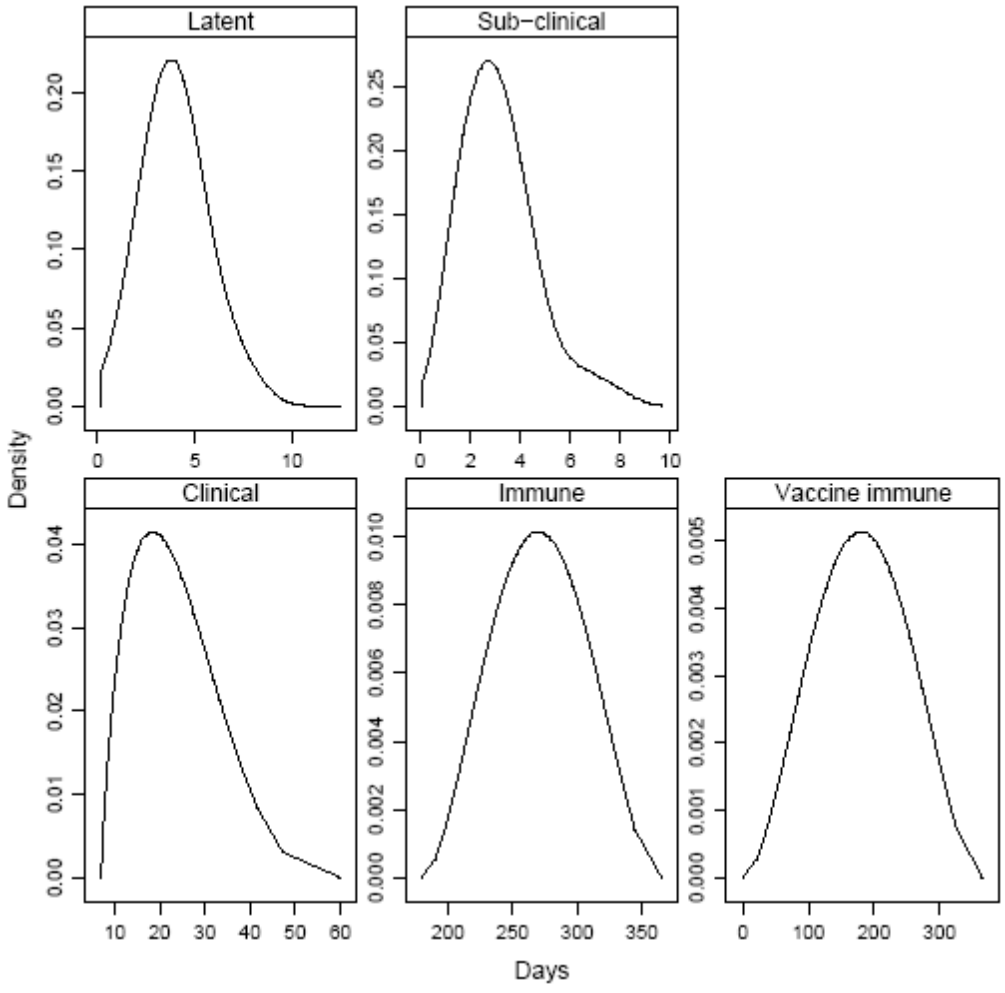

Figure 2.3. Disease states periods used in eight single production type scenarios simulating a hypothetical outbreak of foot-and-mouth disease in a Midwestern US state.

2.4.4 Disease detection and surveillance

The conditional probability of reporting a unit as positive given clinical signs (P_c), and the probability of reporting as a function of the days from the beginning of the outbreak (P_d) for each PT were specified based on expert opinion and previous studies [31]. For the single PT scenarios, compound estimates of the two probabilities of detection were derived by fitting a locally-weighted polynomial regression to the daily probabilities of detection for all the individual production types, with P_c starting at roughly 10% on the first day the herd exhibited clinical disease, 40% on day 5, and 100% by day 10. P_d was set to 20% on the first day of the outbreak, almost linearly increasing to reach 100% by day 60.

For all the scenarios, disease detection, surveillance, and tracing were allowed, and all traced direct contacts were destroyed with unlimited capacity. No ring slaughter was used.

2.4.5 Simulation and output analysis

As some scenarios were very computationally intensive, 300 Monte Carlo iterations were initially simulated for each scenario, based on convergence testing. Additional iterations were run for selected scenarios to reach convergence. The means and 95% prediction intervals (PI) for the cumulative total (epidemic size) and daily number of infected units, and the total outbreak length per scenario were tabulated and plotted. Since all scenarios started with one infected unit, an alternative calculation of the cumulative total number of infected units removing the index case was reported to provide a more realistic estimate of the 2.5% PI.

Given that the results are based on a simulation model where the variance on the input parameters and the sample size is controlled, no statistical analyses were performed to test for statistical significance on the model differences.

All the data manipulation, parameter estimation, spatial analyses, summary statistics, and figures were generated using the R statistical language [74].

3 Results

The units used in the heterogeneous spatial dataset presented significant clustering, as Ripley's K-function of the unit locations was significantly higher than that from a CSR simulation envelope (Figure 2.4)

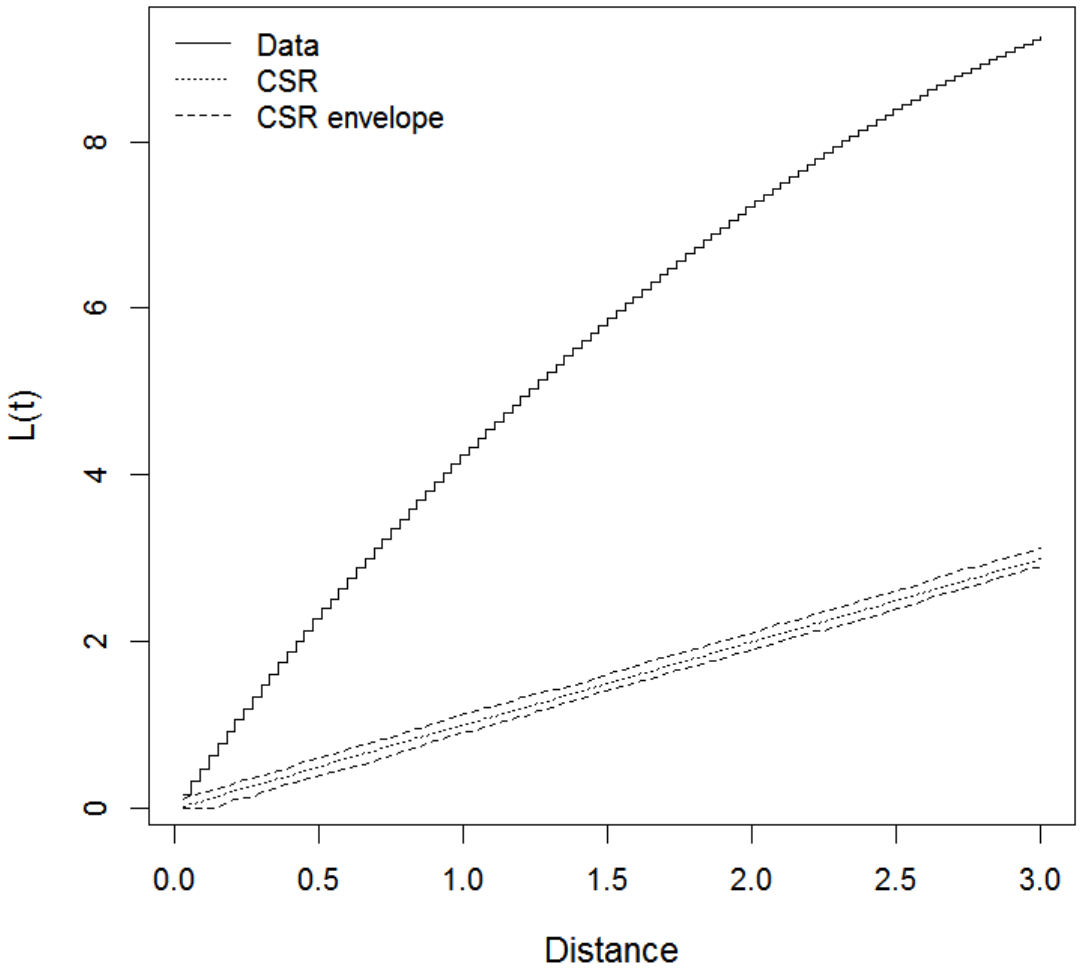

Figure 2.4. Cumulative distribution function of distances between point locations (Ripley's K-function) of actual population units in a Midwestern state in the US (Data), expected K-function from a Complete Spatially Random process (CSR), and simulation envelope of a Poisson CSR process (CSR envelope). Randomly distributed spatial point patterns should fall within the simulation envelopes.

The mean number of total infected units at the end of the outbreak was highest in scenarios combining multiple PTs, high infectivity, and no vaccination (5, 13), followed by equal scenarios that included vaccination (14, 6), and a scenario with multiple PTs, heterogeneous spatial

distribution, and no vaccination (7) (Table 2.5, Figure 2.5). Scenarios 8 and 1 presented similar results, with 196.6 (1.0, 626.1) and 193.2 (1.0, 1023.1) total infected units respectively, with only the heterogeneous spatial population as a common factor. The order above remained after removing the index case from the calculations, whereas the results were slightly modified for the scenarios with lowest total infected units (scenarios 3, 4, 11, and 12).

In some of the scenarios with the highest results, the 2.5th percentile of the total infected units at the end of the outbreak was largely increased when removing the index case (Table 2.5). For example, the 2.5th percentile for scenarios 5 and 6 increased from 2.0 to 1,718.3, and 1.0 to 1,172.8 respectively. In contrast, scenario 13 had the second highest mean total infected units (1,616.4), but the 2.5th percentile of the total infected units only went from 3.0 to 3.9 after removing the index case.

Most of the iterations of the 4 scenarios with the highest cumulative number of infected units predicted large outbreaks, with only a few iterations predicting small outbreaks, or no outbreaks beyond the index case (Figure 2.5).

Table 2.5. Total animal production units infected with a hypothetical outbreak of foot-and-mouth disease in a Midwestern US state, under different assumptions of spatial population distribution, population heterogeneity, infectivity, and vaccination (sorted by total mean infected units, including index case).

Scenario ID	Total infected units mean (95%PI)	Total infected units mean (95%PI) Index case removed	Scenario Spatial/Pop/Inf/Vacc
5	1725 (2, 1836)	1751 (1718, 1836)	He/M/Hi/N
13	1616 (3, 1779)	1649 (4, 1779)	Ho/M/Hi/N
14	1414 (2, 1629)	1450 (12, 1629)	Ho/M/Hi/V
6	1314 (1, 1614)	1362 (1173, 1615)	He/M/Hi/V
7	546 (1, 1195)	590 (4, 1200)	He/M/Lo/N
8	197 (1, 579)	215 (2, 586)	He/M/Lo/V
1	193 (1, 680)	211 (2, 698)	He/S/Hi/N
15	106 (1, 342)	115 (3, 359)	Ho/M/Lo/N
2	104 (1, 367)	118 (2, 375)	He/S/Hi/V
16	74 (1, 262)	78 (3, 263)	Ho/M/Lo/V
9	72 (1, 318)	81 (2, 323)	Ho/S/Hi/N
10	51 (1, 221)	58 (2, 226)	Ho/S/Hi/V
3	10 (1, 38)	13 (2, 38)	He/S/Lo/N
11	10 (1, 42)	12 (2, 44)	Ho/S/Lo/N
4	10 (1, 45)	13 (2, 49)	He/S/Lo/V
12	8 (1, 33)	11 (2, 36)	Ho/S/Lo/V

[†] *He*: Spatially heterogeneous, *Ho*: Spatially homogeneous, *S*: Single Production Type, *M*: Multiple production types, *Hi*: high infectivity, *Lo*: low infectivity, *N*: no vaccination, *V*: vaccination.

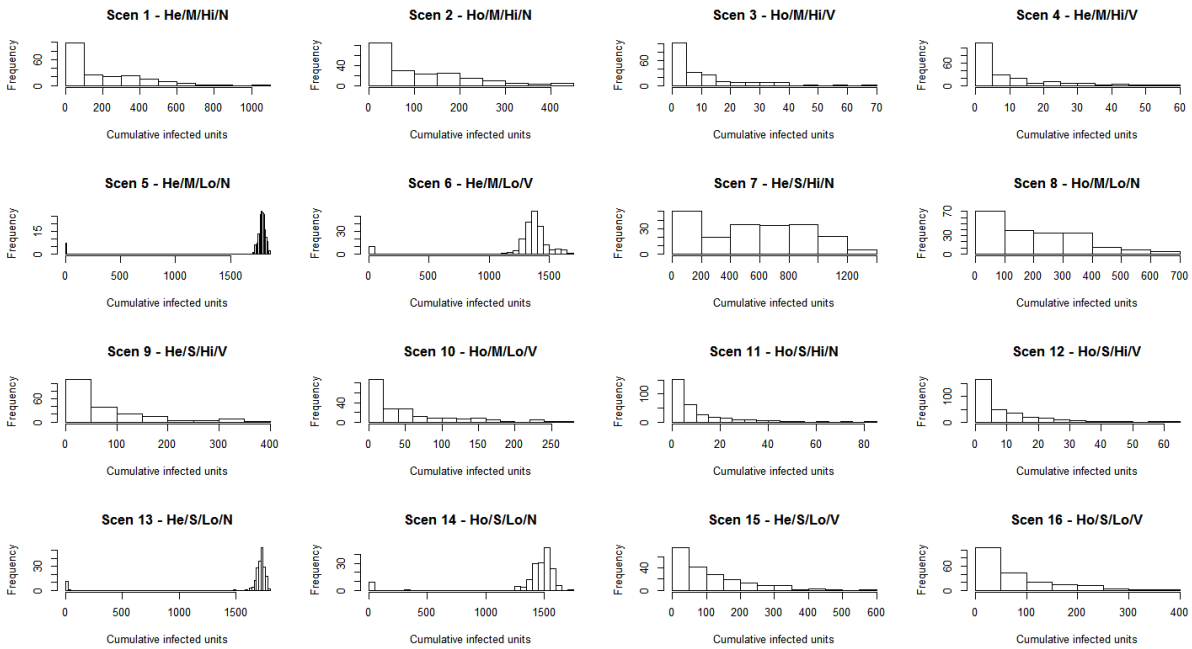

Figure 2.5. Total animal production units infected with a hypothetical outbreak of foot-and-mouth disease in a Midwestern US state, simulated under 16 scenarios with different assumptions of spatial population distribution (*He*: Spatially heterogeneous, *Ho*: Spatially homogeneous), population heterogeneity (*S*: Single Production Type, *M*: Multiple production types), infectivity (*Hi*: high infectivity, *Lo*: low infectivity), and vaccination (*N*: no vaccination, *V*: vaccination).

The cumulative daily number of infected units followed a similar pattern, with scenarios with multiple PTs and high infectivity exhibiting rapidly spreading outbreaks reaching between 1200 and 2000 infected units by day 200 (Figure 2.6.a), and smaller, slower spreading outbreaks for the scenarios with single PTs and low infectivity (Figure 2.6.b). In general, when everything else was held constant, vaccination reduced the mean number of daily and total infected units

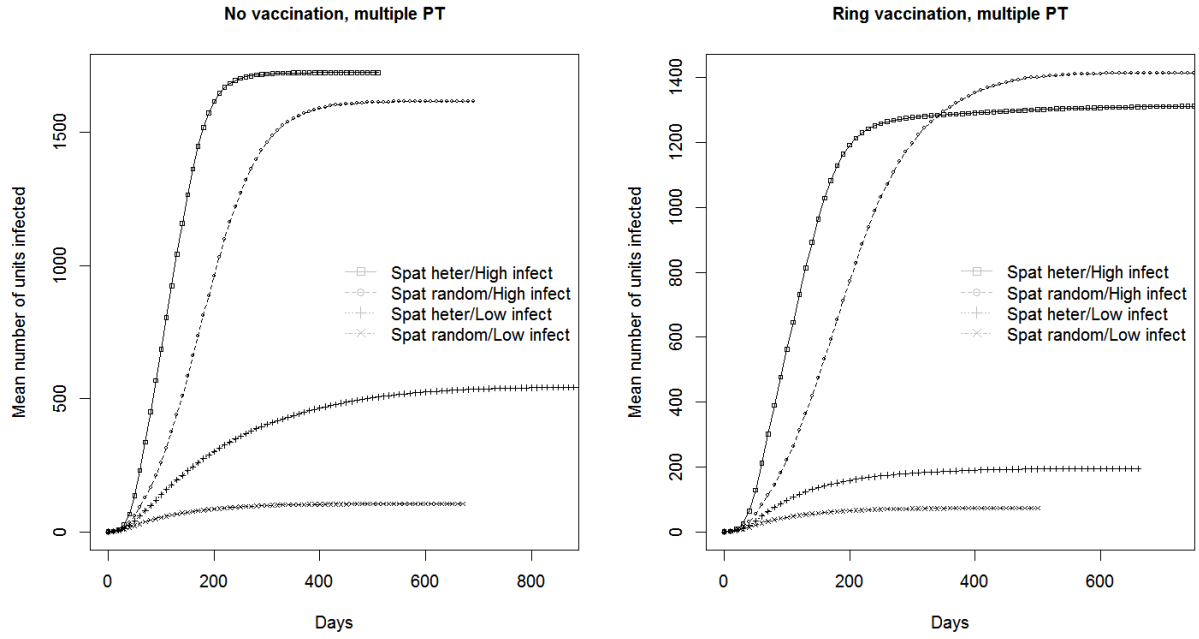

a

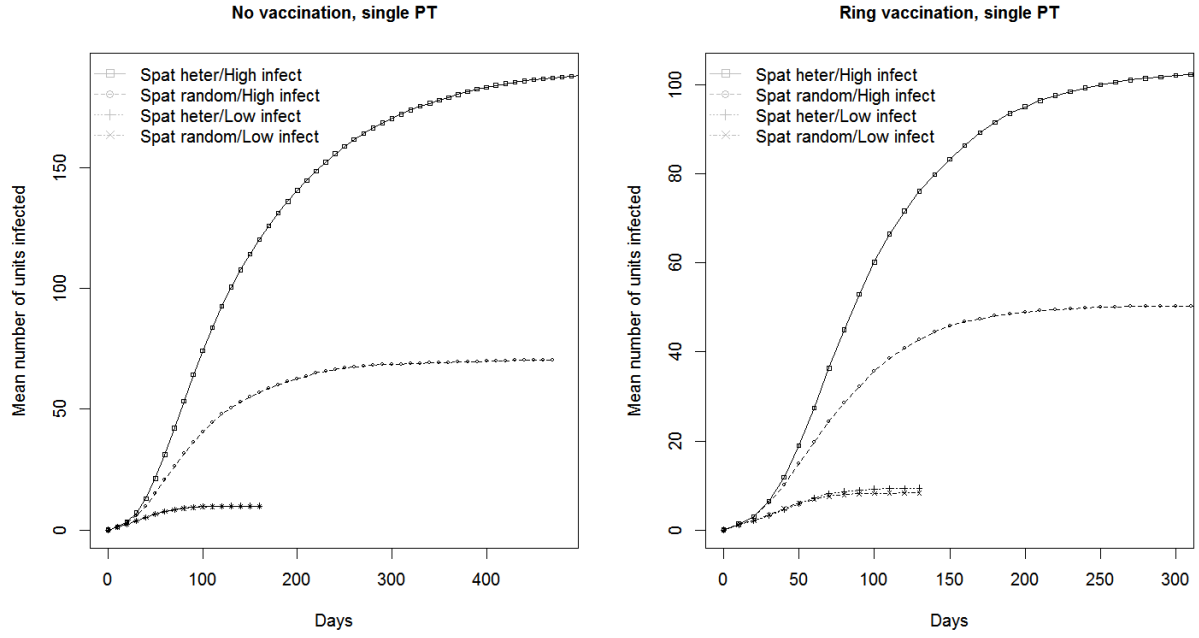

b

Figure 2.6. Mean cumulative number of infected animal production units per day for a hypothetical outbreak of foot-and-mouth disease in a Midwestern US state. Scenario with multiple animal production types (a), and single animal production types (b).

The total outbreak length (Figure 2.7) varied widely, with the longest outbreaks observed in scenarios with multiple PTs (scenarios 5-8, and 13-16), and the shortest outbreaks observed in scenarios with low infectivity and no vaccination. Scenarios 13, 7, and 14 exhibited the overall longest mean outbreak lengths, lasting 422 (12, 800), 415 (24, 625), and 457 (13, 820) respectively, whereas scenarios 12, 4, 11, and 3 each lasted only 46 (10,109), 50 (10, 129), 49 (10,120), and 51 (10, 132) days (Figure 2.7).

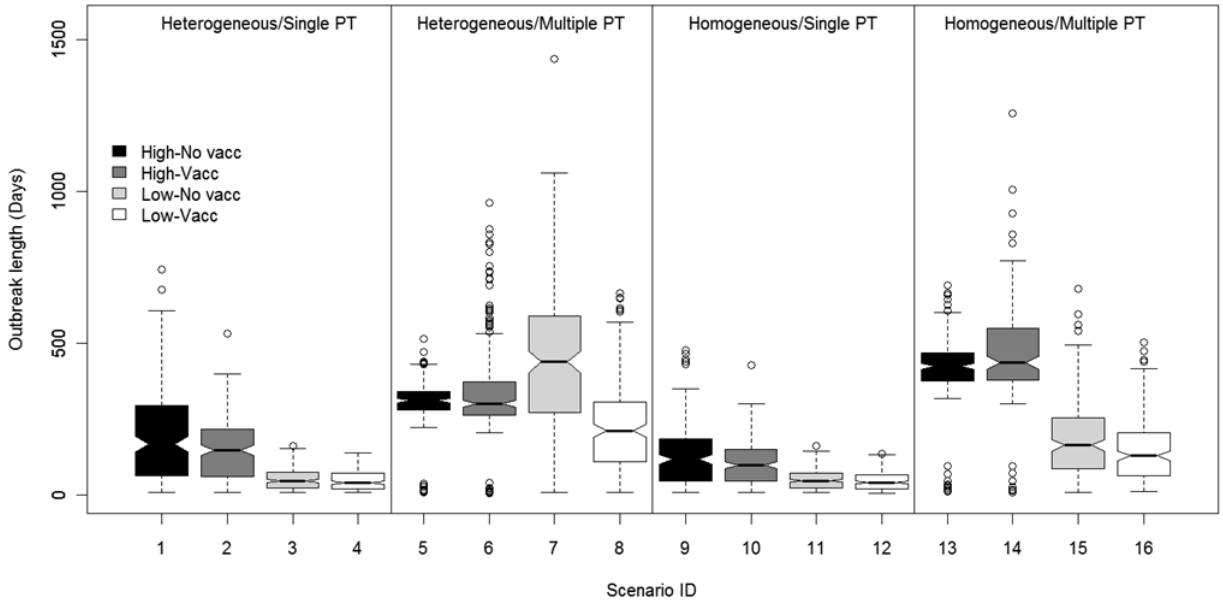

Figure 2.7. Box-and-whiskers plot of total outbreak length for 16 scenarios of a hypothetical outbreak of foot-and-mouth disease in a Midwestern US state. The notches provide an approximate 95%CI (i.e. no overlap provides strong evidence that the medians differ). The center line is the median, the box height shows the inter-quartile range, and the whiskers show the most extreme observation within 1.5 times the inter-quartile range.

4 Discussion

The purpose of this study was to understand the potential role of population, contact, and spatial heterogeneity in the predictions of models for the spread of infectious animal diseases used in animal health policy. For this, several parameterizations of a mechanistic model were

used to isolate the effect of population, contact, and spatial heterogeneity in epidemic size and length, while considering the effect of infectivity and vaccination strategies.

The six scenarios with the highest mean cumulative number of infected units at the end of the outbreak corresponded to parameterizations of the model assuming population and contact heterogeneity (multiple PT), whereas the six scenarios with the lowest number of infected units included single PT and homogeneous contact rates.

Our findings suggest that in our model, the heterogeneity in populations and their respective contact structure has a significant implication in model predictions regardless of the scenarios evaluated, whereas spatial heterogeneity may only have an impact in model predictions under specific disease assumptions.

Differences observed across scenarios

Our findings of consistently larger outbreaks for the scenarios including heterogeneity in the populations and their respective contact rates agree with other studies exploring the effects of contact rates in model predictions. For example, Dickey et al. [67] used a complex mechanistic model to explore the effect of operation-specific contact rates in the prediction of epidemic size, duration of epidemic, and relative risk of infection, and found that models with weighted-average homogeneous contact parameters predicted fewer infected premises. Cook et al.[75] estimated multiple transmission rates from data from a fungal plant pathogen affecting two plant species and concluded that ignoring multiple transmission rates could largely

underestimate the rate of disease spread, but in the same study also some scenarios with multiple transmission rates underestimated the rate of disease spread. In contrast, Brauer [57] compared a simple non-spatial SIR model with one and two populations using weighted averages for the one population model, and found the final epidemic size of both scenarios to be comparable, but still advocated the use of two populations to enable the evaluation of group-specific treatment strategies. However, the authors used a simple SIR model that did not take into account complex population and spatial contact interactions, thus his results are not directly comparable to ours.

Scenarios with high infectivity always yielded bigger outbreaks than comparable scenarios, with lower infectivity. This is consistent with our parameterization as on average, the low infectivity scenarios required roughly 1.5 contacts for every 1 infectious contact in the high infectivity scenario. As expected, ring vaccination also considerably reduced outbreak sizes when compared to identical scenarios without vaccination.

In the scenarios simulating fast spreading epidemics with heterogeneous populations and contact structure (scenarios 5 and 6), knowing the actual spatial location of population units did not provide more predictive accuracy than a simplified model with randomly generated herd locations (scenarios 13 and 14). Several factors could explain this effect, but the most obvious is that for the fast spread scenarios, the effect of population and contact heterogeneity may have overwhelmed the incremental spread created from using actual unit locations that we observed in the lower spread scenarios. In other words, the spread occurred quickly and strongly,

regardless of the clustering of the units. Also, even though we randomly allocated population units, we explicitly modeled the spatial spread of disease (see contact and distance parameters). The importance of modeling the spatial dynamics of disease spread is well documented [54, 58-59, 76], so our findings only suggest that while the spatial component is relevant, having exact population unit locations may not be necessary under certain conditions of disease spread and parameters. Tildesley et al.[35] used a spatially explicit model to evaluate the level of spatial detail required to determine optimal ring vaccination strategies, and found that using herds randomly generated (without spatial clustering) from aggregate US county-scale data was sufficient to closely determine optimal ring culling strategy, and did not significantly modify the prediction of epidemic size when compared against a fully spatial model containing representative herd locations. Although the approach used was different from ours (spread based on spatial kernel vs. our explicit simulation of movements) and relied on the reparameterization of the candidate models to standardize the results, their findings are in line with ours.

Potential relevance to animal health policy

Epidemiological models are commonly used to evaluate disease control and eradication policies and for contingency planning [77]. Yet, the general validity of different modeling approaches is seldom compared [60].

The study described here does not attempt to validate the examined models against real outbreak data, nor does it attempt to make realistic predictions of future disease outbreaks.

Therefore, our findings cannot be used to directly conclude the superiority of the more complex parameterizations of the model to inform policy. However, as the heterogeneous population model provides a more realistic scenario of the dynamics of disease spread in a complex agricultural setting, it would be reasonable to assume that this model could be used as a "gold standard" for the comparisons made here. That is, if the simpler models provided predictions similar to those from the complex model, it would be difficult to advocate the use of a complex model for the purpose of disease prediction, but the meaningful differences between the models reported here, even after adjusting for many potential effect modifiers such as spatial heterogeneity, infectivity rates, and vaccination strategies can be interpreted as an indication that population and contact structure heterogeneity are important to be incorporated in epidemic models used for disease policy.

Heterogeneity in the modeled populations can also be important for informing policy, as many disease control programs target high risk and/or "super-shedder" individuals [(78)], thus these populations must be explicitly modeled to understand the impact of mitigation strategies. For example, Longini et al. [(79)] concluded that treating the highest risk population with antiviral prophylaxis during a pandemic influenza outbreak was almost as effective as vaccinating 80% of the entire population modeled. Such findings have resulted in the so called "20/80 rule" which suggests that roughly 20% of the most infectious individuals in a population are responsible for 80% of the disease transmission [(78)].

Our results could provide useful information for focusing data collection efforts and for the design of models used to inform health decisions. The most relevant finding was that for fast spreading epidemics with heterogeneous populations and contact structure, knowing the actual spatial location of population units did not provide more predictive accuracy than a simplified model with randomly generated herd locations. This suggests that when modeling fast spreading diseases such as certain variants of FMD or African Swine fever, knowing the location of population units may not provide more accurate information for policy and contingency planning purposes (i.e. in a country free of the disease). Nonetheless, knowing unit locations during an outbreak would be relevant not only to model the disease spread in real time, but also for epidemiological investigations such as tracing activities [47].

In contrast, for diseases with lower infectivity and heterogeneous populations and contact structure, ignoring the real spatial location of population units (scenarios 15 and 16) may result in predicted epidemic sizes of as little as 19% of that predicted using actual spatial locations (scenarios 7 and 8). Nonetheless, these differences disappear in similar scenarios with single PT (scenarios 3, 4, 11, and 12).

Study limitations

The parameters used for the scenarios simulated may or may not be representative of the real contact and disease rates in the US livestock industry, as they are mostly based on published parameters for a region in California [70-72] and for a hypothetical FMD outbreak in the US [31]. However, the emphasis of this study was to provide a consistent comparison across scenarios,

while using reasonable parameters. Sensitivity analyses (results not shown) reveal that the model results are very sensitive to relatively small changes in the contact and infectivity parameters used, suggesting that special efforts should be placed in the proper estimation of these parameters when models are to be used for health policy support.

Given the computationally intensive model we developed for this study, only 300 iterations were used for most scenarios. Although convergence testing showed that number to be sufficient, running more iterations may have provided more precise estimates for the scenarios with the smallest spread. However, the differences between scenarios seemed very apparent, suggesting that more iterations may not have changed our main findings.

The model includes many parameters not usually available in other models used for policy, such as tracing activities, on-farm detection, and surveillance. Although these factors were kept constant across scenarios, our results may not directly apply to simpler models, as they may have had an intrinsic effect in our predictions. For example, the effect of disease detection and surveillance, and the resulting culling of animals may have reduced the total epidemic size and length when compared to SIR models without such parameters.

Conclusions

Our results suggest that for a fast spreading epidemic, ignoring heterogeneity in the populations and their respective contact rates greatly underestimated the total outbreak size, whereas using randomly generated population locations rather than actual herd locations had a

limited to nil effect in the final epidemic size. In contrast, when modeling a slower spreading disease with population and contact heterogeneity, ignoring actual herd locations may also underestimate the outbreak size.

In conclusion, in models used to inform health policy and planning, knowing the actual population units (e.g. herds) locations may not be as relevant as understanding the number of unit types and their contact structure when modeling fast spreading epidemics. In contrast, both population and spatial heterogeneity seems to be relevant when modeling slower spreading epidemic diseases. Our findings may provide useful information to prioritize data collection and model building efforts.

CHAPTER 3: DISEASE SPREAD MODELS TO ESTIMATE HIGHLY UNCERTAIN EMERGING DISEASES LOSSES FOR ANIMAL AGRICULTURE INSURANCE POLICIES: AN APPLICATION TO THE U.S. FARM-RAISED CATFISH INDUSTRY[4].

Preface

As discussed in chapter 1, and shown with simulation experiments in chapter 2, the level of structural complexity in a model is dependent among other things, on the epidemiology of the disease modeled, and the level of granularity expected from its results. In this chapter I present a structurally complex set of epidemiological models that were designed to answer a challenging question; what would be the potential inventory losses at the pond, farm, and regional level in case of a new emerging disease affecting catfish in an intensive production environment? The ultimate goal was to provide estimations of losses that could be used within an actuarial framework to calculate disease insurance premiums for catfish producers. The uncertain nature of the new disease to be modeled, and the uncertainty in the frequency of future disease occurrences motivated the use of the detailed epidemiological model described in this chapter.

[4] Article formatted and submitted to the Risk Analysis journal.

Summary

Emerging diseases (ED) can have devastating effects on agriculture. Consequently, agricultural insurance for ED can develop if basic insurability criteria are met, including the capability to estimate the severity of ED outbreaks with associated uncertainty. The U.S. farm-raised channel catfish (*Ictalurus punctatus*) industry was used to evaluate the feasibility of using a disease spread simulation modeling framework to estimate the potential losses from new ED for agricultural insurance purposes. Two stochastic models were used to simulate the spread of emerging diseases between and within channel catfish ponds in Mississippi (MS) under low, medium, and high disease impact scenarios. The mean (95%PI) proportion of ponds infected within disease-impacted farms was 7.6% (3.8%, 22.8%), 24.5% (3.8%, 72.0%), and 45.6% (4.0%, 92.3%), and the mean (95%PI) proportion of fish mortalities in ponds affected by the disease was 9.8% (1.4%, 26.7%), 49.2% (4.7%, 60.7%), and 88.3% (85.9%, 90.5%) for the low, medium and high impact scenarios respectively. The farm-level mortality losses from an ED were up to 40.3% of the total farm inventory and can be used for insurance premium rate development. Disease spread modeling provides a systematic way to organize the current knowledge on the emerging disease perils and, ultimately, use this information to help develop actuarially sound agricultural insurance policies and premiums. However, the estimates obtained will include a large amount of uncertainty driven by the stochastic nature of disease outbreaks, by the uncertainty in the frequency of future ED occurrences, and by the often sparse data available from past outbreaks.

1 Introduction

International trade and movement of live animals represent a major route of disease introduction to new areas in the world [80]. Furthermore, many emerging diseases (ED) are believed to come from pathogens that are already present in the environment and become important due to changing factors that alter the natural equilibrium of the disease agent in the environment [81].

ED can greatly impact animal agriculture. For example, the 2001 outbreak of Foot and Mouth disease (FMD) in the UK alone resulted in £3.1B (US$4.8B) in losses to agriculture and the food chain [82]. Insurance can be a relevant strategy to manage the risk of disease in agriculture, as it allows the producer to transfer the risk of ED losses to an insurer, in exchange for a fee [83]. Insurance including coverage for ED could develop if basic insurability criteria are met, including the capability to estimate the severity of ED outbreaks with associated uncertainty.

Conventional empirical methods are of limited use to estimate the impact of new ED since outbreak data are usually scarce and/or may not be relevant to the new disease. Hence, the feasibility of alternative methods to quantify the impact of ED should be further explored. Disease spread models (DSM) mimic the dynamics of disease spread in populations, and have been extensively applied to a variety of human and animal diseases [7, 84]. DSM can allow for the inclusion of variability in the model predictions and uncertainty in the model structure and accompanying estimates used to parameterize the model [7], making them potentially suitable to calculate impact from ED for which knowledge is limited. DSM have been proposed to

estimate disease impact for both human [85] and livestock agricultural insurance [86], but have not been applied for ED insurance in specific sectors such as aquaculture. Authors exploring the actuarial applications of deterministic DMS suggested that stochastic DSM could provide a more generalized and pragmatic alternative to actuarial applications [85].

There are several examples of ED affecting aquatic animals: Taura Syndrome Virus, an infectious disease agent of shrimp, was originally transmitted to Taiwan from live shrimp imports from Ecuador in the late 1990s, and then further spread throughout Asia [87]. Koi Herpes Virus (KHV) has spread in cyprinid species throughout the world due to international trade and international shows of ornamental fish [88]. In the last two decades, the farmed channel catfish populations have been exposed to emerging diseases such as Visceral Toxicosis of Catfish (VTC), digenetic trematode infestations, and Proliferative Gill Disease (PGD) [89-91]. Also, the farmed salmonid industry has experienced the emergence of a variety of diseases such as Piscirickettsiosis, Infectious Salmon Anemia, and Sea lice [92-94].

Aquaculture producers and researchers have identified disease as the peril of greatest economic concern for several aquaculture industries, including the U.S. farm-raised catfish (*Ictalurus punctatus*) industry [83]. However, the authors of this article are unaware of government-backed insurance policies available to protect U.S. catfish producers from economic losses due to a disease outbreak.

The aim of this study is to evaluate the feasibility of using disease spread models to estimate the magnitude of new ED outbreak losses on a farm level for animal agriculture insurance

policies. The U.S. farm-raised catfish industry was used as an example for the application of this approach.

2 Materials and methods

For insurability purposes, the direct impact of an ED outbreak in a livestock facility such as a farm or aquaculture site is proportional to the total number of animals affected by the outbreak and the severity (i.e. mortality) of the disease outbreak. Impacts such as production losses due to non-covered mortality events or other causes, and loss of marketability of surviving animals are often not considered insurable. The ED impact is influenced not only by the disease agent, but also by the management practices at the facility and the characteristics of the animal population. Animal holding facilities are often comprised of sub-populations of animals such as in separated poultry houses, corrals, or ponds. Therefore, to quantify the ED losses it is necessary to estimate the disease spread between and within such sub-populations. The framework presented here utilizes the U.S. farm-raised catfish industry as an example of using models that simulate the spread of an ED outbreak to quantify the expected total number of animals affected by the outbreak in any given farm.

2.1 Insurability framework

Insurability criteria such as those proposed in Table 3.1 (adapted from Coble et al. [83]) should be considered to evaluate the applicability of the modeling estimates of the expected farm-level loss from an ED. For example, it must be assumed that management practices that reduce the risk or prevent losses for an emerging disease are either non-existent (i.e. new/poorly

understood emerging disease) or not easily applied to the disease affected area (e.g. vaccination is not possible, treatment not approved in the country). Also, attributing death losses to a single disease when other diseases are present can be difficult, unless ED outbreaks are confirmed by the competent authority using recognized diagnostic tests. For this study, it is assumed that the losses are only caused by the ED under investigation, as typically ED outbreaks are confirmed by the competent authority using recognized diagnostic tests. Insurers often pool policies to reduce the variability of losses in their overall policy portfolio [(83)]. However, the standard methods used to model pooled policies can only be applied when the elements pooled (e.g. farms holding individual policies) are sufficiently uncorrelated. As infectious disease outbreaks can often cluster in a region, DSM can be used to calculate pooled estimates while taking into account clustering. The farm-level risk classification for ED could be evaluated considering management and biosecurity practices (e.g. all-in/all-out management, stocking density, mortality removal), that are known to mitigate the introduction and spread of infectious diseases, and could then be used to adjust the premium rate accordingly. Such classification is beyond the scope of this work, but risk factors could be established with observational epidemiological studies. For the purpose of this study it is assumed that the ED modeled satisfy all insurability criteria.

Table3.1. Suitability of disease simulation modeling of an emerging disease in meeting Insurability Criteria for Aquaculture Diseases.

Insurability criteria questions	Answer for an emerging disease and epidemic model predictions	Satisfies criteria?
Determinable loss		
Are losses caused from single disease alone?	Most likely	Most Likely
Is this the primary cause of loss?	Most likely, but all other causes must be ruled out	Most Likely
Measurable loss		
Does the disease cause acute losses?	ED must cause acute losses so they could be easily enumerated	Unknown
Accidental and unintentional		
Are the probabilities of getting these diseases conditioned on management?	Possibly, unless ED is poorly understood	Yes
Are there available control measures to prevent the disease outbreak?	No method to prevent until disease is well understood	Yes
Are there available control measures to mitigate the severity of the outbreak?	There may be minimal control methods outside of standard biosecurity and management practices	Most likely
Sufficient information to conduct risk classification		
Within a region is one farm more prone to this disease than another farm?	Unknown	Unknown
Is the disease endemic or exotic?	Exotic	Yes
Between two regions can one farm be more prone to this disease than another farm?	There may be regional and production differences. The epidemic model takes this into account	Unknown
How contagious is the disease between pond-raised catfish?	The epidemic model takes this into account	Unknown
Sufficient data to establish accurate premium rates		
Can we estimate the frequency of losses from this disease?	Difficult to estimate given emerging pattern of disease	Not at this time, scenario analyses used
Can we estimate the magnitude of losses from this disease?	The epidemic model estimates this value	Yes, through this modeling exercise
Losses sufficiently uncorrelated to allow for pooling		
Are losses largely idiosyncratic or systemic?	Unknown	Unknown
Are there factors that may affect the frequency of occurrence over time?	Unknown	Unknown
Will future outbreaks be more probable after the first outbreak occurs?	Unknown	Unknown

The anticipated *loss cost* is the expected exposure that an insurer would have related to a payout for any given farm. That is, the expected total cost of fish mortalities in foodsize fish ponds due to an ED in a given farm in a year period. Thus, the loss cost for an emerging disease can be defined as:

$$LC_{ed} = Np_i\lambda_f\, p_m c\lambda_{ed} \quad (1)$$

Eq. 1 shows that the expected loss cost from emerging diseases LC_{ed} depends on the number of ponds in a farm *N*, the proportion of infected ponds on an infected farm p_i, the mean number of foodsize fish per pond λ_f, the proportion of mortalities p_m that occur within an infected pond, the cost per fish *c*, and the mean yearly frequency of covered ED infections in the farm λ_{ed}.

The total number of ponds in the farm *N* can be assumed as known at the time the loss cost is estimated. Likewise, the mean number of food size fish per pond λ_f and the cost per fish *c* could be available or estimated from production records, and there would be expected variations from pond to pond. Such variation could be accounted for by calculating a loss cost function for different population strata (e.g. ponds ready to harvest vs. young stock). As *c* would be accessible to the insurer but highly variable over time and regions, it is excluded from the results reported hereafter, but this value could be readily incorporated when calculating the loss cost.

The three parameters p_i, p_m, and λ_{ed} are uncertain as they depend on the epidemiological characteristics of the ED. Thus, two disease spread models were used to estimate p_i and p_m. p_i was estimated using a model that simulated the spatial and temporal spread of a hypothetical transmissible disease between ponds in the region, and p_m was estimated using a separate model that simulated the disease spread and mortality within infected ponds. Both models were stochastic and incorporated variability in the prediction, and uncertainty in their parameters; therefore their results were probability distributions obtained via Monte Carlo simulations. The models provide results at the individual pond and farm level, offering the potential for detailed farm and regional-level analyses. For illustration purposes, the analysis presented in this article uses only the arithmetic means from the simulated values from p_i and p_m in the loss cost calculation, as they represent the expected value of the losses and thus are influenced by the variability and uncertainty in the models predictions. Further details on the models are described in the next sections.

Finally, using historical records of catfish disease emergence to estimate λ_{ed} would assume that the historical rate of disease emergence is a valid estimate of future disease emergence, so instead the effect of λ_{ed} in the estimation of farm-level inventory losses is evaluated via scenario analysis.

The estimated loss cost for the emerging disease LC_{ed} could then be incorporated into a total loss cost estimate for all potential payouts.

$$LC_t = LC_{ed} + \sum LC_p \tag{2}$$

The total estimated loss cost LC_t (Eq. 2) is the estimated mean loss cost from emerging diseases LC_{ed} plus the estimated expected loss costs from all other perils LC_p named in the policy. Finally, the estimated premium rate (excluding overhead and profit margin) for the insurance product can be calculated as:

$$PR = LC_t - d \tag{3}$$

The premium rate *PR* is the estimated total loss cost LC_t minus the deductible *d* (Eq. 3).

This article focuses on the estimation of the farm-level inventory losses (i.e. p_i, p_m) using the DSM methods described hereafter.

2.2 Models for the spread of diseases in farmed catfish populations

Two DSM for the spread of a hypothetical ED in farm-raised catfish populations were developed. The first model simulated the spatial and temporal spread of a transmissible disease between ponds, and the second model simulated the spread of the disease within infected ponds. The models were used to estimate p_i and p_m respectively. Foodsize fish producing farms are the target population for potential insurance products and thus used in LC_{ed}. However, the disease spread was simulated for both foodsize and fingerling catfish as both populations are likely to participate in the transmission of an emerging disease outbreak. Only the simulation results for foodsize fish producing farms are reported.

A meeting with fish disease experts was held to identify the key scenarios and parameters needed to model emerging diseases in aquaculture, including a definition of a representative hypothetical emerging disease to develop the models (further description in parameters estimation and data sources section). The resulting models were based on a hypothetical infectious disease that could be transmitted between and within ponds horizontally via direct contact (e.g. stocking of fingerling into foodsize fish ponds), or indirect contacts (e.g. vehicles, equipment transfer). The disease was detected only by clinical signs (i.e. mortalities) and since the natural occurrence of a new emerging disease was modeled, no interventions (vaccination, quarantine, etc.) on the detected ponds were modeled. However, both models currently accommodate such interventions and could be used for the evaluation of further scenarios.

2.2.1 Model for the spread of disease between ponds (between-ponds model)

A spatial, pond-based, discrete-time, state-transition stochastic model to simulate the spread of an ED between ponds was implemented in Delphi 7[5]. The basic model structure was similar to that of a previously described model [(31)], but also accommodated for multiple farm types (fingerling vs. foodsize) and for the stratification of ponds within farms so the proportion of infected ponds on an infected farm p_i could be estimated. The pond was the individual unit, and had attributes that changed in daily time steps. The attributes of the pond included the number of fish (inventory on hand), the farm type (predominantly fingerling or foodsize), the spatial

[5] Embarcadero Technologies, Inc., San Francisco, California, USA

location (geographical coordinates), and the disease state of the pond (Susceptible, Exposed, Infected, Immune).

When the pond received a successful direct or indirect contact (contact that resulted in infection) it was considered exposed (but not yet infectious). The pond became infected (and infectious) after time γ_e once the fish in the pond started shedding the agent. The pond became immune after infection. After a number of days γ_i, an immune pond could become susceptible again (Figure 3.1).

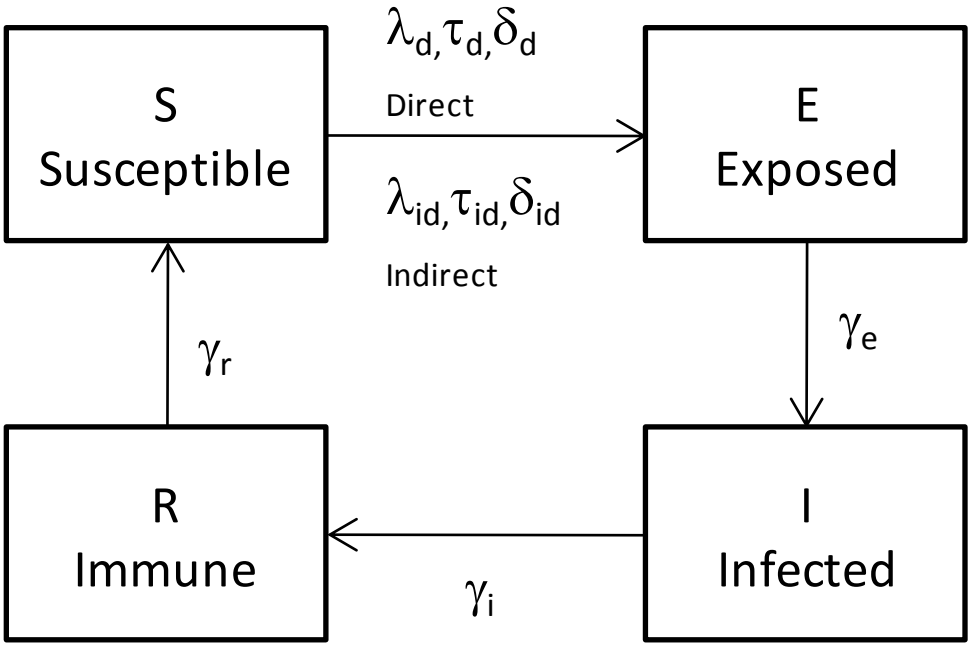

Figure 3.1. A spatially explicit, pond-based, discrete-time, state-transition stochastic model to simulate the spread of an ED between ponds of farmed-raised catfish.
Transitions between states are represented as arrows. Ponds transition from susceptible (S) status to exposed (E) after a successful direct or indirect contact determined by $\lambda_d, \tau_d, \delta_d$ and $\lambda_{id}, \tau_{id}, \delta_{id}$ respectively, from E to infected (I) after γ_e days, from I to immune (R) after γ_i days, and may again become S after γ_r days. Parameters above are randomly sampled from probability distributions.

For each infected pond, the lengths of disease periods (at the pond level) were sampled from Pert distributions (Table 3.2), with minimum, mode, and maximum parameters listed in the parameter estimation and data sources section). A dead state was not considered since mortalities were modeled at the fish level with the more detailed intra-pond model. No intervention strategies such as vaccination and treatments were included since the intention was to simulate the course of the outbreak without interventions.

Table 3.2. Relevant parameters used in three scenarios simulating the spread of a new emerging disease between farmed catfish ponds in Mississippi.

Category	Parameter	Name	Low scenario	Medium scenario	High scenario	Source
Disease duration (days)	γ_e	Exposed	*Pert(0,1,2)*	*Pert(0,1,2)*	*Pert(0,1,2)*	Expert[1]
	γ_i	Infectious	*Pert(0,100,300)*	*Pert(0,100,300)*	*Pert(0,100,300)*	*Expert*
	γ_r	Immune	*Pert(182,300,365)*	*Pert(182,300,365)*	*Pert(182,300,365)*	*Expert*
Movements (days)	λ_d	Direct contact rate	*Poisson(0.02)*	*Poisson(0.025)*	*Poisson(0.03)*	*Expert*
	τ_d	Direct probability of infection transfer	*1*	*1*	*1*	*Expert*
	δ_d	Direct distance	*Uniform(0,300)*	*Uniform(0,300)*	*Uniform(0,300)*	*Expert, spatial dataset*[2]
	λ_{id}	Indirect rate	*Poisson(0.8)*	*Poisson(1)*	*Poisson(1.1)*	*Expert*
	τ_{id}	Indirect probability of infection transfer	*0.01*	*0.025*	*0.035*	*Expert*
	δ_{id}	Indirect distance	*Exponential(1)*	*Exponential(1)*	*Exponential(1)*	Spatial dataset[2]

[1]Estimates derived from the expert elicitation meeting.
[2]Estimates from spatial population dataset of ponds.

The spread of the disease between ponds was modeled by direct and indirect movements. A direct movement was a fish transfer from fingerling ponds to foodsize fish ponds. Indirect movements were all the other movements that could potentially transfer the infection from one pond to another, for example movement of equipment (e.g. seine nets), accidental movement of fish from pond to pond (e.g. bird predation), water transfer from pond to pond (e.g. hill ponds), and personnel.

The daily number of direct *kd* and indirect *ki* contacts from each infected pond was:

$$\begin{aligned} kd_{ij} &= Poisson(\lambda_d) \\ ki_{ij} &= Poisson(\lambda_{id}) \end{aligned} \quad (4)$$

That is, for each *i* infected pond on each *j* day a movement was randomly sampled from a Poisson distribution with direct and indirect contact rates λ_d and λ_{id} respectively. Eq. 4 could be simplified to *Poisson*(λ_{id}+ λ_d), but was separated to take into account the different infectivity (probability of infection transfer to susceptible recipient pond given an infective contact) from direct and indirect contacts (τ_d and τ_{id} respectively). The distance of each direct δ_d and indirect δ_{id} contact was sampled from a Uniform and Exponential probability distribution respectively (Table3.2) and the susceptible pond closest to the distance sampled was identified as the recipient of the contact. The infection transfer (transition from S $\rightarrow$E) was modeled as *Bernoulli*(τ_d) and *Bernoulli*(τ_{id}) for each direct and indirect contact respectively. As the sum of *n* Bernoulli trials with equal probability p is *Binomial*(*n*, *p*) the incidence of all newly infected ponds on any given *j* day can be summarized as:

$$I_j = Binomial(kd_{ij}, \tau_d) + Binomial(ki_{ij}, \tau_{id}) \quad (5)$$

A fingerling pond was randomly infected, and was used as seed to start each simulation and the simulation was run for a year. As the model was very computationally demanding, 300 iterations were used based on tests for convergence of E[p_i]. Histograms were used to visualize the distribution of the total numbers of ponds affected at the end of the outbreak, and the proportion of the cumulative number of ponds affected in infected farms at the end of the outbreak. The mean proportion of the cumulative number of ponds affected in infected farms E[p_i],was used in the farm-level inventory loss calculation, as the expected value is influenced by the variability and uncertainty in the estimates and can be readily added to the expected loss costs from all other perils LC_p named in the policy.

2.2.2 Model for the spread of disease within ponds (Intra-pond model)

A stochastic, continuous-time state transition model that simulates the spread of an infectious disease between fish in ponds was implemented in the R statistical language [(74)]. The model follows the principles of the density-dependent (individual contact rate is proportional to population size) Susceptible-Infectious-Recovered (SIR) Kermack-McKendrick model [(7)], while simulating individual disease transitions in continuous time using a Gillespie-based algorithm [(95)]. An explicit dead state was added to quantify the mortalities for the farm-level inventory loss estimation. Figure 3.2 summarizes the model structure and parameters, and equation 6 is a differential equation representation of the stochastic model.

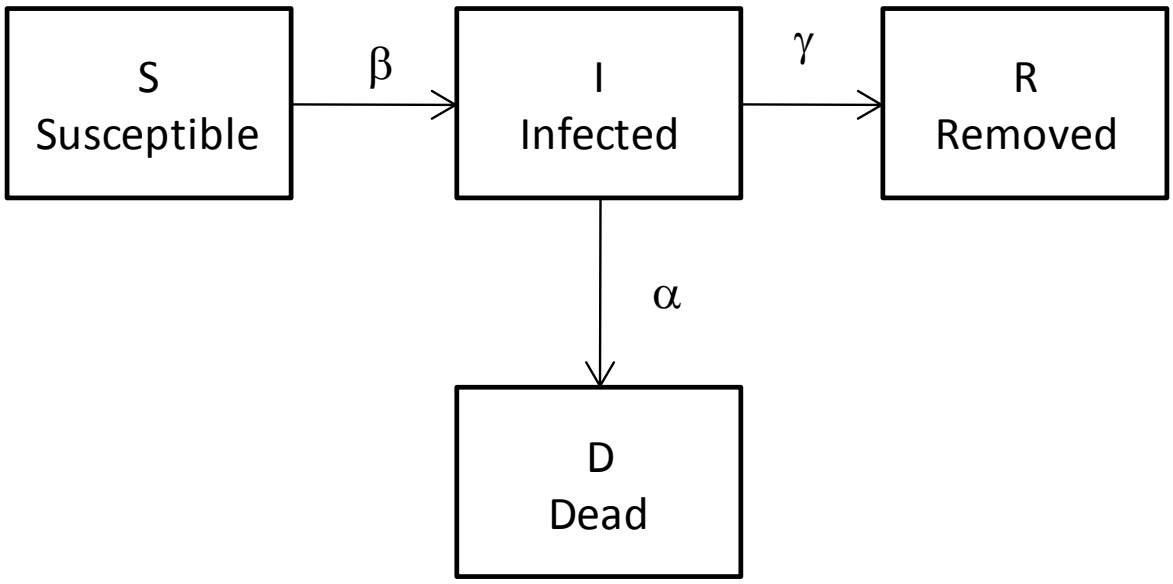

Figure 3.2. Within pond stochastic state-transition model for simulation of a new emerging disease in farmed-catfish ponds in Mississippi.
Transitions between states are represented as arrows. Fish transition from susceptible (S) status to infected (I) at a rate βSI, from I to recovered (R) (e.g. immune) at a rate γI, and from I to dead at a rate αI. The transition times are exponentially distributed.

$$\frac{dS}{dt} = -\beta SI$$

$$\frac{dI}{dt} = \beta SI - \alpha I - \gamma I \qquad (6)$$

$$\frac{dR}{dt} = \gamma I$$

$$\frac{dD}{dt} = \alpha I$$

The susceptible (S) state included all fish in foodsize fish ponds that could be potentially infected by the agent, infected (I) comprised all the fish that were infected and capable of transmitting the disease, the removed (R) state included the fish that were immune, harvested, or that died of causes other than the disease being modeled, and the dead (D) state included all

the fish that died due to the disease. Susceptible fish were infected at rate βSI, and infected fish were either removed at rate γI or dead due to the disease at rate αI. The times at which fish remained in a state was sampled from an exponential(θ) distribution, where θ was the relevant transition rate (βSI, γI, or αI).

Given the uncertainty in the dynamics of an ED outbreak, the model structure was kept simple to avoid over-parameterization. Thus, the following was assumed: (1) closed population; that is no baseline births or deaths other than the mortality caused by the disease, which is reasonable to assume for an epidemic scenario in a confined population such as a fish pond [96]. (2) Every susceptible fish had the same probability of becoming infected. (3) Fish remained in the removal state for the lifetime of the outbreak. (4) the stochastic variability in transition times between fish in a pond was explicitly modeled, while the transition coefficients remained constant. (5) the time scale of the within pond dynamics is independent of that from the between pond model.

The simulation algorithm was fast, but it was computationally implausible (and unnecessary) to simulate all fish in a pond, so the proportion of mortalities p_m in an infected pond was calculated from a population of 1,000 fish/pond. The simulation started with the introduction of infectious fish in a completely susceptible population of catfish in a pond and was run for 1,000 iterations. The mean p_m in infected foodsize fish ponds at the end of the outbreak was calculated and used in the farm-level inventory loss estimation. Histograms were used to

display the simulation summary for the three scenarios, including the distribution of the cumulative proportion of fish mortalities in a pond at the end of the outbreak.

2.3 Parameter estimation and data sources

2.3.1 Expert elicitation to derive key scenarios and parameters

A new ED is by definition unknown; thus the scenarios and parameters to model such ED must be discussed and derived with experts in the disease and production system under evaluation. An elicitation meeting with 14 fish disease experts was held to identify the key scenarios and parameters needed to model emerging diseases in catfish aquaculture. The expert panel included six researchers in aquatic diseases, five epidemiologists, two agricultural economists, and one expert in aquaculture predators. Experts were first presented with conceptual DSM for current catfish diseases and were then asked to discuss approaches to adapt the models for an unknown ED, including the disease characteristics to derive the disease scenarios and parameters. Experts also discussed available sources of data to derive the ponds populations. The elicitation was a panel discussion rather that individual questionnaires, thus a professional moderator was used to guide the discussions and reduce biases resulting from face-to-face meetings, such as dominance and availability bias [(97)].

2.3.2 Pond locations

As the location of catfish ponds was not available, pond locations and attributes were generated based on a combination of census data published by the National Agricultural Statistics Service (NASS) [(98-99)], the National Animal Health Monitoring System (NAHMS) studies

[100-101], and a geospatial dataset of catfish ponds that was created using a classification algorithm on Landsat® satellite imagery for the state of MS. Although a more recent NAHMS Catfish study was published in 2010, the data required to create the pond population was only available in the earlier 2004 publication.

The geospatial dataset was used to calculate the spatial centroids for a total of 3,543 ponds in eastern and western (delta) regions of Mississippi. After all the ponds were geo-referenced, foodsize farms were generated by randomly selecting ponds to represent farm centers, and then *n* ponds closest to the farm center were selected, where *n* was a number randomly sampled (with replacement) from the distribution of the numbers of ponds per farm reported by NAHMS [100-101]. The remaining ponds were assumed to be fingerling ponds. The ponds were then classified by location (east or west MS) and by production goal (fingerling or foodsize fish ponds) to use different parameters for each of the categories in the model. The population calculations were made using the R statistical language and the geospatial manipulations were performed in ESRI ArcGIS 9[6]. Figure 3.3 shows the resulting pond locations used to simulate the disease in MS.

[6] Environmental Systems Research Institute, Inc. (ESRI), Redlands, California, USA

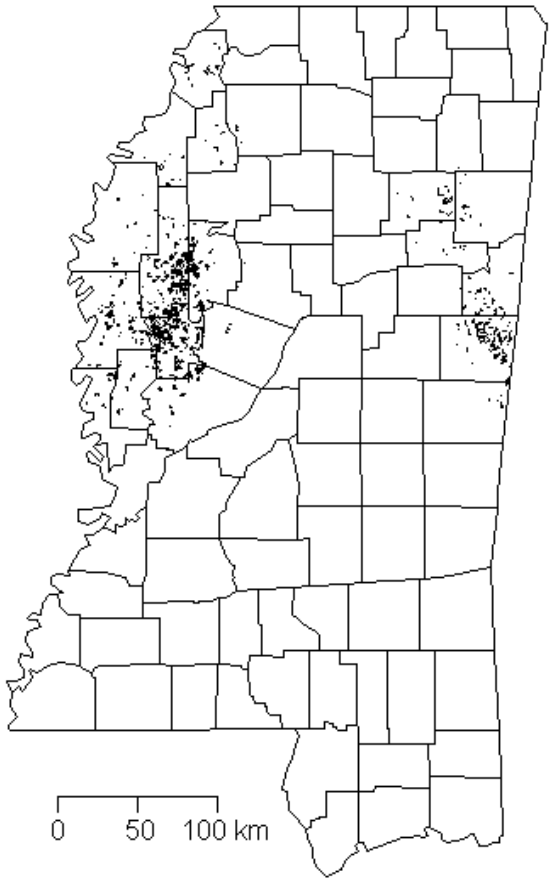

Figure 3.3. Distribution of pond centroids used to simulate an outbreak of an emerging infectious disease in farm-raised catfish in Mississippi.

2.4 Scenarios evaluated

Disease outbreaks can have different impacts on a population depending on the characteristics of the agent (e.g. infectivity, pathogenicity), the host (immune status, species) and the environment (e.g. water quality, fish movement, management). Combinations of those factors were used to develop scenarios for diseases with high, medium and low farm-level impact in

terms of disease incidence and mortality. The scenario and parameters were generated based on published literature and expert opinion. The results from the three scenarios provided a range of possible values of p_i and p_m representing the uncertainty in the epidemiological behavior of the ED considered.

2.4.1 Scenarios for the between-ponds model

The most relevant parameters used for the high, medium and low disease impact scenarios are summarized in table 3.2. The pond-level exposed period (infected not yet infectious) γ_e was assumed to be short (0 to 2 days), the infectious period γ_i was assumed to have a highly variable length to represent the range of pond-level infection (from fast die-off to persistent infection, thus 0 to 300 days), and the immune period γ_r went from half of a year to a full year to simulate the scenario where most ponds would not be restocked while experiencing an outbreak. The direct contact rate λ_d was .02, .025, and .03 contacts/day (roughly 7, 9, and 11 fish movements from fingerling ponds to foodsize fish ponds/year) for the low, medium, and high scenario respectively, whereas indirect contacts λ_{id} happen much more often, with rates 0.8, 1, and 1.1 contacts/day. The probability of infection transfer from direct contacts τ_d was assumed to be 1 since large numbers of fingerlings are usually stocked in foodsize fish ponds. In contrast, as indirect contacts are less likely to result in infection (lower dose of the agent, fewer fish exposed), τ_{id} was 1%, 2.5%, and 3.5% for the three scenarios respectively. Fingerlings could be moved to any pond in the population, so the distance of direct contacts δ_d ranged from 0 to 300 km, based on the maximum distance between ponds in the population database. Indirect movements were assumed to be mostly local (at the farm or pond group level); hence δ_{id} was

exponential (1), effectively simulating most of the distances at a short range, with 99.995% of movements under 10 km. This parameterization was consistent with the distribution of distances between the centroids of pond clusters.

2.4.2 Scenarios for intra-pond model

At the time this study was done there were no catfish-specific disease spread parameters published in the literature and no data were readily available to estimate them. Furthermore, even currently known diseases may not be representative of new ED in catfish; therefore similarly to the between-ponds model, high, medium and low disease impact scenarios were selected to exemplify the use of the model for a broad range of ED losses depending on a combination of parameters that affect disease spread and mortality

The scenarios were discussed with fish disease experts and their parameters were derived from published work for two salmonid diseases; Furunculosis (*Aeromonas salmonicida*) and Infectious Pancreatic Necrosis (Infectious pancreatic necrosis virus) [96, 102-103]. The low scenario simulated a relatively low spreading disease with low mortality rates, whereas the high scenario modeled a fast spreading disease with high mortality. The medium scenario simulated intermediate spread and mortality (table3.3).

Table 3.3. Scenarios and parameters used to simulate the spread of a new emerging disease in catfish ponds in Mississippi

Coefficient	Low spread, low mortality[3]	Intermediate spread and mortality[4]	Fast spread, high mortality[5]
R_0	1	1.45	3.25
Transmission (β)	0.0075	0.0096	0.0214
Mortality (α)[1]	7	6.12	6.08
Removal (γ)[2]	0.5	0.5	0.5
Total population (N)	1,000	1,000	1,000

[1,2] α solved using eq.8 and parameters above. γ assumes 2 days infectious period across all scenarios. For the range of parameters used above, mortality decreases as α increases.
[3]Assumed R_0=1 for epidemic to quickly die-out. β =.001 lowest value reported by (96).
[4]R_0=1.45 and β =.0096 reported for high stocking density experiment in (96).
[5]R_0=3.25 and β =.0214 reported by (102). Highest spread parameters estimated from data found for fish diseases models reviewed.

The studies above report parameters from experimental infections of young (fry/fingerling) salmonids in controlled environments and under different densities ranging from very high to very low fish stocking densities. Thus, the reported parameters may not be interpreted as a direct representation of those from a naturally occurring outbreak. For example, the observed mortality from experimental infection in fingerling fish under high density is likely higher than that of a foodsize catfish in a pond stocked at lower densities. However, the aforementioned studies provide model parameters for different stocking densities and trial designs, providing a range of spread and mortality parameters to parameterize the model. The parameters for each scenario were derived starting from a basic reproductive number, R_0. R_0 represents the mean number of secondary infections caused by an infectious individual in a completely susceptible population (7), and thus provides a measure of the spread potential of the disease. From eq. 6 it can be shown that R_0 is:

$$R_0 = \frac{\beta N}{(\alpha + \gamma)} \quad (7)$$

And since R_0, β, and *N* were known for the three scenarios (Table 3.3), only α and γ had to be derived. γ is the inverse of the average duration of the infectious period and was assumed to be 1/2 across scenarios to match the infectious duration reported by [102]. Rearranging eq. 7, α was solved for using the following equation:

$$\alpha = \frac{\beta N}{R_0} - \gamma \quad (8)$$

This formulation allowed for a consistent usage of the reported data and parameters rather than imposing a pre-defined mortality rate which would defeat the purpose of the modeling work.

2.5 Combined estimates used for the farm-level inventory loss calculation

All possible combinations of the expected values from the three scenarios for P_i (proportion of infected ponds on an infected farm) and P_m (percent mortality of fish within infected ponds) were combined to evaluate their effect on $LC_{ed.}$ Since the yearly frequency of an emerging disease impacting the farm λ_{ed} is unknown, the analysis provides a baseline scenario assuming one ED outbreak per year (λ_{ed}=1). An alternative approach often used in simulation analysis is to calculate the expected value across scenarios via Monte Carlo simulation. With this approach, each scenario is sampled with weights relative to their (often subjective) likelihood of occurrence and the expected value from the combined scenarios is reported. Here the

estimates were reported separately to show the impact that the potential disease dynamics could have in the LC_{ed} estimate.

3 Results

As expected, the high scenario produced the largest outbreak, with a mean of 1,061 infected ponds (29.9% of total, 95%PI: 730 (20.6%), 1,296 (36.6%)) (Table 3.4, Figure 3.4). The proportion of ponds infected within infected farms was high (45.6%) and highly variable (4.0%, 92.3%) (Table 3.4, Figure 3.5), and the mortality within infected ponds was high 88.3%, with fairly small variation (85.9%, 90.5%) relative to the other scenarios (Table 3.4, Figure 3.6).

The medium scenario predicted a mean of 357 (10.0%) infected ponds (95%PI: 122(3.4%), 547(15.4%))

The low scenario exhibited a mean of 7 infected ponds (0.2% of total in region, 95%PI: 0 (0.0%), 29(.8%)), with most scenarios showing no spread of infection between ponds (Table 3.4, Figure 3.4). Of the infected farms, a mean of 7.6% ponds were infected (3.8%, 22.8%) (Table 3.4, Figure 3.5), with a small number of small farms (farms with one or very few ponds) exhibiting 100% pond infection (Table 3.4, Figure 3.5). Pond mortality for this scenario was 9.8% (1.4%, 26.7%), the lowest of the three scenarios (Table 3.4, Figure 3.6)

Table 3.4. Predicted mean and 95%PIs of the proportion of catfish ponds infected in the region, proportion of ponds infected within infected farms (p_i), and proportion of catfish (*Ictalurus punctatus*) mortality due to disease within infected ponds (p_m) in farms infected with a new emerging disease outbreak in a year in Mississippi, USA.

Result	High scenario	Medium scenario	Low scenario
% of total ponds infected in region	29.9% (20.6%, 36.6%)	10.0% (3.4%, 15.4%)	0.2% (0%, 0.81%)
% ponds infected within infected farm (p_i)	45.6% (4.0%, 92.3%)	24.5% (3.8%, 72.0%)	7.6% (3.8%, 22.8%)
Mortality within infected ponds (p_m)	88.3% (85.9%, 90.5%)	49.2% (4.7%, 60.7%)	9.8% (1.4%, 26.7%)

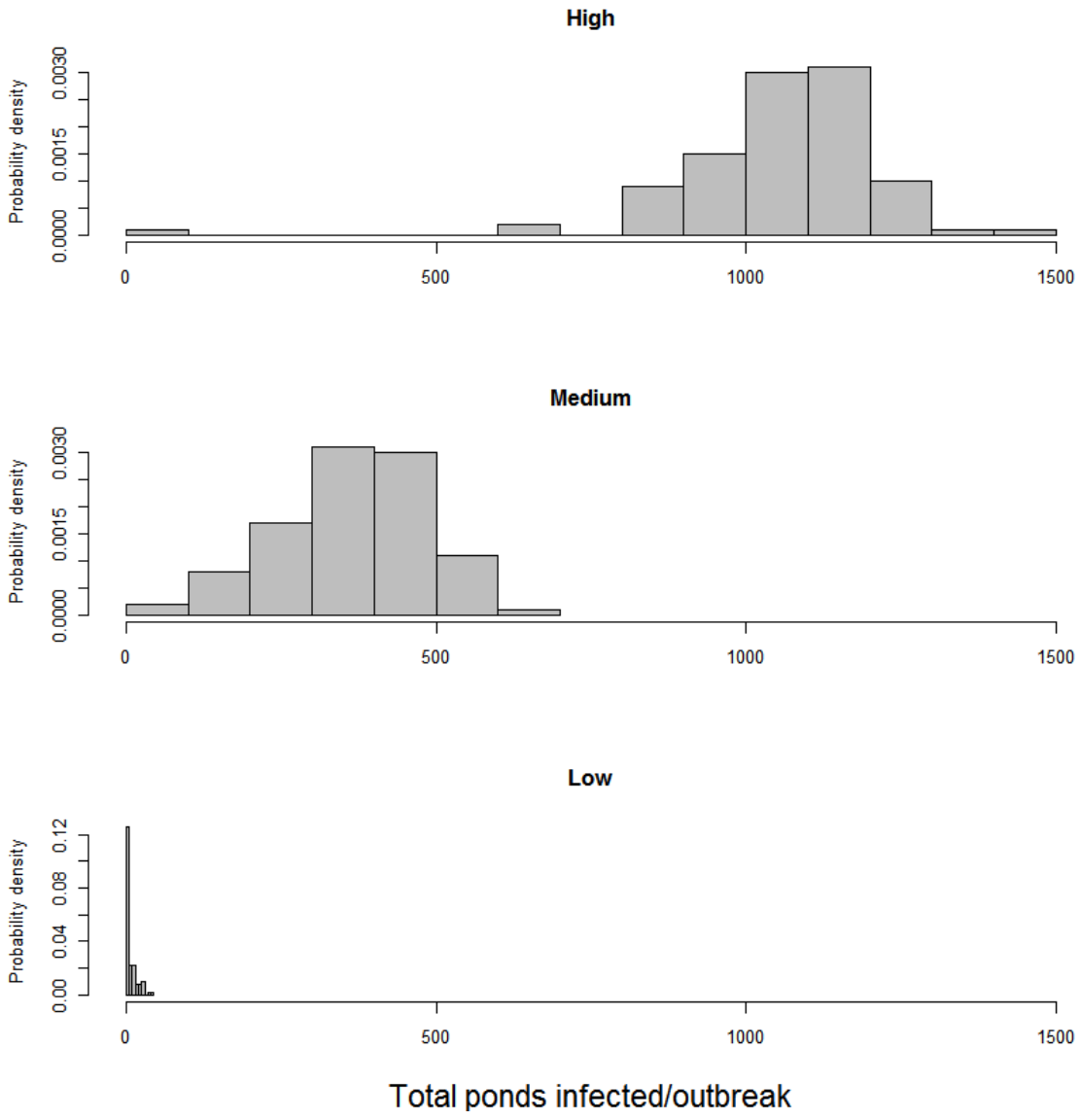

Figure 3.4. Total number of ponds affected at the end of the simulated ED outbreak in catfish, for three scenarios in the state of Mississippi. The index (initially infected) pond is included.

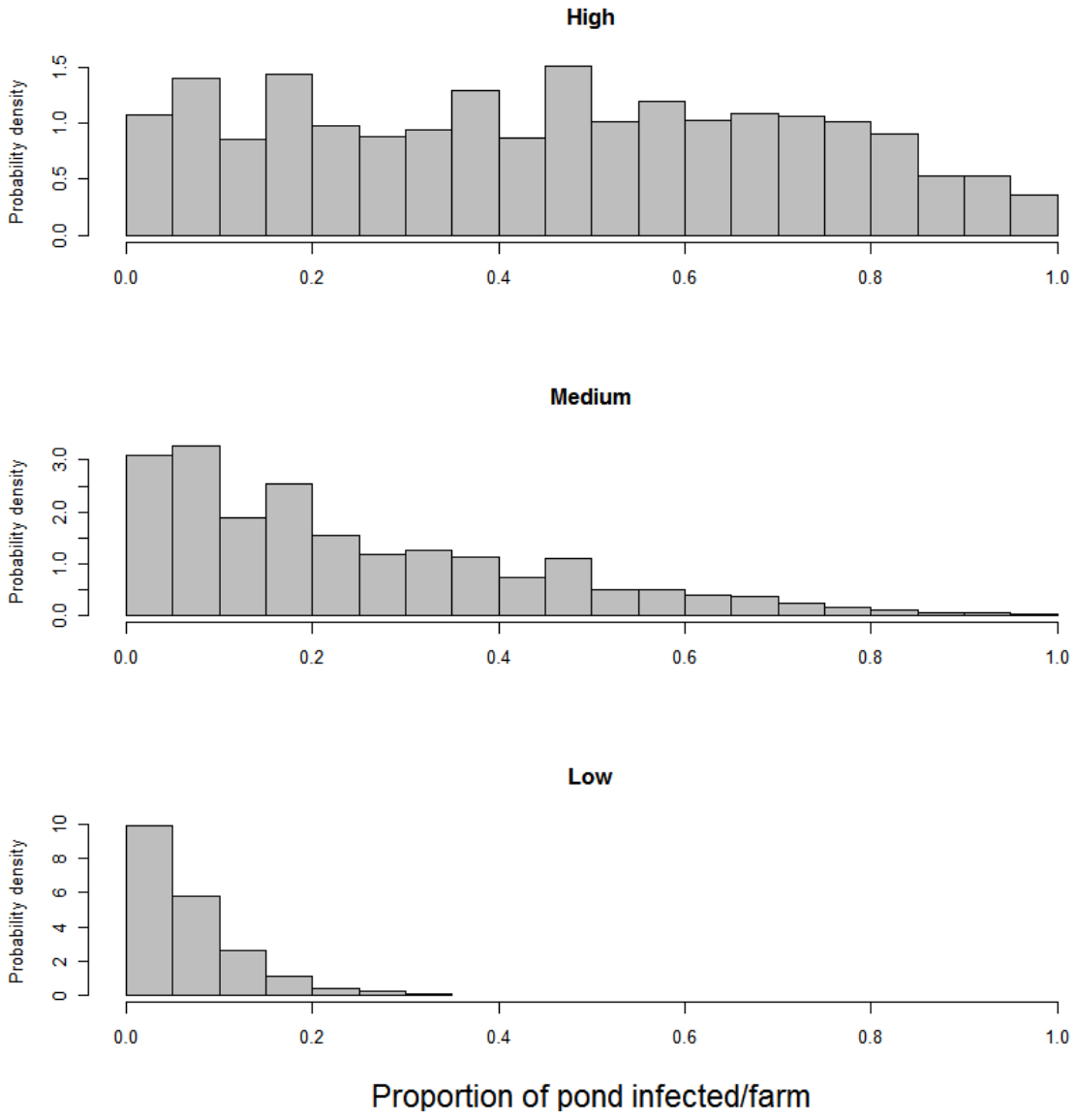

Figure 3.5. Proportion of catfish ponds affected within infected farms (p_i) at the end of an emerging disease outbreak, for three scenarios in the state of Mississippi.

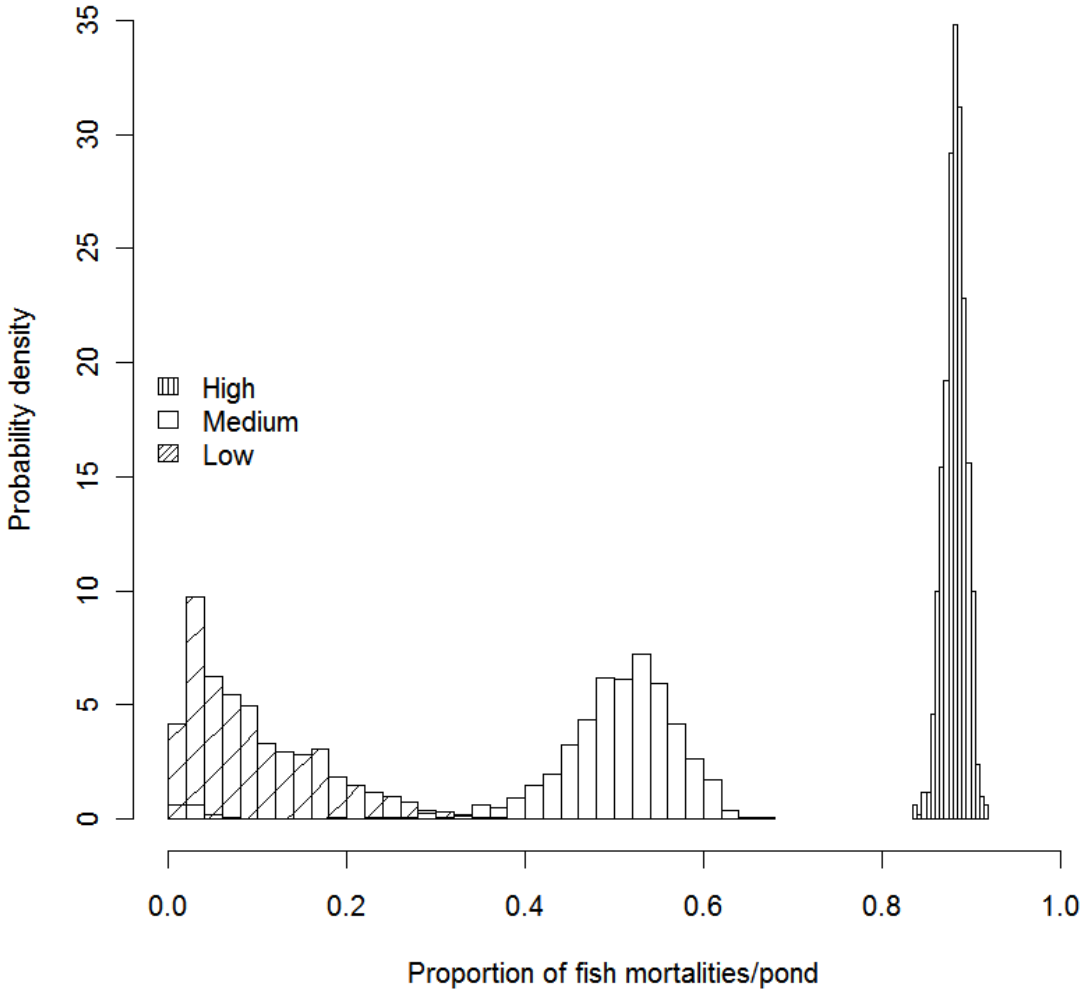

Figure 3.6. Proportion of cumulative fish mortalities due to ED per pond after one year, for three emerging disease spread scenarios in catfish ponds in Mississippi, USA.

3.1 Estimated farm-level inventory loss

The estimated proportion of inventory loss from an outbreak of an ED on an average catfish farm in a year is expected to range from 0.7% to 40.3% depending on the combination of disease spread and mortality exhibited by the ED outbreak (Table 3.5). However, the absolute

maximum losses can be as high as 100% of the farm's inventory, since there were a few farms with only one or a few ponds and all ponds were infected.

Table 3.5. Estimated proportion of total farm-level inventory loss (mean proportion of ponds infected within infected farms (p_i)* mean proportion of catfish (*Ictalurus punctatus*) mortality due to disease within infected ponds (p_m)) in simulated outbreaks of an emerging disease in farmed catfish ponds in Mississippi. Numbers assume one outbreak/year.

Percentage of loss of farm inventory on a given year								
High * High	**High * Med**	**Med * High**	**Med * Med**	**Low * High**	**High * Low**	**Low * Med**	**Med * Low**	**Low * Low**
40.3%	22.5%	21.6%	12.1%	6.7%	4.5%	3.7%	2.4%	0.7%

The estimates in Table 3.5 are based on a frequency of one ED outbreak λ_{ed} per year. If it can be assumed that the risk of ED outbreaks remains constant across the years analyzed (i.e. that the number of ED outbreaks are Poisson distributed with an unknown λ_{ed} intensity), λ_{ed} can be varied to evaluate the effect that the outbreak frequency have on the estimation of farm-level inventory losses. For example, if it is believed that an ED outbreak would occur once every 10 years (λ_{ed}= 1/10), the estimates from Table 3.5 can be multiplied by 0.1 to obtain the expected losses per year. Alternatively, the uncertainty about the true rate of outbreaks per year could be modeled using a Bayesian approach that relies on historical outbreak frequencies. For example, assuming an uninformed prior $\pi(\lambda_{ed})= 1/\lambda_{ed}$, and a Poisson likelihood based on α historical ED outbreaks in τ years, the resulting conjugate posterior is Gamma(α, 1/τ). This distribution could be used to incorporate the uncertainty on λ_{ed} in the loss cost calculation

rather than using a fixed value. However, this approach assumes that future outbreaks will occur with the same frequency as historically so it was not further explored in this study.

4 Discussion

The DSM were useful to estimate the magnitude of ED farm-level outbreak losses for agricultural insurance policies. However, the large uncertainty in the results, driven by the lack of knowledge of several key disease and population parameters warrants a critical discussion of the potential and limitations of the proposed approach. The scenarios and parameters used in this feasibility study are not comprehensive; hence the findings from this study should be used as a reference for further applications of DSM for the insurability of animal ED. For example, the disease duration parameters in the between-ponds model were the same for all scenarios, but these values are likely to vary depending on the disease and population modeled. Likewise, several important parameters of current diseases in aquaculture are not known; consequently, it cannot be expected that the parameters for new ED will be known precisely. Since catfish data were not available to estimate some of disease parameters, they were obtained from expert opinion and/or approximated from experiments for existing diseases [96, 102]. Although this approach is adequate to show the applications of the modeling framework, special attention should be placed in the parameterization of the models if applied in a real loss cost calculation. DSM predictions are particularly sensitive to the contact rates, infectivity, and transmission parameters [7, 104]. Moreover, those parameters are also harder to estimate as, unlike mortality rate and disease duration, they cannot be directly observed under field conditions. Therefore, when using our proposed framework to estimate losses from a disease

newly emerging in an area, the estimation of parameters such as R_0 from outbreak data should be prioritized over other less relevant parameters. Mardones et al. [105] provide an example of such an application to Infectious Salmon Anemia Virus. Likewise, expert opinion was used to model movement parameters, as no empirical data was available to estimate movements. For future analyses, the frequency and distance of shipments of fingerlings to foodsize fish ponds from on-farm (between ponds) and off-farm (private hatcheries) sources, and of indirect movements could be estimated using survey-based methods, while capturing the movement variation between farms and years.

In contrast, if the disease modeled is not yet known and the estimation aims to cover all feasible ED manifestations, further scenarios including other types of ED such as parasitical or vector-borne diseases and an estimate of the frequency of loss should be considered.

The scenarios used here assumed an emerging disease with no readily available mitigation strategies. However, the models used in this study can also accommodate for the modeling of intervention strategies such as movement restrictions, vaccination, slaughter, and quarantine which can then be applied using the proposed framework. Such interventions could be incorporated in the estimation of premiums based on lost cost for individual farms or specific farm types.

Accurate data on the population of animals modeled is also important to generate sound estimates. For this study, the population data required included the location of ponds and farms, the number of fish in the ponds and the number of ponds in a particular farm. Some of that information was not readily available so catfish populations were inferred using a variety

of sources available at the time including categorized satellite images, population studies, and surveys. Although these calculations were feasible to perform for this study, having more detailed population information should be a minimum requirement to establish insurance premium and indemnity payments from/to an individual producer.

The wide variation in estimated farm-level inventory loss depending on the ED characteristics in the three scenarios evaluated highlights the challenge of incorporating coverage for an emerging disease into an insurance product. For example, an insurer may choose to use the highest estimated loss cost estimate for an ED occurring once every five years, but this may make the insurance premium rates cost prohibitive, diminishing the demand for the product. Likewise, if an insurer favors one of the lowest estimates it may be exposing itself to excessive risk, should an ED occur. An insurer may elect to diversify the coverage region and limit the number of policies available in any one given locale so that the risk exposure is minimized. However, an insurance policy provided by a government agency where public welfare, rather than profit, is the motive might allow a lower premium rate and coverage for all individuals regardless of region, hence exposing itself to an increased likelihood of payouts being larger than premiums received, especially when faced with a highly virulent and pathogenic ED such as the one explored in the high scenario in this study. To overcome this, policies may need to cover multiple years to receive premiums during ED loss years and non-ED (non-loss) years.

Previous outbreaks of important catfish diseases include Visceral Toxicosis of Catfish (VTC), digenetic trematode infestations, and Proliferative Gill Disease (PGD) [89-91]**.** Since estimating the frequency of a new ED impacting the farm-raised catfish industry is not readily possible, a

scenario analysis provides a measure of the impact of this lack of knowledge about the value of these parameters; however further statistical methods to estimate this parameter combining historical data and expert opinion should be explored.

Conclusions

Disease spread modeling provides a systematic way to organize the current knowledge on emerging disease perils and this information can be used to estimate ED losses in agricultural insurance policies. However, the estimates obtained will include a large amount of uncertainty driven by the stochastic nature of disease outbreaks, and by the uncertainty in the nature of future ED occurrences. Some parameters such as the direct and indirect contacts are very influential in the results and could be further explored using on-farm surveys, whereas transmission parameters such as R_0 could be estimated early during the emergence of a disease. Scenarios assuming different disease types (e.g. infectious, parasitical, vector-borne) could be explored to broaden the spectrum of the analysis when the purpose is to estimate the impact of a not yet manifested ED. The frequency of ED outbreaks was not explicitly modeled in this study, and requires further attention so the farm-level inventory loss and thus, the loss cost can be more accurately estimated.

CHAPTER 4: A SIMULATION METHOD TO ESTIMATE THE INDIVIDUAL LEVEL INFECTION PROGRESSION AND THE JOINT UNCERTAINTY OF INFECTIOUS DISEASE MODEL PARAMETERS BASED ON LONGITUDINAL SCREENING TEST RESULTS WITH NO GOLD STANDARD: AN APPLICATION TO PARATUBERCULOSIS MODELING[7]

Summary

As gold-standard tests are not always available or feasible to use, evaluating the performance of imperfect tests is important to determine the infection status of individuals screened for disease. Although methods to evaluate performance of longitudinal screening tests with binary outcomes exist [(106)], no methods are available to determine multiple levels of infection/disease states from longitudinal data such as fecal culture tests for *Mycobacterium avium* subsp. *paratuberculosis* (MAP).

The parameters for infectious disease models are often estimated from such imperfect test results. Yet, the joint uncertainty in the test results is rarely considered in the estimation of disease model parameters. The objective of this study was to develop a method to estimate the confidence on the animal-level infection progression using longitudinal screening test results, and use the results to estimate infectious disease model parameters.

[7] Article prepared for submission to *Epidemiology and Infection*.

Test results from a paratuberculosis control program were used to demonstrate the method. The results from 1,034 fecal culture tests (TREK) from 3 Wisconsin dairy herds for 6 years were used to build a stochastic Markov Chain model for the within-herd spread of MAP and estimate its parameters. The infection/disease states were Susceptible, Non-shedder adult, Latent, Low Shedder, Heavy Shedder, Clinical, and Culled. Test parameters estimated with a latent-class Bayesian model were used to simulate a longitudinal disease trajectory for each tested animal and for the herd. The disease trajectories were used to estimate the joint uncertainty distributions of the transition probabilities of the stochastic Markov Chain model, and were then used to project the yearly progression of disease in 20 years.

The joint uncertainties in both the test characteristics and the disease parameters exhibited a significant level of correlation (up to Pearson's r=-.99(-.987, -.989)). Sensitivity analysis showed that ignoring parameter correlation greatly underestimated the variance of the model predictions.

It is concluded that for MAP, in the presence of imperfect disease diagnostic data, the uncertainty distributions of the test characteristics and disease prevalences can considerably impact in the uncertainty distributions of disease parameters estimated from the data. Furthermore, the correlation between the disease parameters can greatly increase the variance of relevant disease model outputs and therefore, this correlation should be taken into account when parameterizing stochastic epidemic models. The simulation method described provides a

likelihood-free alternative to derive the joint uncertainty in the disease parameters, and can be extended to a variety of disease spread models.

1 Introduction

Screening tests are used to determine the disease status of individuals and/or populations. When individuals are repeatedly tested over time, the results from the test provide an indication of their longitudinal disease state. Example of longitudinal disease screening tests include breast or prostate cancer screening in humans [107-108], HIV screening [109], and bovine tuberculosis [110], or paratuberculosis [111] surveillance and/or eradication programs in cattle.

Commonly used disease diagnostic tests are often imperfect and gold standard tests are not always available, practical, or economically feasible to use. Thus, methods to evaluate the performance of diagnostic tests in absence of a gold standard were initially introduced by Hui & Walter [112] and revisited by others [113]. More recently, methods to evaluate the performance of longitudinal screening tests and estimate disease status with binary outcomes [114] and with one binary outcome and one continuous outcome have been proposed [106], but to the authors' knowledge, no methods are available to determine multiple levels of infection and/or disease states from longitudinal screening tests such as those obtained from fecal culture tests for *Mycobacterium avium* subsp. *paratuberculosis* (MAP).

The results from longitudinal diagnostic screening tests are useful to understand the progression (or absence) of disease in individuals and populations, for example, after disease

control policies have been implemented. Likewise, disease spread models (also called infectious disease models) are increasingly relevant tools to evaluate the effects of public health policy options in controlling or eradicating infectious diseases, and have been broadly applied to evaluate mitigation strategies of major infectious diseases affecting humans and animals [7]. As diagnostic test results are an important source of empirical data to parameterize disease spread models, the uncertainty arising from the imperfect test results inevitably propagates to the disease model parameters.

Historically, the "true" disease status of tested individuals and populations is inferred by adjusting test results by the test sensitivity and specificity, and fixed point estimates of the disease parameters are then derived from this "most likely" dataset. For example, Benedictus et al. [115] used a series of subjective rules to interpret infection and shedding states based or multiple test results from individual animals. Alternatively, the uncertainty distributions of disease parameters are assumed to either be uncorrelated to each other [29, 116], or their correlation is modeled using parametric assumptions, typically multivariate Normal distributions with an estimated covariance matrix [117].

Several authors [118-120] have explored the estimation of joint disease parameters in presence of imprecise data. For example, Höhle et al. [121] described a Bayesian method to estimate disease parameters when the time of infection is unknown. However, the method requires an epidemic disease with an established ending time to make inferences about the time of infection (and thus, the population distribution of infection times), and makes no implicit adjustments for

imperfect diagnostic tests. Other methods [120] adjust for imperfect binary diagnostic tests, but also rely on an epidemic disease with a known end time to infer the time of infection and thus, derive transmission parameters. More recently, Nishiura [122] proposed a simple model that simultaneously estimates binary diagnostic test properties and infection dynamics parameters from cross-sectional Influenza tests in humans. However, to the authors' knowledge no attempts have been made to quantify the joint uncertainty of test with more than two outcomes, and disease parameters from longitudinal screening tests of a chronic and/or endemic disease with no ending times.

Paratuberculosis (PTB) represents an interesting example of an infectious disease where screening tests are applied repeatedly to individuals. PTB (also called Johne's disease) is a chronic disease of cattle caused by *Mycobacterium avium* subsp. *paratuberculosis* (MAP) that can cause diarrhea, weight loss, milk production losses, and an increase in culling. However, only a fraction of infected animals may develop clinical signs of the disease, and this may often happen several years after the initial infection [106]. Bacterial culture of feces is a commonly used diagnostic test for MAP, but the accuracy of this test across animals is poor [123]. However, the test accuracy depends on the shedding level of the animals [124]. For example, test sensitivity is intuitively higher for animals shedding large quantities of the bacteria.

The objective of this study was to develop a method to estimate the confidence in the individual level infection progression using longitudinal screening test results, and use the

results to estimate the joint uncertainty of infectious disease model parameters. The estimation method is illustrated using a dataset of longitudinal diagnostic testing for Paratuberculosis.

2 Materials and methods

2.1 Description of dataset

The dataset used for this study has been described elsewhere [125]. The results from the bacterial culture of feces (fecal culture) from three herds (A, B, and C) from the Wisconsin Johne's disease vaccine clinical trial funded by USDA-APHIS-VS were used to parameterize the models. The three herds were previously diagnosed with MAP infection. Within each herd, female calves were systematically assigned at birth to receive MAP vaccine (vaccinated group) or not (control group), until a cohort of 50 animals per group and per herd was formed. A fecal sample from each animal in the cohort was collected at approximately 90 days into pregnancy during each lactation for 6 years. Fecal samples were cultured and evaluated for presence of MAP at the Wisconsin Veterinary Diagnostic Lab (WVDL; Madison, Wisconsin) using a broth-based culture media [126]. The results of the five standard (0 to 4) reported fecal culture categories [127] were classified in three categories: *Negative* (culture= 0), *Low* (culture 1-2), and *High* (culture=3-4) (Table 4.1)

Table 4.1: Grouped results of 6 years of MAP fecal culture test results from three WI herds. C= control, v= vaccinated animals.

Number of tests (% of group)		High	Low	Negative
Herd A				
	C	10 (9.6%)	10 (9.6%)	84 (80.8%)
	V	4 (3.0%)	13 (9.7%)	117 (87.3%)
Herd B				
	C	0 (0.0%)	15 (8.7%)	157 (91.3%)
	V	2 (0.9%)	11 (5.0%)	205 (94.0%)
Herd C				
	C	0 (0.0%)	15 (7.3%)	190 (92.7%)
	V	0 (0.0%)	4 (2.0%)	197 (98.0%)

2.2 Modeling approach

The purpose of the model was twofold: (1) use the results of a fecal culture diagnostic test to infer the longitudinal progression of MAP infection/Johne's disease of individual animals in yearly intervals, and (2) to use the information from (1) to calculate the joint uncertainty distribution of infectious disease model parameters, to simulate disease progression at the herd level. Figure 4.1 summarizes the steps taken to calculate the model parameters and generate projections, as described in the following sections.

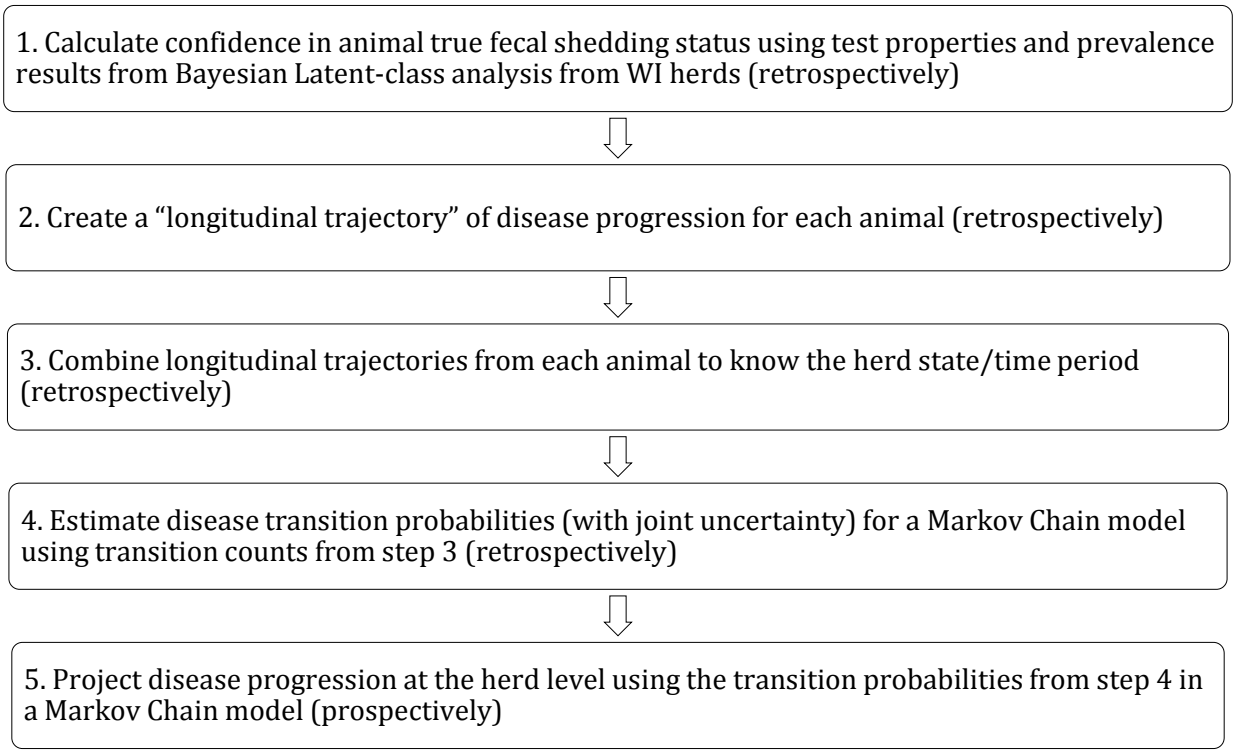

Figure 4.1: Steps to calculate the model parameters and generate projections.

2.2.1 Calculate confidence in animal fecal shedding status

Model

Fecal culture results from the three WI herds were used to evaluate the characteristics of the fecal culture test and estimate herd-level prevalences of animal fecal shedding states. The estimates were then used to estimate the confidence in the true fecal shedding status of animals based on the fecal culture results (Table 4.2).

Table 4.2: Terminology and notation used to differentiate test results and true fecal shedding status of animals

Test result (notation)		True shedding status (notation)	
High	(T_H)	Heavy shedder	(S_H)
Low	(T_L)	Low shedder	(S_L)
Negative	(T_N)	Non- shedder	(S_N)

While shedding rate is a continuum, the three shedding categories utilized were assumed for consistency with the reporting of the fecal culture test [127] and with the common categorization of MAP shedding for infectious disease modeling purposes. Therefore, there were three possible test results and three corresponding shedding states (Table 4.2), yielding nine possible combinations of tests and shedding states.

A Bayesian latent-class model was developed to estimate the conditional probability of correctly identifying the true shedding status of an animal given the observed test results. The model is a ternary extension of the model initially described by Hui & Walter [112] and revisited by Johnson et al. [113] for one test with a binary outcome and no gold standard. The derivation of the model is presented here, whereas the Markov Chain Monte Carlo (MCMC) estimation method is explained in the subsequent section.

The model assumes that the test characteristics are equal for all the herds (conditional on infection status), for all cows within herds (regardless of age), and remain constant over time. Therefore, for each *i* herd, the probability that a randomly sampled animal (pre-test probability) is heavy, low, or non-shedder is equal to the herd-level true shedding prevalences ($p_{H,i}$, $p_{L,i}$, and $p_{N,i}$ respectively). The fecal test results are then conditional on the shedding status of the animals, yielding nine conditional probabilities, $P_{H,H,}$ $P_{L,H,}$ $P_{N,H,}$ $P_{H,L,}$ $P_{L,L,}$ $P_{N,L,}$ $P_{H,N,}$ $P_{L,N,}$ $P_{N,N}$ (Figure 4.2).

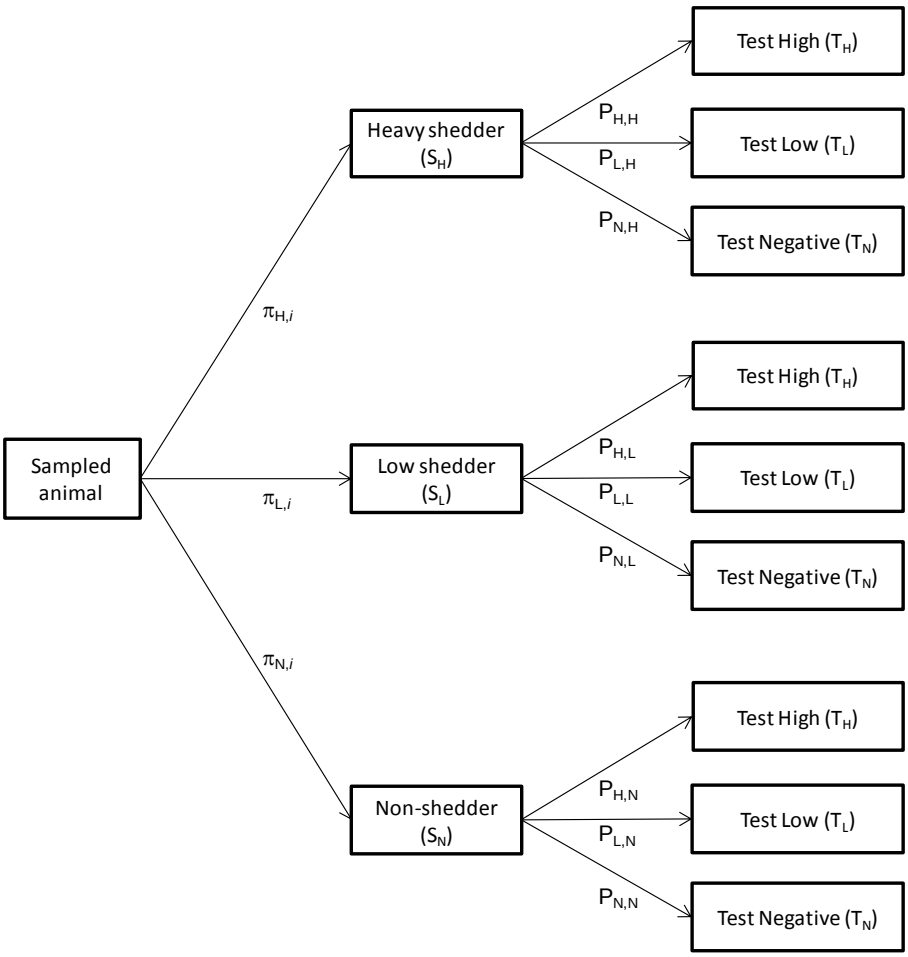

Figure 4.2: Event tree of individual animal sampling, fecal shedding status, test outcomes, and related model parameters.

The joint probability of any possible sample outcome is then the marginal probability of the animal shedding level (true shedding prevalence) multiplied by the conditional probability of the test outcome given the animal shedding level. For example, the joint probability that a randomly sampled animal from herd *i* is a heavy shedder and yields a high test result, $P(S_H \cap T_H)$ is $p_{H,} P_{H,H}$ (or $p_{H,i} P(T_H|S_H)$ using standard probability notation).

However, the shedding status of any sampled animal is unknown so the marginal probabilities of obtaining $T_{H,}$ $T_{L,}$ or T_N test results (grouped as p_i, the apparent prevalences) in herd *i* are respectively:

$$P(T_{H,i}) = p_{H,i} P_{H,H} + p_{L,i} P_{H,L} + p_{N,i} P_{H,N}, \quad i=1,2,3 \tag{1}$$

$$P(T_{L,i}) = p_{H,i} P_{L,H} + p_{L,i} P_{L,L} + p_{N,i} P_{L,N} \tag{2}$$

$$P(T_{N,i}) = p_{H,i} P_{N,H} + p_{L,i} P_{N,L} + p_{N,i} P_{N,N} \tag{3}$$

Applying Bayes's theorem, the confidence of the shedding status of individual animals in herd *i* given the observed test results are:

High test result

$$P(S_{H,i}|T_{H,i}) = P(S_{H,i} \cap T_{H,i}) / P(T_{H,i}) \tag{4}$$

$$P(S_{L,i}|T_{H,i}) = P(S_{L,i} \cap T_{H,i}) / P(T_{H,i}) \tag{5}$$

$$P(S_{N,i}|T_{H,i}) = P(S_{N,i} \cap T_{H,i}) / P(T_{H,i}) \tag{6}$$

Low test result

$$P(S_{H,i}|T_{L,i}) = P(S_{H,i} \cap T_{L,i}) / P(T_{L,I}) \tag{7}$$

$$P(S_{L,i}|T_{L,i}) = P(S_{L,i} \cap T_{L,i}) / P(T_{L,i}) \tag{8}$$

$$P(S_{N,i}|T_{L,i}) = P(S_{N,i} \cap T_{L,i}) / P(T_{L,i}) \tag{9}$$

Negative test result

$$P(S_{H,i}|T_{N,i}) = P(S_{H,i} \cap T_{N,i}) / P(T_{N,i}) \tag{10}$$

$$P(S_{L,i} | T_{N,i}) = P(S_{L,i} \cap T_{N,i}) \,/\, P(T_{N,i}) \quad (11)$$

$$P(S_{N,i} | T_{N,i}) = P(S_{N,i} \cap T_{N,i}) \,/\, P(T_{N,i}) \quad (12)$$

For example, if the result of the fecal culture test in an animal was high, the probability (confidence) that the animal was a heavy shedder at the time the sample was taken is $P(S_{H,i} | T_H) = (p_{H,i}\, P_{H,H}) / (p_{H,i}\, P_{H,H} + p_{L,i}\, P_{H,L} + p_{N,i}\, P_{H,N})$.

Parameter estimation

The parameters were estimated using a Bayesian latent-class model implemented in OpenBUGS 3.2.1 [(128)].

The set T_i represents the count of individual T_H, T_L, and T_N fecal culture results collected in the 6-year period for each *i* herd, for a total of n_i tests per herd (Table 4.1). Likewise, p_i is a set with three elements representing the observed proportion of individual fecal culture results out of the total n_i tests (the apparent prevalences for the three test results, in parentheses in Table 4.1). Assuming that each animal represents an independent random sample from each herd, the distribution of the number of individual fecal culture results was modeled as:

$$T_i \sim \text{Multinomial}(p_i, n_i) \quad (13)$$

where the individual probabilities p_i of obtaining High $P(T_{H,i})$, Low $P(T_{L,i})$, and Negative $P(T_{N,i})$ test results in the *i* herd are calculated as shown in formulas 1-3.

The prior distributions for the true shedding level prevalences p_i of heavy $p_{H,i}$, light $p_{L,i,}$ and non-fecal shedders $p_{N,i}$ for each *i* herd were modeled using a Dirichlet distribution (a multivariate generalization of the Beta distribution). The arithmetic means of the posteriors from a separate analysis done on dairy herds in Minnesota, Pennsylvania, and Colorado [124] were used as the α parameters of the Dirichlet distributions to provide informed priors for all *i* herds:

$$p_i \sim \text{Dirichlet}(\alpha_H, \alpha_L, \alpha_N) \quad (14)$$

where $(\alpha_H, \alpha_L, \alpha_N) = (4,16,80)$ thus, the priors were the same for all three herds.

Likewise, the prior distributions of the conditional test probabilities of the three test outcomes $P_{H,H,}\, P_{L,H,}\, P_{N,H}$ from heavy shedders $P(T_{H,L,N}|S_H)$, $P_{H,L,}\, P_{L,L,}\, P_{N,L}$ from low shedders $P(T_{H,L,N}|S_L)$, and $P_{H,N,}\, P_{L,N,}\, P_{N,N}$ from non-shedders $P(T_{H,L,N}|S_N)$ were modeled using Dirichlet distributions, with informed priors based on posteriors means from a separate analysis done in another population using a similar fecal culture test [124]:

$$P(T_{H,L,N}|S_H) \sim \text{Dirichlet}(\alpha_{HH}, \alpha_{LH}, \alpha_{NH}) \quad (15)$$

$$P(T_{H,L,N}|S_L) \sim \text{Dirichlet}(\alpha_{HL}, \alpha_{LL}, \alpha_{NL}) \quad (16)$$

$$P(T_{H,L,N}|S_N) \sim \text{Dirichlet}(\alpha_{HN}, \alpha_{LN}, \alpha_{NN}) \quad (17)$$

where:

$(\alpha_{HH}, \alpha_{LH}, \alpha_{NH}) = (59,38,3)$

$(\alpha_{HL}, \alpha_{LL}, \alpha_{NL}) = (1,26,73)$

$(\alpha_{HN}, \alpha_{LN}, \alpha_{NN}) = (.1,1.9,98)$

The fit and convergence of the MCMC model was assessed using diagnostics methods including autocorrelation plots, Gelman-Rubin plots, and convergence plots. Scatter plots were used to evaluate correlations between estimates. Three parallel chains were simulated using two diverging sets of initial values to explore convergence and to perform sensitivity analyses.

Also, the initial values for the three chains were changed mid-simulation to stress-test convergence of the estimates. The final estimates were based on a "burn-in" period of 1,000 iterations and a total of 100,000 iterations per chain. Based on convergence tests, to avoid autocorrelation the results from every 3rd iteration from the last 10,000 iterations from a chain with strong evidence of convergence were stored in an Excel® 2007 (Microsoft Corp, Redmond, WA) spreadsheet to be used in the further calculation steps.

The arithmetic means and 95% credible intervals (CrI) for each estimate were reported. To reduce the number of parameters estimated in OpenBUGS, the mean and 95% CrI of the true shedding confidence parameters (eqns. 4-12) were calculated in Excel® using the posteriors from the MCMC samples taken in OpenBUGS.

2.2.2 Create a longitudinal trajectory for each animal

The test parameters estimated in step 1 were used to reconstruct the longitudinal trajectory of each animal based on the repeated results of fecal culture tests, birth date, and date of removal. All calculations for steps 2-5 were implemented in Visual Basic for Applications (VBA)

for Excel 2007 and Monte Carlo simulations were performed using the SDK simulation engine in ModelRisk 4.0 (Vose Software, Ghent, Belgium).

The states considered for the longitudinal trajectories (Figure 4.3) were:

- Susceptible (S): uninfected calves (≤12 months of age)
- Latent (L): calves or cows (> 12 months of age) infected but not yet infectious (not shedding)
- Non-shedder (NS): adult animals not shedding MAP. Assumed to be uninfected and resistant to infection as adult.
- Low shedder (LS): cows shedding low amounts of MAP
- Heavy shedder (HS): cows shedding large amounts of MAP
- Clinical (CL): cows showing clinical signs of MAP infection (Johne's disease)
- Culled (CU): calves or cows removed from the herd

The directions of the arrows in Figure 4.3 indicate the possible transition of individuals between states. For example, after a month, Susceptible individuals can remain Susceptible, become Latently infected, or become Uninfected, whereas Latently infected individuals cannot return to the Susceptible state.

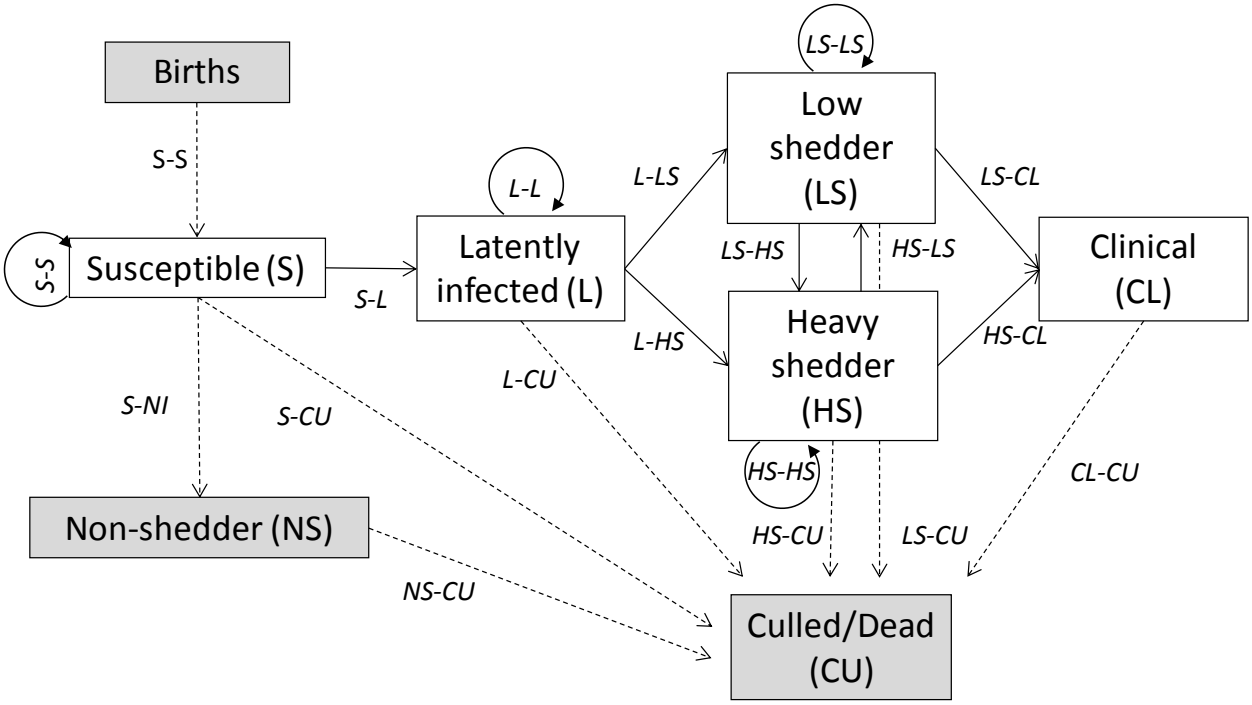

Figure 4.3: Model for the animal-level dynamics of MAP infection and Johne's disease in dairy cattle. The arrows and parameters indicate the possible transition of individuals between states and their respective probabilities of transition on any given year.

The longitudinal trajectory for each animal was calculated in two steps: the first step computes the health status of each animal over time based on historical fecal culture test results, and birth and removal months. The second step uses the results from the first step to establish the initial time of infection. The following pseudo-code describes the calculation steps performed for each animal:

First step: forward calculation

The health status of each animal over time is inferred based on historical fecal culture test results, and birth and removal months (or final month of data available) using the following rules:

1. Define total time: from birth month to removal month (or final month of data available)
2. Set to Susceptible from birth through first test
3. When first test occurs, allocate to NS, LS, or HS based on test results as following:
    a. If NS in the prior month, the new status based on test determination (see section below for details):
        i. If NS, then stays NS
        ii. If LS, then new status is LS
        iii. If HS, then new status is HS
    b. If LS in the prior month, the new status based on test determination:
        i. If NS or LS, then stays LS (assumes that Low shedders always shed at some level)
        ii. If HS, then new status is HS
    c. If HS in the prior month, the new status based on test determination:
        i. HS, then it stays HS
        ii. NS or LS, the new status is LS
4. Maintain status until another test, Clinical, removal or end of data
    a. If Clinical, animal becomes clinical and is consequently removed.
    b. If end of data, animal remains in current state
5. Repeat until animal removed or end of data

Calculation of shedding status based on test determination

Every time that a test result is available for an animal *n* at month *m*, the true shedding status *S* of the animal conditional on the sample result *t* is sampled from a Multinomial distribution with probabilities equal to the posterior probabilities calculated from the test results (eqs.4-12):

$$S_{m,t}\begin{cases} Multinomial\big(n, P(\mathrm{S_H}|\mathrm{T_H}), P(\mathrm{S_L}|\mathrm{T_H}), P(\mathrm{S_N}|\mathrm{T_H})\big) & t = \mathrm{H} \\ Multinomial\big(n, P(\mathrm{S_H}|\mathrm{T_L}), P(\mathrm{S_L}|\mathrm{T_L}), P(\mathrm{S_N}|\mathrm{T_L})\big) & t = \mathrm{L} \\ Multinomial\big(n, P(\mathrm{S_H}|\mathrm{T_N}), P(\mathrm{S_L}|\mathrm{T_N}), P(\mathrm{S_N}|\mathrm{T_N})\big) & t = \mathrm{N} \end{cases} \quad (18)$$

The uncertainty distributions from the posterior probabilities of the test results were sampled jointly to preserve their correlations. That is, for each iteration of the model, the posterior

probabilities from one iteration from the MCMC chain were sampled and used together in the model.

Second step: backward calculation

The results from the first step are used to establish the initial time of infection using the following rules:

1. Go backward in time to determine health status in each month based on information calculated on first pass.
    a. Any animal that has been determined to be LS or HS is assumed to have been latent starting from month 6 (on average, mid-age of a calf).
    b. If an animal has been determined to be HS, it is assumed to have been LS for 12 months prior to the HS determination as long as it is classified as an adult (over 12 months of age).
    c. Animals that end as NS remain Susceptible from birth though first test, and NS for the remainder of the period.

2.2.3 Combine individual animal trajectories to know the herd state at each time period

The individual trajectories from each animal are combined to obtain the aggregate number of individuals in each of the infection/disease states per herd. That is, for any *m* month, the number of animals *n* in each state *s* for the *j*th iteration is summed.

The number of yearly transitions between states t_m occurring at each *j* iteration are also recorded. Although the trajectories are calculated in monthly steps, the transitions are counted on a yearly basis as the fecal culture tests are only performed once a year per animal, and thus the Markov Chain model described in step 4 also takes yearly steps.

The results of both transition counts and animal states per herd per iteration are recorded in Excel® spreadsheets so they can be used in step 4.

2.2.4 Estimate transition probabilities for Markov Chain model

The disease trajectories and/or transition counts from step 3 could have been used to estimate the parameters of a variety of disease spread models, including compartmental state-transition models such as extensions to the population dynamics Kermack-McKendrick SIR model [(129)] in discrete time, mechanistic models of disease spread, or more general models such as Markov Chains. A discrete time stochastic Markov Chain model is used here as an example application.

The model followed the standard Markov Chain form, where future states X in time *y* are conditionally independent of past states, that is:

$$P(X_{y+1}=x|X_1=x_1, X_2=x_2, \ldots, X_n=x_n) = P(X_{y+1}=x|X_n=x_n) \quad (19)$$

Where X are the potential infection/disease states for individual animals in the herd and *y* is a year. In other words, the probability of any given animal in the herd to be in a certain disease state in a future year is only dependent on the state it was in the prior year (and the transition probabilities). The yearly steps were chosen for consistency with the yearly testing performed in the herds analyzed, and based on the relatively slow progression of MAP infection and disease.

Since the states are inferred using the results from the fecal culture test, the model is equivalent to a Hidden Markov model (HMM) where the LS, HS, and NS states (Figure 4.3) are the hidden states, and the three disease diagnostic results (Table 4.1) and the clinical reporting of disease are the observable states. However, the duration of the Susceptible and Latent states cannot be directly estimated using a HMM (as this would require knowing the time of transition to the Latent state and/or the time of infection), thus justifying the dynamic calculation approach described here.

Since the calculation of the test characteristics and herd prevalences was performed using Bayesian methods, the transition probabilities shown in Figure 4.3 were also calculated using a Bayesian approach. The realizations of a Markov Chain for *n* individuals in each *s* state at time (year) *y*+1 were simulated using a Multinomial distribution:

$$n_{s,y+1} = Multinomial\left(n_{s,y}, P_s\right) \quad (20)$$

Where $n_{s,y}$ is a vector with the number of individuals on each *s* state at time *y*, and P_s is a matrix with the transition probabilities from each state.

The conjugate of a Multinomial outcome with an uninformed prior probability of occurring is a *Dirichlet*(α_s), where α_s, are the observed frequencies of transitions between states. Therefore, the relative frequency of the number of yearly transitions between states t_m was used directly to estimate P_s. As described for the sampling of test posteriors in step 2, the transition counts per iteration were sampled sequentially to preserve the joint uncertainties in P_s.

2.2.5 Use transition probabilities to project future disease states at the herd level

The joint uncertainty distributions for the transition probabilities were used directly in the Markov Chain model (Figure 4.3) to create yearly projections of the number of animal in each disease states in a herd for 20 years. Although the number of animals in each state at the end of 20 years could be solved directly, yearly steps were simulated to provide inputs to other analyses that require yearly results (e.g. to perform a farm-level economic analysis).

The model assumes a population with 100% replacement of culled animals to represent a herd with constant size; therefore, the birth and death rates were set to be equal (that is, the transition probability from *CU* to *S* was 1, and calf and heifers that are not kept as replacement animals were not considered in the model). The starting values were set to the mean number of animals in each state, as derived from a medium-sized dairy herd that was not used to derive the transition parameters (Table 4.3). However, to stress-test the model behavior, the scenario starts with no animals culled at year 0, which should result in a reduced number of Susceptible calves on year 1 The calculations assumed a replacement rate of 35% (from total cows in the herd) and a calving interval of 14 months, both considered to be typical management values for the US dairy industry.

Table 4.3: initial values used for the 20-year projection of MAP infection and Johne's disease in an average WI herd

Starting values	Number of animals
Susceptible	132
Non Shedder	271
Latent	68
Heavy shedder	12
Low shedder	90
Clinical	0
Culled	0
Total animals in herd	573

2.3 Sensitivity analysis

The simulation projections of the Latent animals were chosen for the sensitivity analysis, as they represent a direct estimate of the infection progression in the herd. The contribution of the total model variability due to the parameter uncertainty was explored by simulating the disease for 20 years using the means of the parameter posteriors and comparing the results to the simulation sampling from the joint uncertainty of the parameters. The yearly means and 95%CrI of the Latent animals for both scenarios were then plotted. Similarly, to understand the impact of the correlation structure between the transition probabilities, the total Latents simulated after 20 years were compared against the results from a simulation where the transition parameters were assumed to be independent (i.e. Pearson's $r = 0$), and also against a scenario using only the means from the transition probabilities.

The sensitivity of the projections of cumulative Latents after 20 years to the transition parameters was explored via a percentile-fixed sensitivity analysis. In short, each transition parameter was divided in 10 tranches (from 5^{th} to 95^{th} percentile), and fixed to that percentile while all the others parameters were sampled randomly for 3,000 simulations, and the mean of

the total Latents was recorded. This was repeated for each parameter, effectively obtaining the mean total Latents conditional on the i^{th} percentile from each transition parameter. The resulting conditional means from each simulation were graphically displayed. This method has the advantage of showing non-linear relationships between the uncertainty distributions of input parameters and the model outputs.

Also, the rank order correlation between each input parameter and the total Latents after 20 years was visualized as an horizontal bar plot.

Finally, the values of the time assumptions for the backward calculations (latent from month 6 from birth, LS for 12 months prior to HS determination, as described in step 2), where individually changed to 12 and 6 months respectively and the change on the mean and 95%CrI of the total Latents was evaluated.

For reproducibility, all simulations were performed using the same seed value. Unless otherwise specified, simulations were run for 3,000 iterations. Figures were created in the R statistical language [130].

3 Results

3.1 Test characteristics and herd prevalences

The majority of animals were non-shedders, with Non-shedding (p_N) prevalences across the test period of 75.1% (68.2%,81.7%), 82.0% (75.1%,87.4%), 84.8% (78.5%,90.1%) for herds A, B, and

C respectively (Table 4.4). The prevalence of low shedders (p_L) was similar across herds and ranged from 14.0% for herd C, to 17.0% for herd A, whereas the prevalence of heavy shedders (p_H) was more variable, going from as little as 1.2% (0.3%,2.6%) for herd C to as high as 7.9% (4.7%,11.9%) for herd A.

The overall sensitivity of the fecal culture for identification of any shedding level among Heavy shedders ($P_{H,H} + P_{L,H}$) was 97.0% (92.9%,99.4%), whereas the sensitivity for the identification of any shedding among Low shedders ($P_{H,L} + P_{L,L}$) was 26.3% (18.8%,34.1%). The specificity ($P_{N,N}$) of the fecal culture test was 98.6% (table 4.4).

The posteriors of the test characteristics (Table 4.4) were similar to the priors used, suggesting that several of the priors dominated over the test results data. For example, the mean of the prior for $P_{H,H}$ (the probability of a High test given that the animal is a Heavy shedder) was 59% and its posterior probability was 57.4%. In contrast, although the same priors were used for the prevalences of the three herds, the posterior estimates of p_H, p_L, and p_N varied across herds.

Sensitivity analyses show that the posteriors of test parameters for Heavy and Low shedding levels were most sensitive to the priors, which is expected as the majority of the test results were Negative. The posteriors of test parameters for Non-shedders did not vary significantly when the priors were modified (results not shown).

Table 4.4: Posterior probabilities for test characteristics and herd prevalences from fecal culture of feces of MAP from three WI herds with High, Low, and Negative outcomes.

Parameter (test,shedding)	Probability interpretation	Posteriors Means (95%CrI)
$P_{H,H}$ [1]	$P(T_H \mid S_H)$	57.4% (47.7%,66.7%)
$P_{L,H}$ [1]	$P(T_L \mid S_H)$	39.6% (30.3%,49.0%)
$P_{N,H}$	$P(T_N \mid S_H)$	3.0% (0.7%,6.9%)
$P_{H,L}$ [2]	$P(T_H \mid S_L)$	0.6% (0.0%,2.2%)
$P_{L,L}$ [2]	$P(T_L \mid S_L)$	25.7% (18.6%,33.2%)
$P_{N,L}$	$P(T_N \mid S_L)$	73.7% (66.0%,81.0%)
$P_{H,N}$	$P(T_H \mid S_N)$	0.0% (0.0%,0.2%)
$P_{L,N}$	$P(T_L \mid S_N)$	1.3% (0.2%,3.2%)
$P_{N,N}$ [3]	$P(T_N \mid S_N)$	98.6% (96.8%,99.8%)
$p_{H,i}$ [4]	$P(S_{H,i})$	A=7.9% (4.7%,11.9%),B=1.9% (0.7%,3.7%),C=1.2% (0.3%,2.6%)
$p_{L,i}$	$P(S_{L,i})$	A=17.0% (10.5%,24.2%),B=16.2% (10.7%,23.0%),C=14.0% (8.7%,20.2%)
$p_{N,i}$	$P(S_{N,i})$	A=75.1% (68.2%,81.7%),B=82.0% (75.1%,87.4%),C=84.8% (78.5%,90.1%)

[1] Sensitivity for identification of heavy shedders = $P_{H,H} + P_{l,H}$
[2] Sensitivity for identification of heavy shedders = $P_{H,L} + P_{L,L}$
[3] Specificity of the test = $P_{N,N}$
[4] i is an index for the three herds: A, B, and C.

The uncertainty distributions of the test parameters (Figure 4.4) ranged from very positively skewed (e.g. Skew[$P_{H,L}$]=2.1, Skew[$P_{H,N}$]=6.7), to moderately left skewed (Skew[$P_{N,N}$]=-0.7), while the joint uncertainties of several parameters exhibited a high level of negative correlation (Figure 4.4). For example, the Pearson correlation coefficient (r) of parameter pairs $P_{H,H}/P_{L,H}$, $P_{L,L}/P_{N,L}$, and $P_{L,N}/P_{N,N}$ was -.93(,-.929, -.939), -.99(-.987, -.989), and -.99(-.996, -.997) respectively, whereas other pairs exhibited a moderate positive correlation or no correlation.

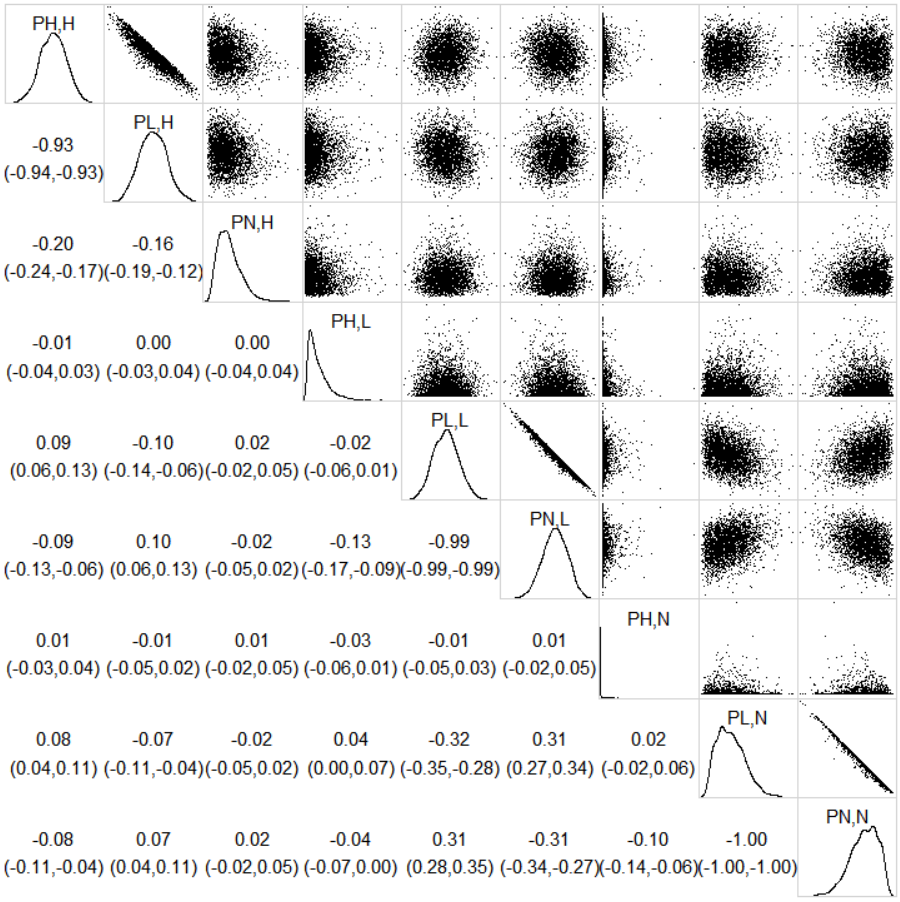

Figure 4.4: Posterior probabilities for parameters from fecal culture of feces of MAP from three WI herds with three outcomes: High, Low, and Negative (estimated herd prevalences excluded). Empirical density plots for each probability are shown in the diagonal. For example $P_{H,H}$ is the probability of a High test result, given that the animal is a heavy shedder. Figures above the diagonal are scatterplots of two parameters pairs, and numbers below the diagonal are Pearson's correlation coefficient and corresponding 95% CI for each parameter pair.

The probabilities of correctly identifying the shedding level of an animal given the results of the fecal culture test for herds A, B, and C were 97.4%, 89.7%, and 86.3% for Heavy shedders, 51.1%, 68.8%, and 68.7% for Low shedders, and 85.2%, 87.0%, and 89.0% for Non-shedders (Table 4.4).

Table 4.4: Mean (95%CrI) posterior probabilities of correctly and incorrectly identifying the shedding level of an animal given the results of a fecal culture test (TREK) with High, Low, and Negative outcomes, for three WI herds.

Posterior probability	Herd A	Herd B	Herd C
$P(S_H \mid T_H)$	97.4% (90.2%,99.9%)	89.7% (63.4%,99.6%)	86.3% (52.1%,99.5%)
$P(S_H \mid T_L)$	36.8% (20.4%,55.3%)	12.6% (4.0%,25.2%)	9.3% (2.5%,21.0%)
$P(S_H \mid T_N)$	0.3% (0.0%,0.7%)	0.1% (0.0%,0.2%)	0.0% (0.0%,0.1%)
$P(S_L \mid T_H)$	2.3% (0.0%,8.9%)	8.8% (0.2%,34.3%)	11.5% (0.3%,43.6%)
$P(S_L \mid T_L)$	51.1% (30.5%,71.3%)	68.8% (46.1%,87.4%)	68.7% (44.7%,89.1%)
$P(S_L \mid T_N)$	14.6% (9.0%,21.7%)	12.9% (8.0%,18.9%)	11.0% (6.7%,16.4%)
$P(S_N \mid T_H)$	0.3% (0.0%,3.3%)	1.4% (0.0%,14.2%)	2.2% (0.0%,20.3%)
$P(S_N \mid T_L)$	12.0% (1.9%,27.2%)	18.7% (3.1%,41.2%)	22.0% (3.8%,45.5%)
$P(S_N \mid T_N)$	85.2% (78.0%,90.7%)	87.0% (81.0%,92.0%)	89.0% (83.5%,93.3%)

3.2 Transition probabilities from disease trajectories

For brevity, the transition probabilities from the vaccinated individuals in only one herd are reported (Table 4.5, Figure 4.5). The yearly probability of transitioning from Susceptible to Latent was 17.4%, and provides a measure of the risk of infection. Latent individuals had a 26.4% chance of starting to shed low level of MAP in any given year, and 46.3% chance of remaining Latent for a year. Low shedders had a 50.0% probability of remaining in the same shedding state for a year, a 10.2% of becoming Heavy shedders, and a 27.3% chance of being removed (culled) from the herd. Once an individual was a Heavy shedder, it had a 16.1% chance of remaining HS, a 20.0% probability of returning to the Low shedder state, and a 38.9% probability of being culled from the herd, which was almost 10% higher than the culling rate of Low shedders.

Table 4.5: Means of posterior transition probabilities for animals vaccinated against MAP in a WI herd. Culled (CU) is a terminal state, thus the transitions to other states are excluded.

Transition probability	S	NS	L	LS	HS	CL	CU-S	CU-NS	CU-L	CU-LS	CU-HS	CU-CL
S	27.6%	20.0%	17.4%	0.0%	0.0%	0.0%	35.0%[1]	0.0%	0.0%	0.0%	0.0%	0.0%
NS	0.0%	71.4%	0.0%	0.0%	0.0%	0.0%	0.0%	28.6%	0.0%	0.0%	0.0%	0.0%
L	0.0%	0.0%	46.3%	26.4%	0.0%	0.0%	0.0%	0.0%	27.3%[2]	0.0%	0.0%	0.0%
LS	0.0%	0.0%	0.0%	50.0%	10.2%	12.5%[3]	0.0%	0.0%	0.0%	27.3%	0.0%	0.0%
HS	0.0%	0.0%	0.0%	20.0%	16.1%	25.0%[3]	0.0%	0.0%	0.0%	0.0%	38.9%	0.0%
CL	0.0%	0.0%	0.0%	0.0%	0.0%	0.0%	0.0%	0.0%	0.0%	0.0%	0.0%	100.0%[4]

[1] Culling of 35% of young stock (Susceptible calve states) assumed.
[2] No culling data was available for Latents so it was assumed to be the same as calculated for Low shedders
[3] Transition from Low-shedder (LS) to Clinical (CL) and HS to CL assumed to be 12.5% and 25% respectively.
[4] Transition from Clinical (CL) to Culled (CU_CL) assumed to be 100% in any given year.

The joint uncertainties of several transition probabilities exhibited significant correlation (Figure 4.5). For example, there was a strong negative correlation *r*= -.92 (-.91,-.93) between the L-L and L-LS transition probabilities, as the only other possible transition from L was HS. The HS-HS transition probability was negatively correlated to HS-CU (-1) as Heavy shedder animals were culled from the herd within a year, and NS-NS was also 100% negatively correlated to CU as NS animals remained in that state until culled.

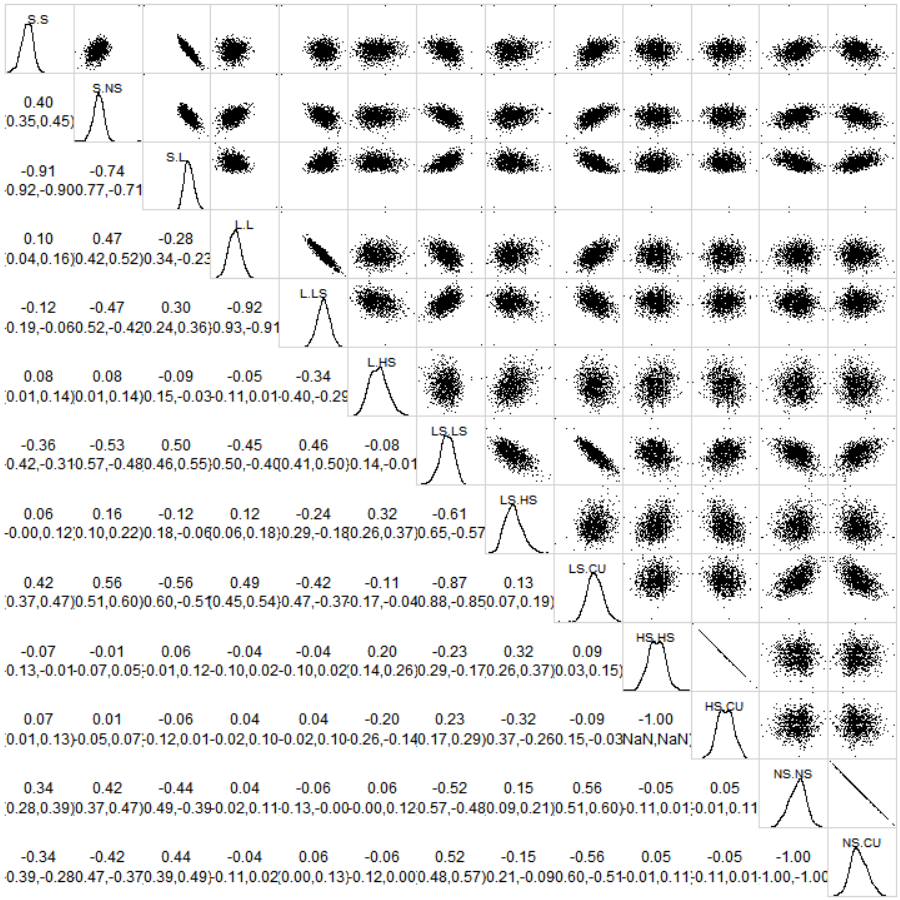

Figure 4.5: Posterior transition probabilities for a within-herd Markov Chain model of Paratuberculosis spread. Empirical density plots for each posterior are shown in the diagonal. Figures above the diagonal are scatterplots of two parameters pairs, and numbers below the diagonal are Pearson's correlation coefficient and corresponding 95% CI for each parameter pair.

3.3 Disease projections

The 20-year projection of the mean (95%CrI) yearly number of Latents (Figure 4.6.a), and the mean yearly number of individuals in multiple states (Figure 4.6.b) shows that the number of Latent individuals drops in the first two years, to quickly increase and reach a steady state by year 6 or 7. Following the same pattern, the Low shedding animals drop until reaching an

average of 30 individuals/year. This initial drop is expected, as the scenario shown here purposely starts with no animals culled at year 0. As the replacement calves are calculated from the culled animals, the number of Susceptible calves on year 1 is reduced, effectively reducing the number of calves that can become Latent on year 1. As the Susceptible population reaches a stable number, the Latent individuals also reach equilibrium at year 6-7. This initial drop is not observed in scenarios using reasonable starting numbers of culled animals, as derived from the herds used (results not shown).

Finally, the number of Latent individuals in earlier years will result in a lagged number of Heavy shedder and Clinical individuals, which is reflected in the increased number of HS and CL individuals in the first years.

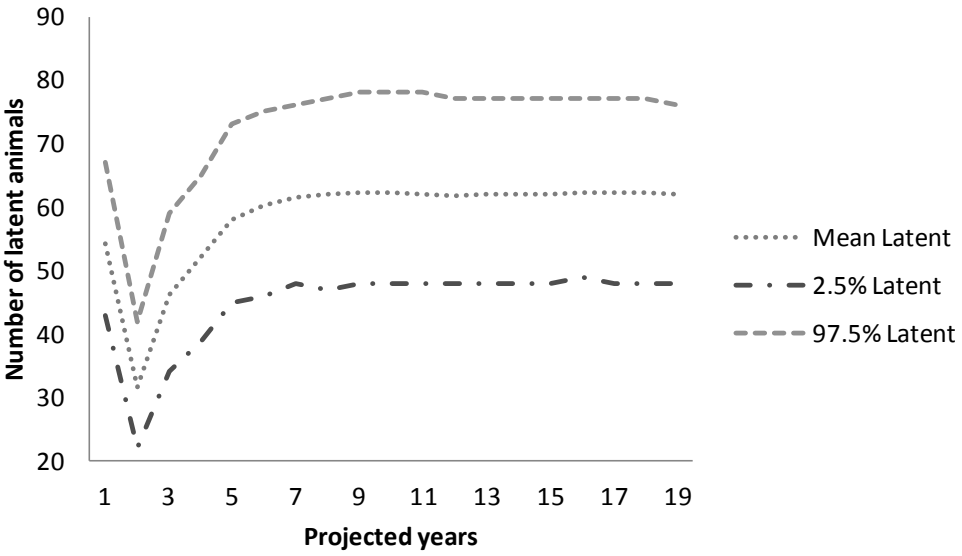

(a)

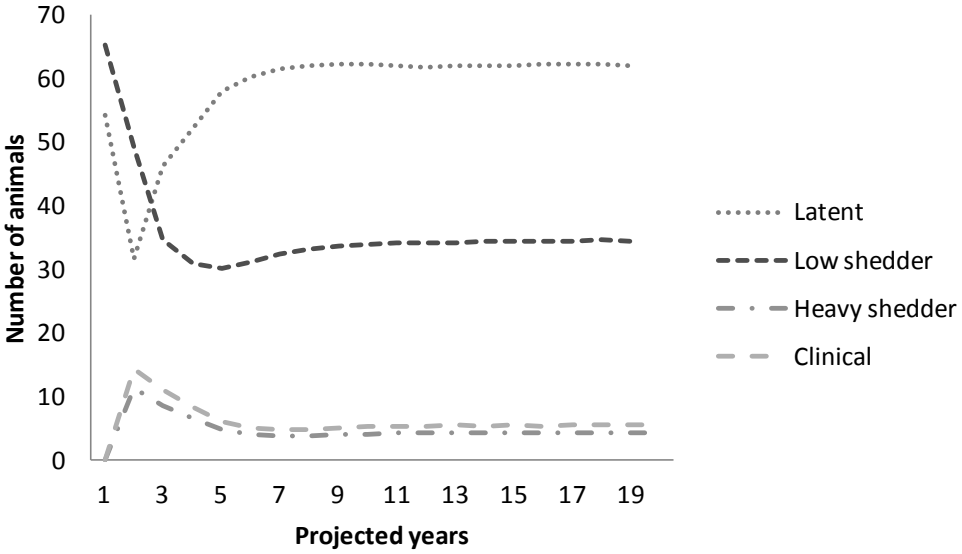

(b)

Figure 4.6: Yearly projection of the mean (95%CrI) yearly number of Latents (a), and the mean yearly number of individuals in L, LS, HS, and CL states of Paratuberculosis (b) in a dairy herd from Wisconsin, USA. Non-shedders excluded to ease the interpretation of the plot (as they represent the large majority of the total animals predicted).

3.4 Sensitivity analysis

The results from simulating only variability with the model vs. including both variability and uncertainty in the model results (Figure 4.7) suggest that the uncertainty in the transition probabilities increased the percentiles (and thus, the variance) of the model prediction of total Latents. Similar results were observed for the other state projected (results not shown).

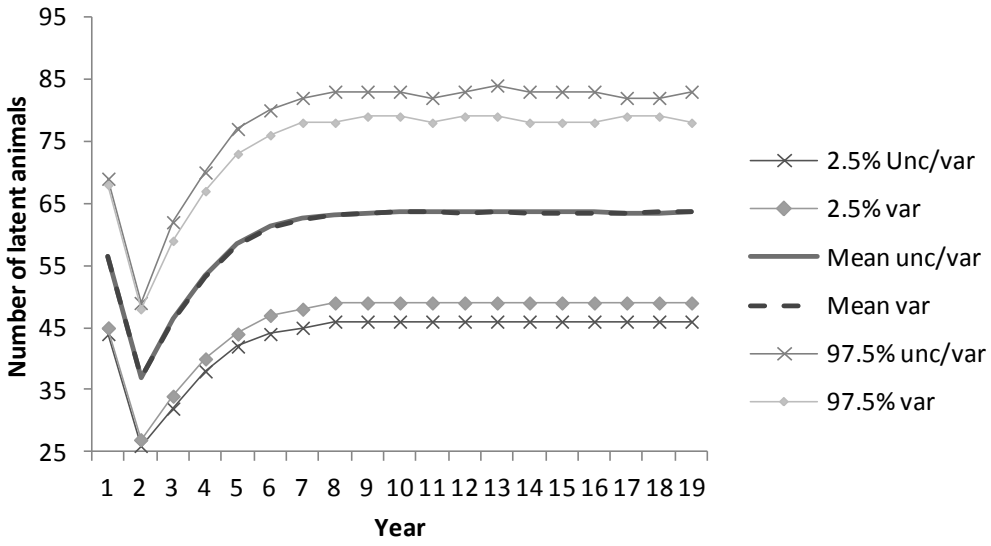

Figure 4.7: Yearly projection of the mean (95%CrI) number of individuals with latent MAP infection. The projections include individual variability only (*var*) and individual variability and uncertainty (*unc/var*) in the transition probabilities.

The projection of total number of latent individuals after 20 years (Figure 4.8) shows that while keeping everything else constant, the distribution of Latent individuals was narrower when ignoring the parameter correlation (SD :188.5 and 250.3 for correlated and uncorrelated scenarios respectively), and further reduced when only variability was modeled (SD: 45.1).

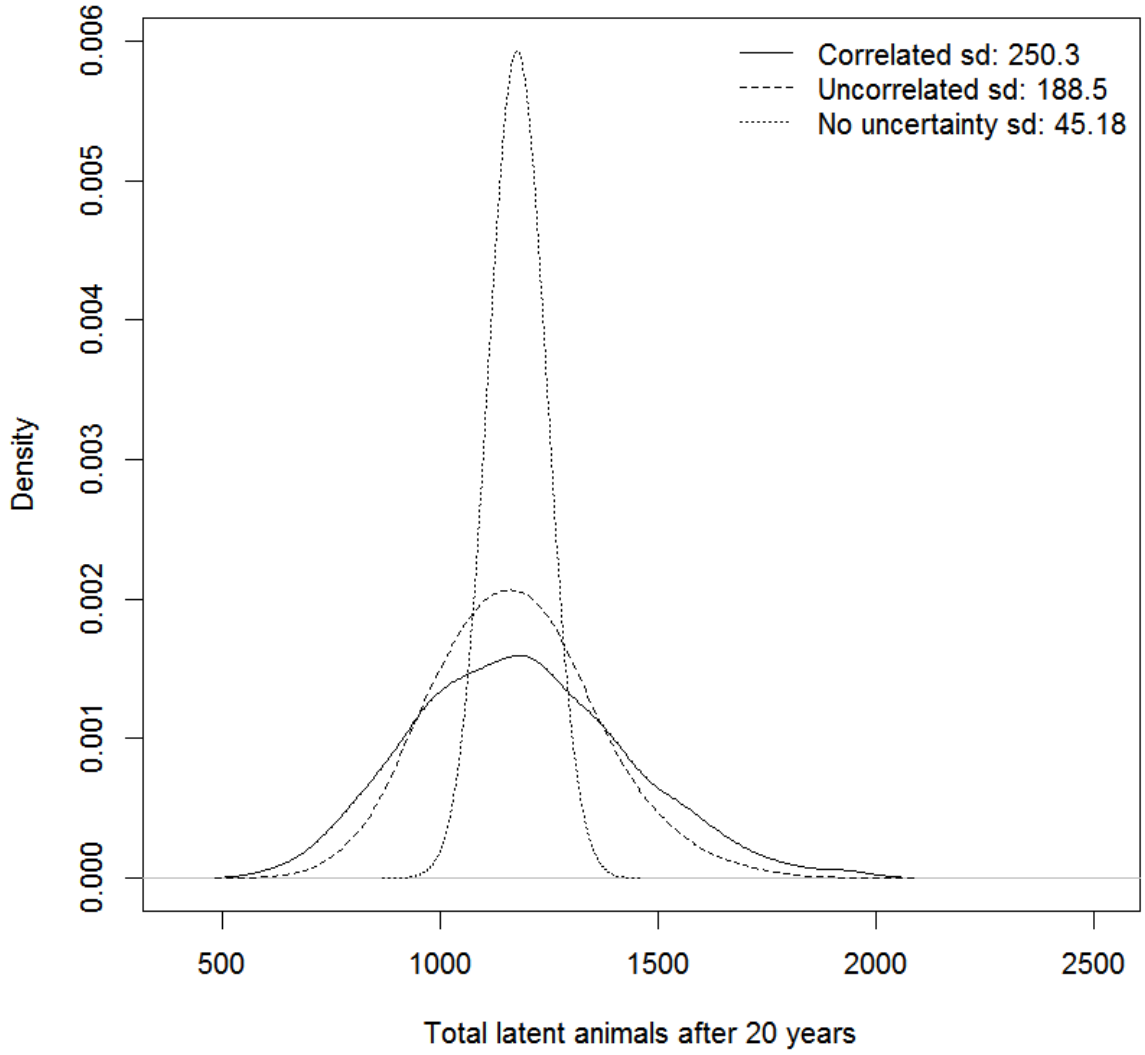

Figure 4.8: Empirical density of the simulated total number of individuals with latent MAP infection after 20 years. The *Correlated* scenario assumes correlation between the transition probabilities, and an alternative *Uncorrelated* scenario assumes uncorrelated transition probabilities. The *No uncertainty* scenario uses the mean of the transition probabilities.

The total number of latent individuals projected after 20 years was influenced by several of the transition parameters (Figure 4.9), with the most influential being the transition probability from S to L, S to NS, and S to S. Expectedly, S-L had a positive rank-order correlation to the

number of Latent individuals (.90), whereas S-NS and S-S had negative correlation (-.87 and -.84 respectively) (Figure 4.10).

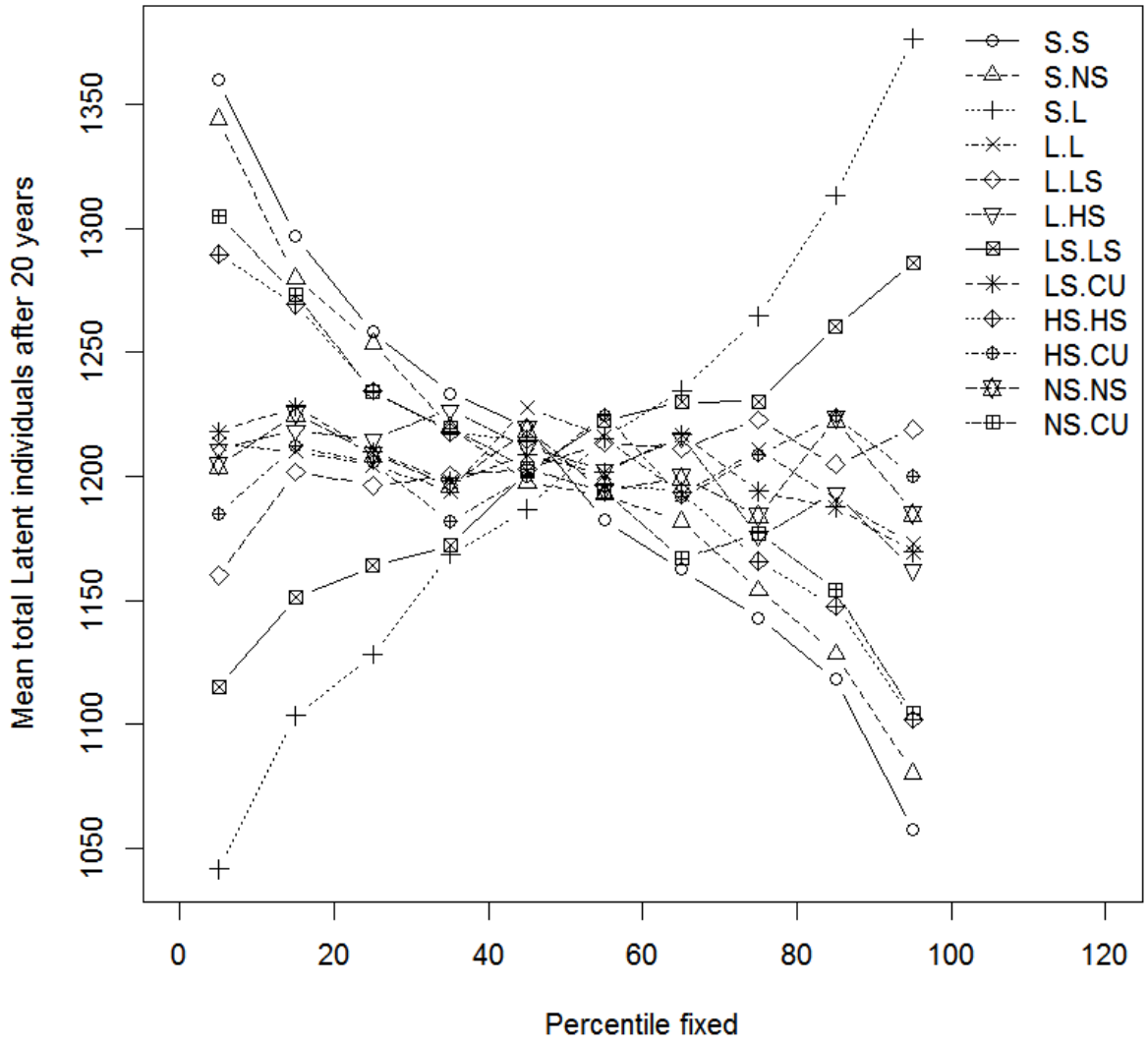

Figure 4.9: Sensitivity of the mean simulated total individuals with latent MAP infection after 20 years, in a dairy herd in Wisconsin, USA. The horizontal axis shows the percentile fixed for each input distribution, and the vertical axis reports the mean of the total Latent individuals after 20 years, conditional on the percentile of each input distribution. A horizontal line suggests that the input variable doesn't affect the mean results of the output, whereas a sloped line indicates an influential input variable.

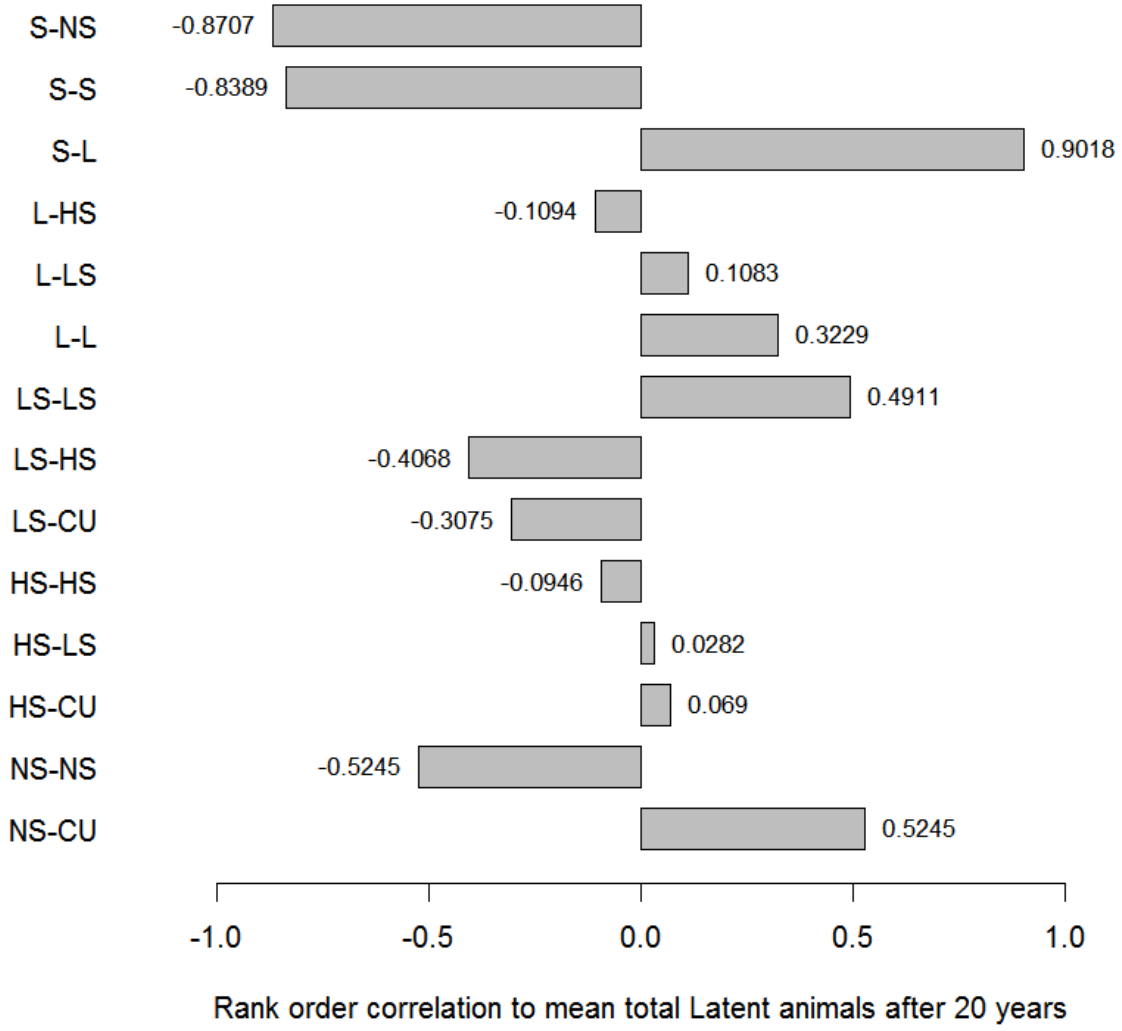

Figure 4.10: Rank order correlation of transition probabilities and the mean simulated total individuals with latent MAP infection after 20 years, in a dairy herd in Wisconsin, USA. The transition probabilities are listed on the vertical axis, and their respective rank order correlation values are shown as horizontal bars.

No relevant changes in the total predicted Latents were observed by changing the Latent delay from month 6 from birth, or Low shedder time to 12 months prior to HS determination (results not shown).

4 Discussion

The modeling approach discussed here provides a general framework to estimate disease transmission parameters for a chronic disease with multiple levels of shedding, while taking into account the uncertainties in test characteristics and their respective correlations. Although several methods for statistical inference for infectious disease models have been proposed [118-122], to the authors' knowledge this is the only work that addresses statistical inference for an endemic disease with multiple levels of shedding.

The sensitivity analysis ignoring parameter correlation yielded a SD of the total Latent individual projected that was roughly 75.3% of the SD from the simulation accounting for correlated parameters (figure 4.8). This underestimation can have a considerable impact in the applicability of a disease model, as the lower SD will result in narrower estimates such as the 95%PI typically reported from stochastic simulation models. Also, the Markov Chain model reported here was applied to a small population of 573 animals/year so the overall SD of the projection was contained. However, when modeling larger populations, the effect on the SD would increase[8], further amplifying the effect of ignoring the parameter correlation.

Given the number of test and prevalence parameters estimated it was necessary to provide informative priors for the parameters to be identifiable; an issue well described in diagnostic test evaluation as discussed elsewhere [53, 131]. The stratification of results by different

[8] Assuming that the Central Limit Theorem applies to the simulation results, it is reasonable to assume that the total SD of *n* simulated individuals/year $SD_n \rightarrow SD/\sqrt{n}$

populations (e.g. the three herds used in this study) is also a strategy commonly used to estimate parameters of unidentifiable models, as this increases the degrees of freedom available for estimation [132]. From a practical standpoint, although some of the test parameters estimated were sensitive to the choice of priors, the prior values used in this study were derived from a subset of herds from a larger study based on more herds and test results that used a fecal culture test together with the results of a serum ELISA tests run concurrently [124]. Therefore, the priors were informed by relevant data under similar conditions to those used here.

A series of simplistic assumptions were made to facilitate the derivation of this application. However, the framework proposed could be expanded to accommodate more realistic assumptions. For example, the Markov Chain model used to project the disease assumes that the infection probabilities remain constant (but uncertain) over time, whereas other infectious disease models assume that the transition probabilities may change over time. Since the model derives the full historical trajectories for every individual in the population, the parameters for other disease models could also be estimated for example, using Generalized Linear Models fitted iteratively to each the different disease trajectories.

Paratuberculosis is a chronic disease with poorly predictive test results and a significant lag between infection and shedding and/or clinical signs of the disease, so several years of data were required to estimate the disease transition parameters and even under those circumstances, the scarce number of High test results presented difficulties for the estimation

of some of the parameters. Also, the time of infection and the duration of some of the shedding periods had to be assumed, as unlike for epidemic diseases, no outbreak end times could be used to infer some of these values. However, the sensitivity analysis of these assumptions suggested that they did not have a substantial impact in the model predictions. Thus, the proposed model could also be applied to other chronic or slow progressing diseases for which there are several years of longitudinal screening data and potentially multiple disease states, such as Bovine tuberculosis or prostate cancer screening in humans. Likewise, the model could also be applied to other faster spreading diseases that may require less longitudinal data, and could be expanded to accommodate for algorithms to establish time of infection such as the ones described by Höhle et al. [121].

Finally, the technique described here departs from those described in other Bayesian studies as it takes a two-stage approach, with the test parameter estimation performed in OpenBUGS and the estimation of the transition probabilities and disease model projections in Excel® (coded in VBA, and using the simulation engine from a commercial add-in). Although this approach is infrequent in the statistical literature, it can be found in the medical decision analysis literature. For example Dias et al. [133] argue that for decision models requiring meta-analytical parameters estimated in WinBUGS (an alternate version of OpenBUGS), the output chains can be imported in Excel® and sampled directly, yielding the exact technical properties as a one-stage Bayesian approach. The authors also highlight the need to sample all parameter values from the same MCMC iteration to ensure that the correlations in the parameter estimates are preserved, which was the approach taken here.

Conclusions

In presence of imperfect disease diagnostic data, the uncertainty distributions of the test characteristics and disease prevalences may have a major impact in the uncertainty distributions of disease parameters estimated from the data. Furthermore, the correlation between the disease parameters can greatly impact the variance of relevant disease model outputs and therefore, this correlation should be taken into account when parameterizing stochastic epidemic models. The simulation method described provides a likelihood-free alternative to derive the joint uncertainty in the disease parameters, and can be extended to a variety of disease spread models.

CHAPTER 5: CONCLUDING REMARKS

"I believe that no one who is familiar, either with mathematical advances in other fields, or with the range of special biological conditions to be considered, would ever conceive that everything could be summed up in a single mathematical formula, however complex."

- Ronald Fisher

"Sufficiently simple natural structures are predictable but uncontrollable, whereas sufficiently complex symbolic descriptions are controllable but unpredictable."

- Howard Patte

1. Relevance of this work

As epidemiological models become increasingly popular to support policy, a closer examination of the models' structure and assumptions is warranted. In this thesis, I focused on the subject of simplicity (parsimony) and complexity in epidemiological models for both epidemic and endemic diseases. For this, I developed several models with the goal of addressing parsimony and complexity both in the models structure, and in their parameterization. The application of such models yielded interesting findings that may have direct application in models used for animal health policy.

Chapters 2 and 3 focused on parsimony and complexity in model structure. Probably the most interesting (and somehow unforeseen) finding from the scenarios evaluated in chapter 2 was that for fast spreading epidemics diseases such as those created by introduction of FMD in naïve populations, the actual locations of animal population units may not be as relevant to predict outbreak size and duration as more detailed information on population and contact heterogeneity. In contrast, in our scenarios the extra granularity provided by having the actual population units seems to be important when modeling slower spreading epidemic diseases, as

ignoring this aspect produced outbreak sizes roughly 1/5th smaller. These findings can have a direct implication for the modeling of contingency planning strategies for Transboundary diseases. For example, the United States Department of Agriculture performs a national census twice per decade, but only aggregate county-level data is available to the public and scientific community [35]. This has often been seen as a limitation to parameterized disease models, and researchers have resourced to a variety of approximation methods to create synthetic datasets to model populate epidemiological models[134]. Based on our findings, efforts to obtain actual unit locations or alternative, sophisticated methods to create synthetic population datasets may not be prioritized when modeling highly infectious animal diseases that are typically in the top list for contingency planning purposes, such as FMD, Classical Swine Fever (CSF), and African Swine Fever (ASF). Nonetheless, having access to actual farm locations can be of great value during an outbreak, for example, to perform tracing investigations, apply farm level intervention measures such as prophylactic vaccination, and to enforce movement restrictions, so our recommendations are specific to tactical epidemiological modeling for planning purposes.

In contrast, our findings stress that detailed information on the contact structure between populations is necessary to produce accurate disease predictions. This concept has been discussed considerably in the literature [66-67, 73, 76] but often the models used, and the interpretations derived from them were biased towards explaining theoretical patterns in disease ecology rather than focusing directly on animal health policy, so our findings provide a validation of these principles using a more mechanistic model similar to those applied in practice.

The findings in chapter 3 are not directly applicable to national animal health policy, but nonetheless have a direct application to another important alternative to disease risk management; farm-level insurance against catastrophic disease events. A structurally complex modeling framework was necessary to make inferences about a hypothetical ED for which no empirical data was available, resulting in highly uncertainty fish inventory loss estimates. Nonetheless, the models and analysis provided a systematic framework to organize the current knowledge on the emerging diseases affecting the catfish industry, and this information was used by a US government agency (USDA-Risk Management Agency) to evaluate the feasibility of developing actuarially sound agricultural insurance policies and premiums in aquaculture.

In chapter 4, the focus is shifted to parsimony and complexity in the parameterization of epidemiological models, and used a model to simulate the spread of Paratuberculosis (also called Johne's disease), a cattle disease endemic to most areas in the world. To my knowledge, this model is the first attempt to estimate the joint uncertainty parameters of a Johne's model using longitudinal data, so this represents a novel contribution to the field. Another interesting finding from this work was that the joint uncertainties in the diagnostic test characteristics and the disease parameters exhibited a significant level of correlation, and sensitivity analysis showed that ignoring parameter correlation considerably underestimated the variance of the model prediction of the total number of latent animals. The practical implication from this chapter is that the correlation between disease parameters can greatly impact the variance of relevant disease model outputs and therefore, this correlation should be taken into account when parameterizing stochastic epidemic models. In other words, assuming a more

parsimonious structure in the correlation parameters underestimated the variance of the results, justifying the methodology used to derive the correlated parameters. Unlike in other analytical fields such as risk modeling, the study of parameter correlation seems to be an area mostly ignored by researchers and practitioners in epidemiological modeling, perhaps because methods to estimate the joint uncertainty in such parameters can be complex, and were not computationally possible until relatively recently. Our findings warrant more research on this area.

2. Future research

This thesis only addressed a very small subset of an otherwise vast field that is rapidly expanding, so I can only make recommendations based on the specific findings from this work. From my evaluation of structural parsimony and complexity, it is clear that much work is needed not only to establish a formal framework to test for structural parsimony, but also to create models that can be consistently used and validated for policy support in both human and animal health. The model selection work recently developed in ecological modeling [22-23] should provide an encouraging example for epidemiological modelers.

Also, the models I used in chapters 2 and 3 were very computationally intensive, limiting the scalability of the scenarios I tested to only individual states in the US as all my models were developed for a single desktop application. Although many countries are smaller than the US states evaluated, perhaps scenarios created at a national or continental scale may provide findings in disagreement with mine. Such large scenarios could be evaluated using distributed

computing; a platform that provides exciting possibilities to the development of large scale epidemiological models [27, 135].

Much research is needed in the field of statistical inference from epidemiological models. The approach I used to model the joint uncertainties in epidemiological model parameters was adequate, but there are exciting developments particularly in the field of Bayesian statistics that should be further investigated. For example, Approximate Bayesian Computation (ABC) methods that don't require the specification of a likelihood function seem particularly suitable for the estimation of parameters of complex epidemiological models[136-137], while still providing a direct estimation of parameter correlation.

REFERENCES

1. Zepeda C, Salman M, & Ruppanner R (2001) International trade, animal health and veterinary epidemiology: challenges and opportunities. *Prev Vet Med* 48(4):261-271.
2. Christou L (2011) The global burden of bacterial and viral zoonotic infections. *Clin Microbiol Infect* 17(3):326-330.
3. Singer A, Salman M, & Thulke HH (2011) Reviewing model application to support animal health decision making. *Prev Vet Med* 99(1):60-67.
4. Bolker B (2008) *Ecological Models and Data in R* (Princeton University Press, Princeton, NJ.).
5. Kermack WO & McKendrick AG (1927) A Contribution to the Mathematical Theory of Epidemics. *Proc. Roy. Soc. Lond. A* 115(772):700-721.
6. Anderson RM & May RM eds (1991) *Infectious Diseases of Humans: Dynamics and control* (Oxford University Press, Oxford).
7. Vynnycky E & White RG (2010) *An Introduction to Infectious Disease Modeling* (Oxford University Press, Oxford, UK).
8. Keeling MJ & Rohani P (2008) *Modeling Infectious Diseases in Humans and Animals* (Princeton University Press, Princeton, NJ.).
9. Hollingsworth TD (2009) Controlling infectious disease outbreaks: Lessons from mathematical modelling. *J Public Health Pol* 30(3):328-341.
10. Eisenberg JN, Brookhart MA, Rice G, Brown M, & Colford JM, Jr. (2002) Disease transmission models for public health decision making: analysis of epidemic and endemic conditions caused by waterborne pathogens. *Environ Health Perspect* 110(8):783-790.
11. Garner MG & Hamilton SA (2011) Principles of epidemiological modelling. *Rev Sci Tech* 30(2):407-416.
12. Premashthira S, Salman MD, Hill AE, Reich RM, & Wagner BA (2011) Epidemiological simulation modeling and spatial analysis for foot-and-mouth disease control strategies: a comprehensive review. *Anim Health Res Rev* 12(2):225-234.
13. Dorjee S*, et al.* (2012) A Review of Simulation Modelling Approaches Used for the Spread of Zoonotic Influenza Viruses in Animal and Human Populations. *Zoonoses Public Health*.
14. Woolhouse M (2011) How to make predictions about future infectious disease risks. *Philosophical Transactions of the Royal Society B: Biological Sciences* 366(1573):2045-2054.
15. Jefferys W & Berger J (1991) Sharpening Ockham's Razor on a Bayesian Strop. Purdue University Tech. Report #91-44C.
16. Kelly KT & Mayo-Wilson C (2010) Ockham Efficiency Theorem for Stochastic Empirical Methods. *Journal of Philosophical Logic* 39(6):679-712.
17. Hirschman AO (1985) Against Parsimony: Three Easy Ways of Complicating some Categories of Economic Discourse. *Economics and Philosophy* 1(01):7-21.

18. Gelman A, Bois F, & Jiang J (1996) Physiological pharmacokinetic analysis using population modeling and informative prior distributions. *Journal of the American Statistical Association* 91(436):1400-1412.
19. Hitchcock C & Sober E (2004) Prediction versus Accommodation and the Risk of Overfitting. *The British Journal for the Philosophy of Science* 55(1):1-34.
20. Forster MR (2000) Key Concepts in Model Selection: Performance and Generalizability. *Journal of Mathematical Psychology* 44(1):205-231.
21. Ginzburg LR & Jensen CXJ (2004) Rules of thumb for judging ecological theories. *Trends in Ecology & Evolution* 19(3):121-126.
22. Asgharbeygi N, Langley P, Bay S, & Arrigo K (2006) Inductive revision of quantitative process models. *Ecological Modelling* 194(1–3):70-79.
23. Cox GM*, et al.* (2006) *Towards the systematic simplification of mechanistic models* (Elsevier, Amsterdam, PAYS-BAS), p 7.
24. Bauch CT & Bhattacharyya S (2012) Evolutionary Game Theory and Social Learning Can Determine How Vaccine Scares Unfold. *PLoS Comput Biol* 8(4):e1002452.
25. Breban R, Drake JM, Stallknecht DE, & Rohani P (2009) The Role of Environmental Transmission in Recurrent Avian Influenza Epidemics. *PLoS Comput Biol* 5(4):e1000346.
26. Wearing HJ, Rohani P, & Keeling MJ (2005) Appropriate Models for the Management of Infectious Diseases. *PLoS Med* 2(7):e174.
27. Eubank S*, et al.* (2004) Modelling disease outbreaks in realistic urban social networks. *Nature* 429(6988):180-184.
28. Garner MG & Beckett SD (2005) Modelling the spread of foot-and-mouth disease in Australia. *Aust Vet J* 83(12):758-766.
29. Harvey N*, et al.* (2007) The North American Animal Disease Spread Model: a simulation model to assist decision making in evaluating animal disease incursions. *Prev Vet Med* 82(3-4):176-197.
30. Stevenson MA*, et al.* (In-press) InterSpread Plus: a spatial and stochastic simulation model of disease in animal populations. *Preventive Veterinary Medicine* (0).
31. Schoenbaum MA & Disney TW (2003) Modeling alternative mitigation strategies for a hypothetical outbreak of foot-and-mouth disease in the United States. *Prev Vet Med* 58(1-2):25-52.
32. Saegerman C, Porter SR, & Humblet MF (2011) The use of modelling to evaluate and adapt strategies for animal disease control. *Rev Sci Tech* 30(2):555-569.
33. Garner MG*, et al.* (2007) Evaluating alternative approaches to managing animal disease outbreaks--the role of modelling in policy formulation. *Vet Ital* 43(2):285-298.
34. Keeling MJ (2005) Models of foot-and-mouth disease. *Proceedings of the Royal Society B: Biological Sciences* 272(1569):1195-1202.
35. Tildesley MJ*, et al.* (2010) Impact of spatial clustering on disease transmission and optimal control. *Proc Natl Acad Sci U S A* 107(3):1041-1046.
36. Mansley LM, Donaldson AI, Thrusfield MV, & Honhold N (2011) Destructive tension: mathematics versus experience--the progress and control of the 2001 foot and mouth disease epidemic in Great Britain. *Rev Sci Tech* 30(2):483-498.

37. Kitching RP, Thrusfield MV, & Taylor NM (2006) Use and abuse of mathematical models: an illustration from the 2001 foot and mouth disease epidemic in the United Kingdom. *Rev Sci Tech* 25(1):293-311.
38. Taylor NM (2003) Review of the use of models in informing disease control policy development and adjustment. (The University of Reading, Reading, U.K.), p 94.
39. Ferguson NM, Donnelly CA, & Anderson RM (2001) The foot-and-mouth epidemic in Great Britain: pattern of spread and impact of interventions. *Science* 292(5519):1155-1160.
40. Morris RS, Wilesmith JW, Stern MW, Sanson RL, & Stevenson MA (2001) Predictive spatial modelling of alternative control strategies for the foot-and-mouth disease epidemic in Great Britain, 2001. *Vet Rec* 149(5):137-144.
41. Velthuis AG & Mourits MC (2007) Effectiveness of movement-prevention regulations to reduce the spread of foot-and-mouth disease in The Netherlands. *Prev Vet Med* 82(3-4):262-281.
42. Yoon H*, et al.* (2006) Simulation analyses to evaluate alternative control strategies for the 2002 foot-and-mouth disease outbreak in the Republic of Korea. *Prev Vet Med* 74(2-3):212-225.
43. Boklund A, Toft N, Alban L, & Uttenthal A (2009) Comparing the epidemiological and economic effects of control strategies against classical swine fever in Denmark. *Prev Vet Med* 90(3-4):180-193.
44. Ribbens S, Goris N, Neyts J, & Dewulf J (2012) Classical swine fever outbreak containment using antiviral supplementation: a potential alternative to emergency vaccination and stamping-out. *Prev Vet Med* 106(1):34-41.
45. Lewis N SJVJDC (2009) *T6-1.4.1 - Analysis of a large number of simulated outbreaks of highly pathogenic avian influenza in Ontario from the North American Animal Disease Spread Model*, pp 109-109.
46. Pendell DL & Hill AE (2009) Economic impacts for alternate depopulation capacities for a FMD outbreak in the US. *International Symposia on Veterinary Epidemiology and Economics*, pp 461-461.
47. Pendell DL (2006) Value of Animal Traceability Systems in Managing a Foot-and-Mouth Disease Outbreak in Southwest Kansas. PhD thesis dissertation (Kansas State University, Manhattan, Kansas).
48. Dubé C*, et al.* (2007) A comparison of predictions made by three simulation models of foot-and-mouth disease. *N Z Vet J* 55(6):280-288.
49. Groenendaal H, Nielen M, & Hesselink JW (2003) Development of the Dutch Johne's disease control program supported by a simulation model. *Prev Vet Med* 60(1):69-90.
50. Wilkinson D*, et al.* (2009) Cost-benefit analysis model of badger (Meles meles) culling to reduce cattle herd tuberculosis breakdowns in Britain, with particular reference to badger perturbation. *J Wildl Dis* 45(4):1062-1088.
51. Rovira A, Reicks D, & Munoz-Zanzi C (2007) Evaluation of surveillance protocols for detecting porcine reproductive and respiratory syndrome virus infection in boar studs by simulation modeling. *J Vet Diagn Invest* 19(5):492-501.
52. Danon L, House T, & Keeling MJ (2009) The role of routine versus random movements on the spread of disease in Great Britain. *Epidemics* 1(4):250-258.

53. Branscum AJ, Gardner IA, & Johnson WO (2004) Bayesian modeling of animal- and herd-level prevalences. *Preventive Veterinary Medicine* 66(1–4):101-112.
54. Durrett R & Levin S (1994) The Importance of Being Discrete (and Spatial). *Theoretical Population Biology* 46(3):363-394.
55. Capaldi A*, et al.* (2012) Parameter estimation and uncertainty quantification for an epidemic model. *Math Biosci Eng* 9(3):553-576.
56. Torres A, David MJ, & Bowman QP (2002) Risk management of international trade: emergency preparedness. *Rev Sci Tech* 21(3):493-498.
57. Brauer F (2008) Epidemic models with heterogeneous mixing and treatment. *Bull Math Biol* 70(7):1869-1885.
58. Colizza V, Barthelemy M, Barrat A, & Vespignani A (2007) Epidemic modeling in complex realities. *L'épidémiologie : une science en développement / Epidemiology : a developing science* 330(4):364-374.
59. Keeling MJ*, et al.* (2001) Dynamics of the 2001 UK foot and mouth epidemic: stochastic dispersal in a heterogeneous landscape. *Science* 294(5543):813-817.
60. Sanson RL*, et al.* (2011) Foot and mouth disease model verification and 'relative validation' through a formal model comparison. *Rev Sci Tech* 30(2):527-540.
61. Rhodes CJ & Hollingsworth TD (2009) Variational data assimilation with epidemic models. *J Theor Biol* 258(4):591-602.
62. Clancy D (1996) Carrier-borne epidemic models incorporating population mobility. *Math Biosci* 132(2):185-204.
63. Hufnagel L, Brockmann D, & Geisel T (2004) Forecast and control of epidemics in a globalized world. *PNAS* 101(42):15124-15129.
64. Bombardt JN (2006) Congruent epidemic models for unstructured and structured populations: Analytical reconstruction of a 2003 SARS outbreak. *Mathematical Biosciences* 203(2):171-203.
65. Diekmann O, Jong MCMD, & Metz JAJ (1998) A deterministic epidemic model taking account of repeated contacts between the same individuals. *J. Appl. Probab.* 35(2):448.
66. Kiss IZ, Green DM, & Kao RR (2006) The effect of contact heterogeneity and multiple routes of transmission on final epidemic size. *Mathematical Biosciences* 203(1):124-136.
67. Dickey BF, Carpenter TE, & Bartell SM (2008) Use of heterogeneous operation-specific contact parameters changes predictions for foot-and-mouth disease outbreaks in complex simulation models. *Prev Vet Med* 87(3-4):272-287.
68. Ripley BD (1977) Modelling spatial patterns. *Journal of the Royal Statistical Society, Series B* 39(2):172-212.
69. USDA (2002) Census Volume 1, Chapter 1: State Level Data: Minnesota Cattle and Calves - Inventory. . (National Agricultural Statistics Service (US), Washington, DC), p 1.
70. Bates TW, Thurmond MC, & Carpenter TE (2001) Direct and indirect contact rates among beef, dairy, goat, sheep, and swine herds in three California counties, with reference to control of potential foot-and-mouth disease transmission. *Am J Vet Res* 62(7):1121-1129.
71. Bates TW, Thurmond MC, & Carpenter TE (2003) Results of epidemic simulation modeling to evaluate strategies to control an outbreak of foot-and-mouth disease. *Am J Vet Res* 64(2):205-210.

72. Carpenter TE, Thurmond MC, & Bates TW (2004) A simulation model of intraherd transmission of foot and mouth disease with reference to disease spread before and after clinical diagnosis. *J Vet Diagn Invest* 16(1):11-16.
73. Green DM, Kiss IZ, & Kao RR (2006) Modelling the initial spread of foot-and-mouth disease through animal movements. *Proceedings of the Royal Society B: Biological Sciences* 273(1602):2729-2735.
74. R Development Core Team (2011) R: A language and environment for statistical computing. (R Foundation for Statistical Computing, Vienna, Austria).
75. Cook AR, Otten W, Marion G, Gibson GJ, & Gilligan CA (2007) Estimation of multiple transmission rates for epidemics in heterogeneous populations. *Proc Natl Acad Sci U S A* 104(51):20392-20397.
76. Keeling MJ (1999) The effects of local spatial structure on epidemiological invasions. *Proc Biol Sci* 266(1421):859-867.
77. Dubé C*, et al.* (2007) The use of epidemiological models for the management of animal diseases. in *Technical item I presented at the 75th OIE General session, Paris, 20-25 May 2007*.
78. Galvani AP & May RM (2005) Epidemiology: Dimensions of superspreading. *Nature* 438(7066):293-295.
79. Longini IM, Halloran ME, Nizam A, & Yang Y (2004) Containing Pandemic Influenza with Antiviral Agents. *American Journal of Epidemiology* 159(7):623-633.
80. Thiermann A (2004) Emerging diseases and implications for global trade. *Rev Sci Tech* 23(2):701-707.
81. Morens DM, Folkers GK, & Fauci AS (2004) The challenge of emerging and re-emerging infectious diseases. *Nature* 430(6996):242-249.
82. Thompson D*, et al.* (2002) Economic costs of the foot and mouth disease outbreak in the United Kingdom in 2001. *Rev Sci Tech* 21(3):675-687.
83. Coble KH, Hanson TR, Sempier SH, Shaik S, & Miller JC (2006) Investigating the Feasibility of Livestock Disease Insurance: A Case Study in Aquaculture. *The Economics of Livestock Disease Insurance: Concepts, Issues and International Case Studies*, eds Koontz SR, Hoag DL, Thilmany DD, Green JW, & Grannis JL (CABI Publishing, Wallingford, UK).
84. Murray AG (2008) Existing and potential use of models in the control and prevention of disease emergencies affecting aquatic animals. *Rev Sci Tech* 27(1):211-228.
85. Feng R & Garrido J (2011) Actuarial application of epidemiological models. *North American Actuarial Journal* 15(1):112-136.
86. Meuwissen MPM, van Asseldonk MAPM, Skees JR, & Huirne RBM (2006) Designing Epidemic Livestock Insurance. *The Economics of Livestock Disease Insurance: Concepts, Issues and International Case Studies*, eds Koontz SR, Hoag DL, Thilmany DD, Green JW, & Grannis JL (CABI Publishing, Wallingford, UK).
87. Nielsen L, Sang-oum W, Cheevadhanarak S, & Flegel TW (2005) Taura syndrome virus (TSV) in Thailand and its relationship to TSV in China and the Americas. *Dis Aquat Organ* 63(2-3):101-106.
88. Haenen OLM & Engelsma MY (2004) Global distribution of KHV with particular reference to Europe. *International Workshop on Koi Herpesvirus*, pp 13-15.

89. Khoo L & Holmes W (2003) Visceral Toxicosis of Catfish: An Emerging Disease. *28th Annual Eastern Fish Health Workshop*, (Gettysburg, PA).
90. Plumb JA (2001) Overview of Warm-Water Fish Diseases. *Nutrition and Fish Health*, eds Lim C & Webster D (Food Products Press, New York), pp 1-9.
91. Terhune JS, Wise DJ, & Khoo LH (2002) Bolbophorus confusus Infections in Channel Catfish in Northwestern Mississippi and Effects of Water Temperature on Emergence of Cercariae from Infected Snails. *North American Journal of Aquaculture* 64(1):70-74.
92. Fryer JL & Mauel MJ (1997) The rickettsia: an emerging group of pathogens in fish. *Emerg Infect Dis* 3(2):137-144.
93. Mardones FO, Perez AM, & Carpenter TE (2009) Epidemiologic investigation of the re-emergence of infectious salmon anemia virus in Chile. *Diseases of Aquatic Organisms* 84(2):105-114.
94. Peeler EJ & Taylor NG (2011) The application of epidemiology in aquatic animal health - opportunities and challenges. *Vet Res* 42(1):94.
95. Gillespie DT (1976) A general method for numerically simulating the stochastic time evolution of coupled chemical reactions. *Journal of Computational Physics* 22(4):403-434.
96. Ogut H, Lapatra SE, & Reno PW (2005) Effects of host density on furunculosis epidemics determined by the simple SIR model. *Prev Vet Med* 71(1-2):83-90.
97. Knol AB, Slottje P, van der Sluijs JP, & Lebret E (2010) The use of expert elicitation in environmental health impact assessment: a seven step procedure. *Environ Health* 9:19.
98. USDA (2004) Catfish Processing report. (National Agricultural Statistics Service (US), Washington, D.C.), p 5.
99. USDA (2004) Catfish Production report. (National Agricultural Statistics Service (US), Washington, D.C.), p 19.
100. USDA (2003) Part I: Reference of Fingerling Catfish Health and Production Practices in the United States. (USDA:APHIS:VS:CEAH, National Animal Health Monitoring System, Fort Collins, CO #N406.1103), p 85.
101. USDA (2003) Part II: Reference of Foodsize Catfish Health and Production Practices in the United States. (USDA:APHIS:VS:CEAH, National Animal Health Monitoring System, Fort Collins, CO #N406.1103), p 86.
102. Ogut H, Reno PW, & Sampson D (2004) A deterministic model for the dynamics of furunculosis in chinook salmon Oncorhynchus tshawytscha. *Dis Aquat Organ* 62(1-2):57-63.
103. Smith G, Bebak J, & McAllister PE (2000) Experimental infectious pancreatic necrosis infections: propagative or point-source epidemic? *Prev Vet Med* 47(4):221-241.
104. Blower SM & Dowlatabadi H (1994) Sensitivity and Uncertainty Analysis of Complex Models of Disease Transmission: An HIV Model, as an Example. *International Statistical Review / Revue Internationale de Statistique* 62(2):229-243.
105. Mardones FO, Perez AM, Valdes-Donoso P, & Carpenter TE (2011) Farm-level reproduction number during an epidemic of infectious salmon anemia virus in southern Chile in 2007-2009. *Prev Vet Med* 102(3):175-184.
106. Norris M, Johnson WO, & Gardner IA (2009) Modeling bivariate longitudinal diagnostic outcome data in the absence of a gold standard. *Statistics and its interface* 2:171-185.

107. Chamberlain J, Clifford RE, Nathan BE, Price JL, & Burn I (1984) Repeated screening for breast cancer. *J Epidemiol Community Health* 38(1):54-57.
108. Roobol MJ*, et al.* (2012) A Calculator for Prostate Cancer Risk 4 Years After an Initially Negative Screen: Findings from ERSPC Rotterdam. *Eur Urol*.
109. Kaplan EH & Satten GA (2000) Repeat screening for HIV: when to test and why. *J Acquir Immune Defic Syndr* 23(4):339-345.
110. Tschopp R*, et al.* (2010) Repeated cross-sectional skin testing for bovine tuberculosis in cattle kept in a traditional husbandry system in Ethiopia. *Vet Rec* 167(7):250-256.
111. Espejo LA, Godden S, Hartmann WL, & Wells SJ (2012) Reduction in incidence of Johne's disease associated with implementation of a disease control program in Minnesota demonstration herds. *J Dairy Sci* 95(7):4141-4152.
112. Hui SL & Walter SD (1980) Estimating the error rates of diagnostic tests. *Biometrics* 36(1):167-171.
113. Johnson WO, Gastwirth JL, & Pearson LM (2001) Screening without a "gold standard": the Hui-Walter paradigm revisited. *Am J Epidemiol* 153(9):921-924.
114. Engel B, Backer J, & Buist W (2010) Evaluation of the Accuracy of Diagnostic Tests From Repeated Measurements Without a Gold Standard. (1):83-100.
115. Benedictus A*, et al.* (2008) Transmission parameters of Mycobacterium avium subspecies paratuberculosis infections in a dairy herd going through a control program. *Preventive Veterinary Medicine* 83(3–4):215-227.
116. Nielsen SS, Weber MF, Kudahl AB, Marce C, & Toft N (2011) Stochastic models to simulate paratuberculosis in dairy herds. *Rev Sci Tech* 30(2):615-625.
117. Capaldi A*, et al.* (2012) Parameter estimation and uncertainty quantification for an epidemic model. *Mathematical Biosciences and Engineering* 9(3):553 - 576.
118. Gibson GJ & Renshaw E (1998) Estimating parameters in stochastic compartmental models using Markov chain methods. *Mathematical Medicine and Biology* 15(1):19-40.
119. Lekone PE & Finkenstadt BF (2006) Statistical inference in a stochastic epidemic SEIR model with control intervention: Ebola as a case study. *Biometrics* 62(4):1170-1177.
120. Streftaris G & Gibson GJ (2004) Bayesian inference for stochastic epidemics in closed populations. *Statistical Modelling* 4(1):63-75.
121. Höhle M, Jørgensen E, & O'Neill PD (2005) Inference in disease transmission experiments by using stochastic epidemic models. *Journal of the Royal Statistical Society: Series C (Applied Statistics)* 54(2):349-366.
122. Nishiura H (2011) Joint quantification of transmission dynamics and diagnostic accuracy applied to influenza. *Math Biosci Eng* 8(1):49-64.
123. Whitlock RH, Wells SJ, Sweeney RW, & Van Tiem J (2000) ELISA and fecal culture for paratuberculosis (Johne's disease): sensitivity and specificity of each method. *Vet Microbiol* 77(3-4):387-398.
124. Espejo LA, Zagmutt FJ, Groenendaal H, Muñoz-Zanzi C, & Wells SJ (2012) Evaluation of performance of bacterial culture of feces and serum ELISA across stages of Johne's disease in cattle using a Bayesian approach. *Manuscript submitted for publication*.
125. Knust B, Patton E, Ribeiro-Lima J, Bohn J, & Wells SJ (2012) Controlled trial demonstrates effectiveness of whole-cell killed Johne's disease vaccine with natural exposure in three Wisconsin dairy herds. *J Am Vet Med Association (accepted for publication)*.

126. Okwumabua O*, et al.* (2010) Growth Rate Retardation and Inhibitory Effect of para-JEM® BLUE on Mycobacterium Avium Subspecies Paratuberculosis. *Journal of Veterinary Diagnostic Investigation* 22(5):734-737.
127. Crossley BM, Zagmutt-Vergara FJ, Fyock TL, Whitlock RH, & Gardner IA (2005) Fecal shedding of Mycobacterium avium subsp. paratuberculosis by dairy cows. *Vet Microbiol* 107(3-4):257-263.
128. Lunn D, Spiegelhalter D, Thomas A, & Best N (2009) The BUGS project: Evolution, critique and future directions. *Stat Med* 28(25):3049-3067.
129. Kermack WO & McKendrick AG (1927) A Contribution to the Mathematical Theory of Epidemics. *Proceedings of the Royal Society of London. Series A* 115(772):700-721.
130. R Core Team (2012) R: A Language and Environment for Statistical Computing. (R Foundation for Statistical Computing, Vienna, Austria).
131. Joseph L, Gyorkos TW, & Coupal L (1995) Bayesian estimation of disease prevalence and the parameters of diagnostic tests in the absence of a gold standard. *Am J Epidemiol* 141(3):263-272.
132. Gustafson P (2005) On Model Expansion, Model Contraction,Identifiability and Prior Information:Two Illustrative Scenarios Involving Mismeasured Variables. *Statistical Science* 20(2):111–140.
133. Dias S, Sutton AJ, Welton NJ, & Ades AE (2011) NICE DSU technical support document 6: Embedding evidence synthesis in probabilistic cost-effectiveness analysis: software choices. (last updated April 2012; available from http://www.nicedsu.org.uk), p 20.
134. Rorres C, Pelletier ST, & Smith G (2011) Stochastic modeling of animal epidemics using data collected over three different spatial scales. *Epidemics* 3(2):61-70.
135. Van den Broeck W*, et al.* (2011) The GLEaMviz computational tool, a publicly available software to explore realistic epidemic spreading scenarios at the global scale. *BMC Infect Dis* 11:37.
136. Toni T, Welch D, Strelkowa N, Ipsen A, & Stumpf MPH (2009) Approximate Bayesian computation scheme for parameter inference and model selection in dynamical systems. *Journal of The Royal Society Interface* 6(31):187-202.
137. Tanaka MM, Francis AR, Luciani F, & Sisson SA (2006) Using approximate Bayesian computation to estimate tuberculosis transmission parameters from genotype data. *Genetics* 173(3):1511-1520.